

UNIVERSIDADE FEDERAL DE UBERLÂNDIA
INSTITUTO DE CIÊNCIAS BIOMÉDICAS
PROGRAMA DE PÓS-GRADUAÇÃO EM IMUNOLOGIA E PARASITOLOGIA
APLICADAS

COMPLEXO DE RUTÊNIO E *para*-CIMENO INIBE O VÍRUS CHIKUNGUNYA *in vitro*

DÉBORA MORAES DE OLIVEIRA ROSSINI

UBERLÂNDIA - MG
Fevereiro - 2020

UNIVERSIDADE FEDERAL DE UBERLÂNDIA
INSTITUTO DE CIÊNCIAS BIOMÉDICAS
PROGRAMA DE PÓS-GRADUAÇÃO EM IMUNOLOGIA E PARASITOLOGIA
APLICADAS

COMPLEXO DE RUTÊNIO E *para*-CIMENO INIBE O VÍRUS CHIKUNGUNYA *in vitro*

DÉBORA MORAES DE OLIVEIRA ROSSINI

Dissertação apresentada ao colegiado do Programa de Pós-Graduação em Imunologia e Parasitologia Aplicadas como parte de obtenção do título de Mestre.

Orientadora: Ana Carolina Gomes Jardim
Co-orientadora: Carolina Colombelli Pacca

UBERLÂNDIA - MG
Fevereiro - 2020

Ficha Catalográfica Online do Sistema de Bibliotecas da UFU
com dados informados pelo(a) próprio(a) autor(a).

R835 Rossini, Débora Moraes de Oliveira, 1995-
2020 COMPLEXO DE RUTÊNIO E para-CIMENO INIBE O VÍRUS
CHIKUNGUNYA in vitro [recurso eletrônico] : Análise da atividade
antiviral do complexo de rutênio e para-cimeno contra o vírus
chikungunya in vitro. / Débora Moraes de Oliveira Rossini. - 2020.

Orientadora: Ana Carolina Gomes Jardim.
Coorientadora: Carolina Colombelli Pacca.
Dissertação (Mestrado) - Universidade Federal de Uberlândia,
Pós-graduação em Imunologia e Parasitologia Aplicadas.
Modo de acesso: Internet.
Disponível em: <http://doi.org/10.14393/ufu.di.2020.209>
Inclui bibliografia.
Inclui ilustrações.

1. Imunologia. I. Jardim, Ana Carolina Gomes, 1981-, (Orient.). II.
Pacca, Carolina Colombelli, 1977-, (Coorient.). III. Universidade
Federal de Uberlândia. Pós-graduação em Imunologia e
Parasitologia Aplicadas. IV. Título.

CDU: 612.017

Bibliotecários responsáveis pela estrutura de acordo com o AACR2:
Gizele Cristine Nunes do Couto - CRB6/2091
Nelson Marcos Ferreira - CRB6/3074



UNIVERSIDADE FEDERAL DE UBERLÂNDIA
 Coordenação do Programa de Pós-Graduação em Imunologia e Parasitologia Aplicada
 Av. Amazonas, s/n, Bloco 4C, Sala 4C218 - Bairro Umuarama, Uberlândia-MG, CEP 38400-902
 Telefone: (34) 3225-8672 - www.imunoparasito.ufu.br - coipa@ufu.br



ATA DE DEFESA - PÓS-GRADUAÇÃO

Programa de Pós-Graduação em:	Imunologia e Parasitologia Aplicadas				
Defesa de:	Tese de mestrado número 260 do PPIPA				
Data:	vinte e sete de fevereiro de dois mil e vinte	Hora de início:	13h30	Hora de encerramento:	17h30
Matrícula do Discente:	11812IPA002				
Nome do Discente:	Débora Moraes de Oliveira Rossini				
Título do Trabalho:	Complexo de rutênio e para-cimeno inibe o vírus cikungunya in vitro				
Área de concentração:	Imunologia e Parasitologia Aplicadas				
Linha de pesquisa:	Biologia das interações entre patógenos e seus hospedeiros e Biotecnologia empregada no diagnóstico e controle de doenças				
Projeto de Pesquisa de vinculação:	Desenvolvimento E Validacao De Moléculas Sintéticas Com Aplicabilidade No Tratamento De Infeccoes Pelos Virus Da Zika E Chikungunya, E Outros Virus Relacionados				

Reuniu-se no bloco 6T Sala 6T210, Campus Umuarama da Universidade Federal de Uberlândia, a Banca Examinadora, designada pelo Colegiado do Programa de Pós-graduação em Imunologia e Parasitologia Aplicadas, assim composta: Prof^ª. Dr^ª. Cintia Bittar - UNESP/SP, Prof. Dr. Samuel Cota Teixeira - ICBIM / UFU , Prof^ª. Dr^ª. Ana Carolina Gomes Jardim - PPIPA/ICBIM/UFU - orientador(a) do(a) candidato(a).

Iniciando os trabalhos o(a) presidente da mesa, a Sra. Ana Carolina Gomes Jardim, apresentou a Comissão Examinadora e o candidato(a), agradeceu a presença do público, e concedeu ao discente a palavra para a exposição do seu trabalho. A duração da apresentação do discente e o tempo de arguição e resposta foram conforme as normas do Programa.

A seguir o senhor(a) presidente concedeu a palavra, pela ordem sucessivamente, aos(às) examinadores(as), que passaram a arguir o(a) candidato(a). Ultimada a arguição, que se desenvolveu dentro dos termos regimentais, a Banca, em sessão secreta, atribuiu o resultado final, considerando o(a) candidato(a):

Aprovado(a).

Esta defesa faz parte dos requisitos necessários à obtenção do título de Mestre.

O competente diploma será expedido após cumprimento dos demais requisitos, conforme as normas do Programa, a legislação pertinente e a regulamentação interna da UFU.

Nada mais havendo a tratar foram encerrados os trabalhos. Foi lavrada a presente ata que após lida e achada conforme foi assinada pela Banca Examinadora.



Documento assinado eletronicamente por **Ana Carolina Gomes Jardim, Professor(a) do Magistério Superior**, em 04/06/2020, às 21:00, conforme horário oficial de Brasília, com fundamento no art. 6º, § 1º, do [Decreto nº 8.539, de 8 de outubro de 2015](#).



Documento assinado eletronicamente por **Samuel Cota Teixeira, Professor(a) Substituto(a) do Magistério Superior**, em 04/06/2020, às 21:10, conforme horário oficial de Brasília, com fundamento no art. 6º, § 1º, do [Decreto nº 8.539, de 8 de outubro de 2015](#).



Documento assinado eletronicamente por **Cintia Bittar Oliva, Usuário Externo**, em 05/06/2020, às 16:57, conforme horário oficial de Brasília, com fundamento no art. 6º, § 1º, do [Decreto nº 8.539, de 8 de outubro de 2015](#).



A autenticidade deste documento pode ser conferida no site https://www.sei.ufu.br/sei/controlador_externo.php?acao=documento_conferir&id_orgao_acesso_externo=0, informando o código verificador **2070084** e o código CRC **0C1226BB**.

RESUMO

A febre chikungunya é uma doença causada pelo vírus Chikungunya (CHIKV) transmitida pela picada da fêmea do mosquito *Aedes* sp. Os sintomas incluem febre, dores musculares, erupção cutânea e fortes dores nas articulações. A doença pode evoluir para uma condição crônica apresentando dores nas articulações por meses ou anos. Atualmente, não existe tratamento antiviral eficaz contra a infecção pelo CHIKV, sendo necessário o desenvolvimento de novas terapias. Tratamentos baseados em compostos naturais têm sido amplamente estudados, pois muitos medicamentos foram produzidos usando moléculas naturais e seus derivados. O para-cimeno (pCYM) é um composto orgânico aromático de ocorrência natural que é um ligante comum para o rutênio, formando o complexo organometálico de rutênio e pCYM. Os complexos organometálicos mostraram-se promissores como uma nova geração de compostos que apresentaram propriedades biológicas relevantes, no entanto, há um desconhecimento sobre a atividade anti-CHIKV desses complexos. Neste contexto, o presente trabalho avaliou os efeitos do complexo de rutênio e pCYM ($[\text{Ru}_2\text{Cl}_4(\eta^6\text{-p-cimeno})_2]$) (RcP) e seus precursores na infecção por CHIKV *in vitro*. Para isso, as células BHK21 foram infectadas com CHIKV-*nanoluciferase* (CHIKV-*nanoluc*), uma construção viral com o gene repórter -*nanoluc*, na presença ou ausência dos compostos por 16 horas e taxas de citotoxicidade (MTT) e infectividade (luciferase) foram acessados. Os resultados demonstraram que oRcP exibiu um forte índice terapêutico avaliado pelo índice seletivo de 43,1 (razão entre citotoxicidade e potência antiviral). Os efeitos antivirais da RcP em diferentes estágios do ciclo replicativo do CHIKV foram investigados e os resultados mostraram que reduziu 77% da entrada do vírus nas células hospedeiras em concentrações não tóxicas. Ensaios adicionais demonstraram a atividade virucida do composto que inibiu completamente a infectividade do vírus. Análises de docking molecular foram realizados para investigar possíveis interações entre as glicoproteínas pCYM e CHIKV e os resultados sugeriram ligações entre pCYM e um local localizado atrás do loop de fusão entre as glicoproteínas E3 e E2. Além disso, a análise espectral por espectroscopia de infravermelho indicou interações de RcP com glicoproteínas CHIKV. Esses dados sugerem que a RcP pode atuar nas partículas virais do CHIKV, impedindo a entrada do vírus nas células hospedeiras. Análises adicionais estão sendo realizadas para avaliar o modo de ação desse complexo.

Palavras-chave: vírus Chikungunya; antiviral; areno complexo; complexo de rutênio e *para-cimeno*; complexos organometálicos.

LISTA DE ABREVIATURAS E SIGLAS

C	Proteína do capsídeo
CHIKV	Vírus do Chikungunya
DMEM	Dulbecco's Modified Eagle Medium (Meio básico modificado por Dulbecco)
DMSO	Dimetilsulfóxido
E	Proteína do envelope
ECSA	East/Central/South Africa (Leste/Centro/Sul da África)
HSV	Vírus do herpes simples
MOI	Multiplicity of infection (Multiplicidade de infecção)
MTT	3-(4,5-dimethylthiazol-2-yl)-2,5-diphenyltetrazolium-bromide (Brometo de 3-(4',5'-dimetilthiazol-2'-ila)-2,5-difeniltetrazol)
nsP	non-structural proteins (Proteínas não estruturais)
OMS	Organização Mundial da Saúde
ORFs	Open Reading Frame (Regiões de leitura aberta)
RE	Retículo endoplasmático
RNA	Ribonucleic acid (Ácido ribonucleico)
Ru	Rutênio
WA	West African (Oeste Africano)
uL	Microlitro
uM	Micromolar

SUMÁRIO

CAPÍTULO I.....	6
INTRODUÇÃO	7
Histórico e epidemiologia	7
O vírus Chikungunya	8
Transmissão.....	12
Patogênese e implicações na saúde	12
Tratamento	14
Compostos com potencial terapêutico.....	14
OBJETIVOS.....	16
Objetivo geral.....	16
Objetivos específicos.....	16
REFERÊNCIAS	17
CAPÍTULO II	24
CAPÍTULO III	52
Considerações Finais.....	53
Material Suplementar	54

CAPÍTULO I

Fundamentação Teórica

Vírus Chikungunya

INTRODUÇÃO

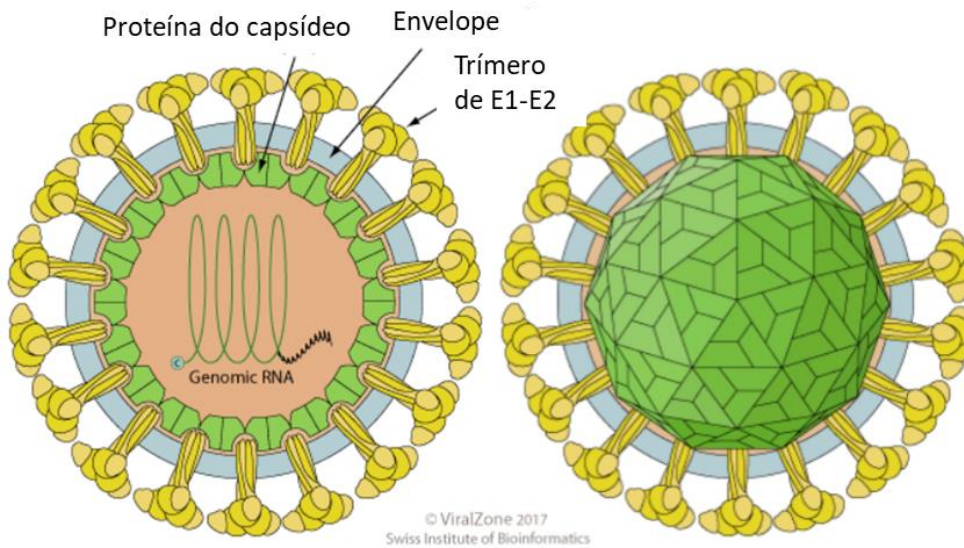
Histórico e epidemiologia

O vírus Chikungunya (CHIKV) é o agente causador da febre Chikungunya e está relacionado a epidemias principalmente em regiões tropicais e subtropicais (KHAN et al., 2002; PAIXÃO et al., 2018; STEGMANN-PLANCHARD et al., 2019). O CHIKV foi isolado pela primeira vez durante uma epidemia na Tanzânia em 1953 (Robinson, 1955; Wintachai et al., 2012). Por muitos anos o vírus permaneceu endêmico apenas em áreas da África e Ásia (NJENGA et al., 2008), mas nos anos de 2005 e 2006, foram notificados surtos de CHIKV em várias ilhas do Oceano Índico e cerca de 250 pessoas morreram devido à doença na ilha francesa de *La Réunion* (SCHUFFENECKER et al., 2006). Já no ano de 2007 foram registrados casos na Europa, em países como França e Itália (GRANDADAM et al., 2011; REZZA et al., 2007).

Em 2013, o vírus chegou às Américas com casos relatados nas ilhas do Caribe (CARVALHO; LOURENÇO-DE-OLIVEIRA; BRAGA, 2014; KAUR; CHU, 2013)(**Figura 1**). No Brasil, os primeiros casos alóctones foram registrados em 2010 no estado de São Paulo (DO SOCORRO SOUZA et al., 2012), mas só em 2014 foi registrado o primeiro caso autóctone em Oiapoque, na Amazônia. A partir de então, relatou-se diversos casos no nordeste do Brasil (CARVALHO; LOURENÇO-DE-OLIVEIRA; BRAGA, 2014; CUNHA; TRINTA, 2017).

O CHIKV foi responsável por mais de 47.000 casos nos anos de 2014 e 2015, e mais de 63.000 casos confirmados até o ano de 2016 (SILVA et al., 2018). Em 2017, foram registrados 184.694 casos prováveis de febre de CHIKV com 192 óbitos confirmados. No ano de 2018 foram registrados 85.221 casos prováveis da doença e 36 óbitos confirmados (EPIDEMIOLOGICO et al., 2018). Segundo o ministério da saúde, os casos da doença voltaram a aumentarem 2019, sendo notificados 132.205 casos prováveis, com 92 óbitos confirmados. A taxa de letalidade por CHIKV foi maior entre pessoas a partir dos 60 anos. Além disso, o CHIKV também acometeu morte em crianças menores de 1 ano (EPIDEMIOLOGICO, 2020).

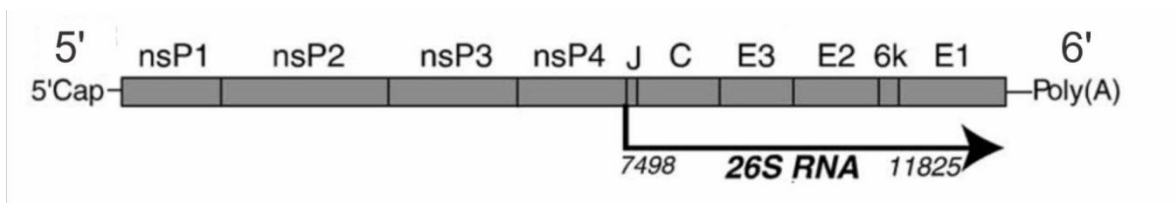
Figura 2: Vírus CHIKV. Esquema representativo da partícula viral do CHIKV.



Adaptado de Instituto de Bioinformática da Suíça (SwissInstituteofBioinformatics).
Fonte: (http://viralzone.expasy.org/625?outline=all_by_species)

O genoma viral é constituído de RNA de fita simples polaridade positiva, de aproximadamente 12 kb (SCHUFFENECKER et al., 2006). Possui duas regiões de leitura aberta (*open read frame* - ORF) que codificam proteínas não estruturais (nsP1 - nsP4), relacionadas ao complexo replicativo, e proteínas estruturais (C, E1, E2, E3), presentes no capsídeo ou envelope do vírus (LUM; NG, 2015; STRAUSS; STRAUSS, 1994) (Figura 3).

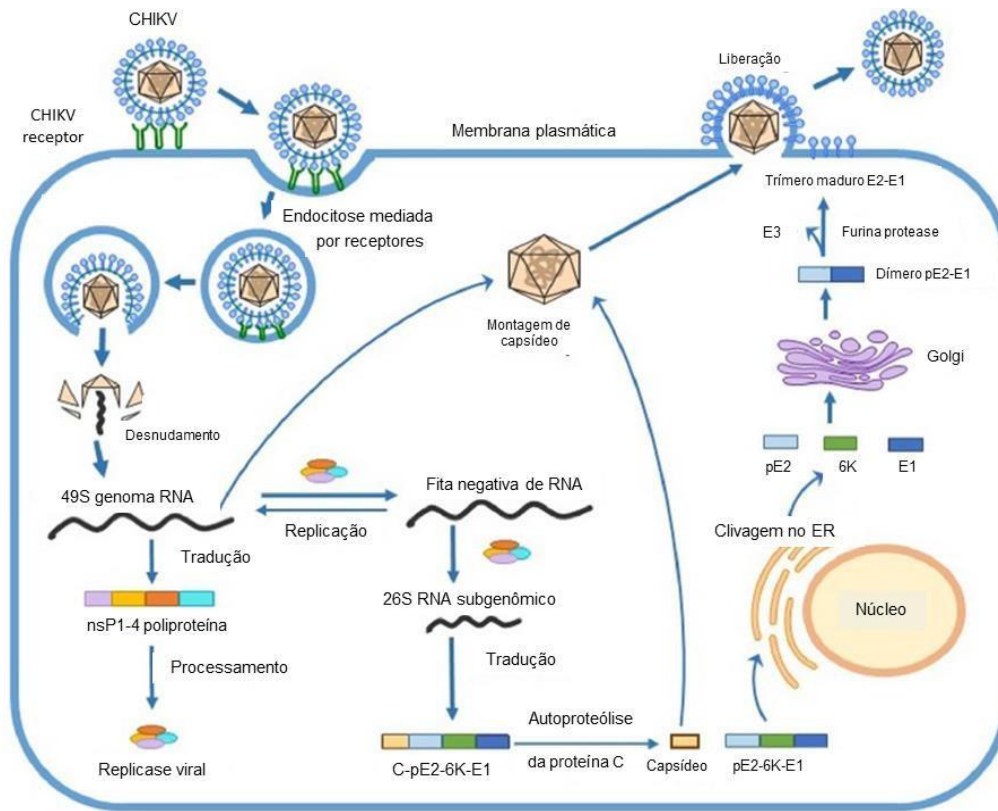
Figura 3: Ilustração do genoma do CHIKV. Genes que codificam proteínas não estruturais e proteínas não estruturais.



Adaptado de (SOLIGNAT et al., 2009).

O ciclo replicativo do CHIKV ocorre no citoplasma das células hospedeiras (**Figura 4**). Inicialmente, a glicoproteína de envelope viral denominada E2 se liga aos receptores proibitina (PHB) (WINTACHAI et al., 2012), fosfatidilserina (PtdSer) (MOLLER-TANK et al., 2013a), glicosaminoglicanos (SILVA et al., 2014) ou ATP sintase β (FONGSARAN et al., 2014) da membrana da célula, onde se constitui um poro celular. A glicoproteína de envelope E1 facilita o reconhecimento de receptores de membrana, permitindo que o vírus seja endocitado. O desnudamento do capsídeo faz com que o genoma viral seja liberado no citoplasma celular. A replicação viral se inicia a partir da tradução do genoma viral em proteínas não estruturais (nsP) do vírus, denominadas nsP1, nsP2, nsP3 e nsP4, formando então um complexo replicativo. O complexo catalisará a síntese de uma fita de RNAm de polaridade negativa, que servirá de molde para sintetizar novas fitas com polaridade positiva e de RNA subgenômico 26S (KHAN et al., 2002). O RNA subgenômico 26S é traduzido em uma poliproteína precursora que será posteriormente clivada nas proteínas estruturais C, E3, E2, 6K e E1. No retículo endoplasmático, essas proteínas sofrem modificações pós-traducionais, e complexo de Golgi, são amadurecidas e depositadas na membrana plasmática. Ocorre então a montagem dos componentes virais, onde a proteína E3 parece estar envolvida (UCHIME; FIELDS; KIELIAN, 2013). As novas partículas virais são liberadas por brotamento na membrana plasmática (ABDELNABI; NEYTS; DELANG, 2015)(**Figura 4**).

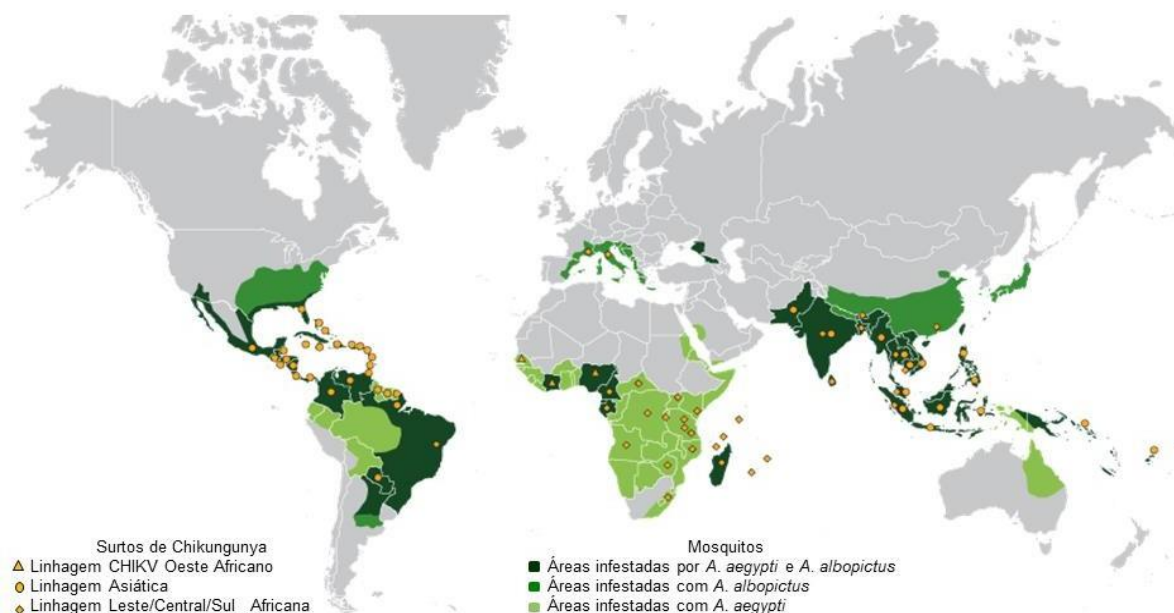
Figura 4: Esquema representativo do ciclo replicativo do CHIKV.



Adaptado de (ABDELNABI; NEYTS; DELANG, 2015).

Análises filogenéticas identificaram que a partir de uma linhagem comum se originou duas linhagens distintas, sendo uma do Oeste Africano (WA) e outra do Leste/Centro/Sul da África (ECSA) (CUNHA et al., 2017; VOLK et al., 2010). A ocorrência de um surto causado pela linhagem ECSA cerca de 70 a 150 anos atrás na Ásia levou a uma diferenciação para uma nova linhagem conhecida como Asiática (BURT et al., 2017; CUNHA et al., 2017; VOLK et al., 2010)(Figura 5).

Figura 5: Linhagens de CHIKV e espécies de *Aedes* sp no mundo. Distribuição das linhagens de CHIKV em cada país, relacionado à presença das espécies de mosquitos *Aedes aegypti* e *Aedes albopictus*.



Adaptado de (JOHANSSON,2015).

Transmissão

O CHIKV é transmitido através da picada do mosquito fêmea de *Aedes* sp(VU; JUNGKIND; LABEAUD, 2017).As espécies que mais se destacam na transmissão são o *A.aegypti* e *A. albopictus*, ambas distribuídas amplamente em zonas tropicais e subtropicais, destacando a capacidade de adaptação do *A.albopictus* a áreas mais frias (KRAEMER et al., 2015b). O *A. aegypti* e concentra em áreas mais quentes como as regiões norte, nordeste e centro-oeste do Brasil (CARVALHO; LOURENÇO-DE-OLIVEIRA; BRAGA, 2014; KRAEMER et al., 2015a)(Figura 5).

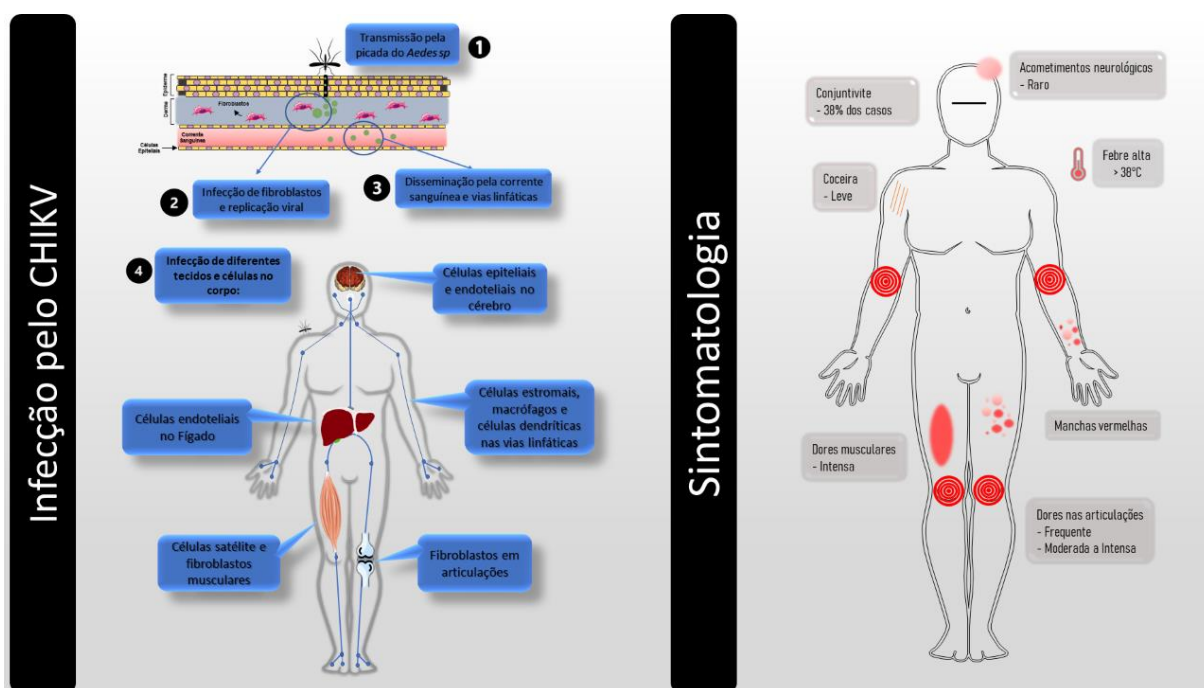
Patogênese e implicações na saúde

A febre de Chikungunya apresenta sintomas como febre, prostração, dores musculares, linfopenia e a artralgia, o principal sintoma relacionado a esta doença (CUNHA et al., 2017; PAIXÃO et al., 2018). A dor associada à artralgia nas falanges, pulsos e tornozelos é recorrente em até 98% dos casos (THIBERVILLE et al., 2013).A infecção pode progredir para uma fase crônica em até 70% dos pacientes infectados (DE ANDRADE et al., 2010;

SIMON et al., 2011), causando dores musculares e artralgias persistentes por períodos que variam de meses a anos (MATHEW et al., 2017)(Figura 6).

Através da picada da fêmea do mosquito *Aedes* sp, o vírus é disseminado para as células epiteliais, se multiplicando em fibroblastos e macrófagos (HER et al., 2010). Através da corrente sanguínea, o CHIKV atinge articulações e tecidos musculares, havendo relatos de infecção de células do fígado e cérebro (HOARAU et al., 2010). Durante a infecção aguda, há uma extensiva multiplicação do CHIKV em macrófagos nos tecidos, levando a uma resposta inflamatória. Há ativação da resposta imunidade inata, estando relacionada com elevado nível de citocinas pro-inflamatórias, tais como interferon e interleucinas. Devido à alta multiplicação do vírus nas articulações e sua consequente resposta inflamatória, surge a artralgia, um dos sintomas mais marcantes da febre Chikungunya (CASTRO; LIMA; NASCIMENTO, 2016; HER et al., 2010; HOARAU et al., 2010; RODRÍGUEZ-MORALES et al., 2016)(Figura 6).

Figura 6: Esquema demonstrativo da infecção pelo CHIKV e sintomas consequentes da infecção.



Adaptado de (BRASIL, 2020)e(SCHWARTZ; ALBERT, 2010).

Estudos demonstram que aproximadamente 43% dos pacientes diagnosticados com CHIKV desenvolvem a infecção crônica 3 meses após a infecção, e 21% após 1 ano. Nesses casos, o movimento das articulações fica limitado devido às fortes dores na região estão observados altos níveis de interleucinas nos pacientes (HOARAU et al., 2010; PAIXÃO et al., 2018).

Tratamento

Atualmente, não existe vacina (ROUGERON et al., 2015) ou terapia específica contra a infecção pelo CHIKV (DEY et al., 2019; YANG et al., 2017). O tratamento de infecções sintomáticas é paliativo, baseado no uso de analgésicos não salicilatos e anti-inflamatórios não esteroides para amenizar os sintomas provocados pela infecção (MATHEW et al., 2017; PARASHAR; CHERIAN, 2014).

O desenvolvimento de antivirais contra o CHIKV é de extrema importância devido à habilidade que os vetores possuem em instalar a infecção em várias regiões, podendo gerar epidemias, e pela falta de vacinas e terapêuticas eficazes para tratar os indivíduos infectados (KAUR; CHU, 2013).

Compostos com potencial terapêutico

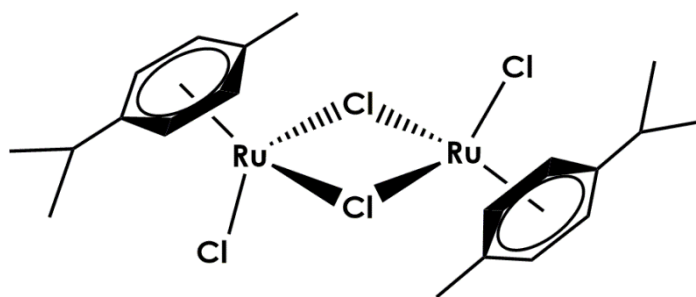
Os produtos naturais sempre tiveram importante papel na produção de fármacos, dada a diversidade de substâncias químicas com estruturas variadas, permitindo a sobrevivência de diversas populações ao clima e às doenças (VIEGAS; DA SILVA BOLZANI; BARREIRO, 2006). Muitos dos medicamentos utilizados atualmente para diversas patologias são de origem natural, ou foram desenvolvidos com base em modelos isolados da natureza (DA SILVA-JÚNIOR et al., 2017; TEIXEIRA et al., 2014).

O *para-cimeno* (*p*-cimeno) é um hidrocarboneto aromático orgânico natural, proveniente da classe dos monoterpenos (FAVRE; POWELL, 2013), que demonstrou possuir propriedades biológicas como antioxidante natural (DE OLIVEIRA et al., 2015), anti-inflamatória (Kummer et al., 2015), antifúngica (KORDALI et al., 2008) e antiviral (ASTANI; REICHLING; SCHNITZLER, 2009).

O rutênio é um metal pertencente ao grupo do ferro que demonstra possuir atividades biológicas efetivas, como antimicrobianas, quando complexado a outras moléculas (PAVAN et al., 2010).

O *p*-cimeno é um ligante comum para o rutênio (BENNETT et al., 2007) e esse complexo denominado complexo de rutênio e *para*-cimeno(**Figura 7**) já demonstrou possuir atividades antitumorais (CLARKE; ZHU; FRASCA, 1999; DOUGAN; SADLER, 2007; DYSON, 2007; HABTEMARIAM et al., 2006; SAVIĆ et al., 2020; VAJS et al., 2015).

Figura 7: Estrutura do complexo de rutênio e *para*-cimeno.



(JENSEN; RODGER; SPICER, 1998)

As moléculas orgânicas que podem ser complexadas com metais podem ter sua biodisponibilidade aumentada no organismo. Portanto, se apresentam como uma abordagem alternativa para o desenvolvimento de novas terapias, uma vez que estes se apresentam de forma vantajosa para a produção em escala comercial de um possível tratamento contra o CHIKV.

OBJETIVOS

Objetivo geral

O presente trabalho teve como objetivo avaliar o potencial antiviral do *para*-cimeno complexado ao rutênio (RcP) e seus precursores no ciclo replicativo do CHIKV *in vitro*.

Objetivos específicos

- Avaliar a citotoxicidade do RcP e seus precursores na linhagem de células BHK 21, por meio de ensaios de viabilidade celular (MTT), e estabelecer a concentração viável para tratamento das células;
- Produzir CHIKV *in vitro* para infecção de células BHK 21, na presença ou na ausência dos compostos em concentrações específicas, e avaliar a atividade antiviral do RcP e seus precursores;
- Determinar a concentração efetiva de inibição em 50% (EC₅₀), concentração citotóxica em 50% (CC₅₀) e Índice de Seletividade (IS = CC₅₀/EC₅₀) de cada composto ativo, avaliando assim os valores ótimos de concentração para o tratamento celular e o potencial antiviral de cada composto;
- Analisar as etapas do ciclo replicativo do CHIKV inibidas pelo tratamento com os compostos ativos;
- Investigar *in silico* as interações dos compostos ativos com proteínas do CHIKV por meio de docking molecular;
- Analisar por espectroscopia de infravermelho (FTIR) as interações químicas dos compostos ativos com o CHIKV.

REFERÊNCIAS

- ABDELNABI, R.; NEYTS, J.; DELANG, L. Towards antivirals against chikungunya virus. **Antiviral Research**, v. 121, n. June, p. 59–68, 2015. <https://doi.org/10.1016/j.antiviral.2015.06.017>
- ASTANI, A.; REICHLING, J.; SCHNITZLER, P. Comparative study on the antiviral activity of selected monoterpenes derived from essential oils. **Phytotherapy Research**, v. 23, n. 9, p. n/a-n/a, 2009. <https://doi.org/10.1002/ptr.2955>
- BENNETT, M. A. et al. 16. (η^6 -Hexamethylbenzene)Ruthenium Complexes. In: [s.l: s.n.]. p. 74–78. <https://doi.org/10.1002/9780470132524.ch16>
- BRASIL, M. DA S. **Chikungunya: causas, sintomas, tratamento e prevenção**. Disponível em: <<http://saude.gov.br/saude-de-a-z/chikungunya>>. Acesso em: 30 jan. 2020.
- BURT, F. J. et al. Chikungunya virus: an update on the biology and pathogenesis of this emerging pathogen. **The Lancet Infectious Diseases**, v. 17, n. 4, p. e107–e117, 2017. [https://doi.org/10.1016/S1473-3099\(16\)30385-1](https://doi.org/10.1016/S1473-3099(16)30385-1)
- CARRAVILLA, P. et al. Effects of HIV-1 gp41-Derived Virucidal Peptides on Virus-like Lipid Membranes. **Biophysical Journal**, v. 113, n. 6, p. 1301–1310, 2017. <https://doi.org/10.1016/j.bpj.2017.06.061>
- CARVALHO, R. G.; LOURENÇO-DE-OLIVEIRA, R.; BRAGA, I. A. Updating the geographical distribution and frequency of *Aedes albopictus* in Brazil with remarks regarding its range in the Americas. **Memórias do Instituto Oswaldo Cruz**, v. 109, n. 6, p. 787–796, 2014.
- CASTRO, A. P. C. R. DE; LIMA, R. A.; NASCIMENTO, J. DOS S. Chikungunya: vision of the pain clinician. **Revista Dor**, v. 17, n. 4, p. 299–302, 2016. <https://doi.org/10.5935/1806-0013.20160093>
- CENTERS FOR DISEASE CONTROL AND PREVENTION (CDC). Countries and territories where chikungunya cases have been reported. **Cdc**, p. 1, 2018.
- CLARKE, M. J.; ZHU, F.; FRASCA, D. R. Non-platinum chemotherapeutic metallopharmaceuticals. **Chemical Reviews**, v. 99, n. 9, p. 2511–2533, 1999. <https://doi.org/10.1021/cr9804238>
- CUNHA, R. V. DA; TRINTA, K. S. Chikungunya virus: clinical aspects and treatment - A Review. **Memórias do Instituto Oswaldo Cruz**, v. 112, n. 8, p. 523–531, 2017. <https://doi.org/10.1590/0074-02760170044>

CUNHA, M. S. et al. Autochthonous Transmission of East/Central/South African Genotype Chikungunya Virus, Brazil. **Emerging Infectious Diseases**, v. 23, n. 10, p. 2015–2017, 2017. <https://doi.org/10.3201/eid2310.161855>

DA SILVA-JÚNIOR, E. F. et al. The medicinal chemistry of Chikungunya virus. **Bioorganic & Medicinal Chemistry**, v. 25, n. 16, p. 4219–4244, 2017. <https://doi.org/10.1016/j.bmc.2017.06.049>

DE ANDRADE, D. C. et al. Chronic pain associated with the Chikungunya Fever: long lasting burden of an acute illness. **BMC Infectious Diseases**, v. 10, n. 1, p. 31, 2010. <https://doi.org/10.1186/1471-2334-10-31>

DE OLIVEIRA, T. M. et al. Evaluation of p-cymene, a natural antioxidant. **Pharmaceutical Biology**, v. 53, n. 3, p. 423–428, 2015. <https://doi.org/10.3109/13880209.2014.923003>

DEY, D. et al. The effect of amantadine on an ion channel protein from Chikungunya virus. **PLOS Neglected Tropical Diseases**, v. 13, n. 7, p. e0007548, 2019. <https://doi.org/10.1371/journal.pntd.0007548>

DO SOCORRO SOUZA, T. et al. Travelers as sentinels for chikungunya fever, Brazil. **Emerging Infectious Diseases**, v. 18, n. 3, p. 529–530, 2012. <https://doi.org/10.3201/eid1803.110838>

DOUGAN, S. J.; SADLER, P. J. The design of organometallic ruthenium arene anticancer agents. **Chimia**, v. 61, n. 11, p. 704–715, 2007. <https://doi.org/10.2533/chimia.2007.704>

DYSON, P. J. Systematic design of a targeted organometallic antitumour drug in pre-clinical development. **Chimia**, v. 61, n. 11, p. 698–703, 2007.

EPIDEMIOLOGICO, B. et al. N° 59 | Dez. v. 49, 2018.

EPIDEMIOLOGICO, B. **Sumário Coordenação-Geral de Vigilância das Arboviroses (CGARB/DEIDT/SVS)***. [s.l.: s.n.].

FAVRE, H. A.; POWELL, W. H. **Nomenclature of Organic Chemistry**. [s.l.] Royal Society of Chemistry, 2013.

FONGSARAN, C. et al. Involvement of ATP synthase β subunit in chikungunya virus entry into insect cells. **Archives of Virology**, v. 159, n. 12, p. 3353–3364, 2014. <https://doi.org/10.1007/s00705-014-2210-4>

GAROZZO, A. et al. In vitro antiviral activity of Melaleuca alternifolia essential oil. **Letters in Applied Microbiology**, v. 49, n. 6, p. 806–808, dez. 2009. <https://doi.org/10.1111/j.1472-765X.2009.02740.x>

GOULD, E. et al. Emerging arboviruses: Why today? **One Health**, v. 4, n. April, p. 1–13,

2017. <https://doi.org/10.1016/j.onehlt.2017.06.001>

GRANDADAM, M. et al. Chikungunya virus, Southeastern France. **Emerging Infectious Diseases**, v. 17, n. 5, p. 910–913, 2011. <https://doi.org/10.3201/eid1705.101873>

HABTEMARIAM, A. et al. Structure-activity relationships for cytotoxic ruthenium(II) arene complexes containing N,N-, N,O-, and O,O-chelating ligands. **Journal of Medicinal Chemistry**, v. 49, n. 23, p. 6858–6868, 2006.

HER, Z. et al. Active Infection of Human Blood Monocytes by Chikungunya Virus Triggers an Innate Immune Response. **The Journal of Immunology**, v. 184, n. 10, p. 5903–5913, 15 maio 2010. <https://doi.org/10.4049/jimmunol.0904181>

HOARAU, J.-J. et al. Persistent Chronic Inflammation and Infection by Chikungunya Arthritogenic Alphavirus in Spite of a Robust Host Immune Response. **The Journal of Immunology**, v. 184, n. 10, p. 5914–5927, 15 maio 2010. <https://doi.org/10.4049/jimmunol.0900255>

JENSEN, S. B.; RODGER, S. J.; SPICER, M. D. Facile preparation of η^6 -p-cymene ruthenium diphosphine complexes. Crystal structure of $[(\eta^6\text{-p-cymene})\text{Ru}(\text{dppf})\text{Cl}]\text{PF}_6$ **Journal of Organometallic Chemistry**, 1998. [https://doi.org/10.1016/S0022-328X\(97\)00776-6](https://doi.org/10.1016/S0022-328X(97)00776-6)

KAUR, P.; CHU, J. J. H. Chikungunya virus: An update on antiviral development and challenges. **Drug Discovery Today**, v. 18, n. 19–20, p. 969–983, 2013. <https://doi.org/10.1016/j.drudis.2013.05.002>

KHAN, A. H. et al. Complete nucleotide sequence of chikungunya virus and evidence for an internal polyadenylation site. **The Journal of general virology**, v. 83, n. Pt 12, p. 3075–84, dez. 2002. <https://doi.org/10.1099/0022-1317-83-12-3075>

KONG, B. et al. Virucidal nano-perforator of viral membrane trapping viral RNAs in the endosome. **Nature Communications**, v. 10, n. 1, p. 1–10, 2019. <https://doi.org/10.1038/s41467-018-08138-1>

KORDALI, S. et al. Antifungal, phytotoxic and insecticidal properties of essential oil isolated from Turkish *Origanum acutidens* and its three components, carvacrol, thymol and p-cymene. **Bioresource Technology**, v. 99, n. 18, p. 8788–8795, 2008. <https://doi.org/10.1016/j.biortech.2008.04.048>

KRAEMER, M. U. G. et al. The global distribution of the arbovirus vectors *Aedes aegypti* and *Ae. Albopictus*. **eLife**, v. 4, n. JUNE2015, p. 1–18, 2015a.

KRAEMER, M. U. G. et al. The global distribution of the arbovirus vectors *Aedes aegypti*

and *Ae. albopictus*. **eLife**, v. 4, n. JUNE2015, jun. 2015b.

KUMMER, R. et al. Effect of p-cymene on chemotaxis, phagocytosis and leukocyte behaviors. **International Journal of Applied Research in Natural Products**, v. 8, n. 2, p. 20–27, 2015.

LUM, F. M.; NG, L. F. P. Cellular and molecular mechanisms of chikungunya pathogenesis. **Antiviral Research**, v. 120, p. 165–174, 2015. <https://doi.org/10.1016/j.antiviral.2015.06.009>

MATHEW, A. J. et al. Chikungunya Infection : a Global Public Health Menace. p. 1–9, 2017. <https://doi.org/10.1007/s11882-017-0680-7>

MATKOVIC, R. et al. The Host DHX9 DExH-Box Helicase Is Recruited to Chikungunya Virus Replication Complexes for Optimal Genomic RNA Translation. **Journal of Virology**, v. 93, n. 4, p. 1–17, 2018. <https://doi.org/10.1128/JVI.01764-18>

MOLLER-TANK, S. et al. Role of the Phosphatidylserine Receptor TIM-1 in Enveloped-Virus Entry. **Journal of Virology**, v. 87, n. 15, p. 8327–8341, 2013a. <https://doi.org/10.1128/JVI.01025-13>

MOLLER-TANK, S. et al. Role of the Phosphatidylserine Receptor TIM-1 in Enveloped-Virus Entry. v. 87, n. 15, p. 8327–8341, 2013b. <https://doi.org/10.1128/JVI.01025-13>

NJENGA, M. K. et al. Tracking epidemic Chikungunya virus into the Indian Ocean from East Africa. **Journal of General Virology**, v. 89, n. 11, p. 2754–2760, nov. 2008. <https://doi.org/10.1099/vir.0.2008/005413-0>

PAIXÃO, E. S. et al. Chikungunya chronic disease: A systematic review and meta-analysis. **Transactions of the Royal Society of Tropical Medicine and Hygiene**, v. 112, n. 7, p. 301–316, 2018. <https://doi.org/10.1093/trstmh/try063>

PARASHAR, D.; CHERIAN, S. Antiviral perspectives for chikungunya virus. **BioMed Research International**, v. 2014, 2014. <https://doi.org/10.1155/2014/631642>

PAVAN, F. R. et al. Ruthenium (II) phosphine/picolinate complexes as antimycobacterial agents. **European Journal of Medicinal Chemistry**, v. 45, n. 2, p. 598–601, 2010. <https://doi.org/10.1016/j.ejmech.2009.10.049>

POHJALA, L. et al. Inhibitors of alphavirus entry and replication identified with a stable Chikungunya replicon cell line and virus-based assays. **PLoS ONE**, v. 6, n. 12, 2011. <https://doi.org/10.1371/journal.pone.0028923>

RASHAD, A. A.; KELLER, P. A. Structure based design towards the identification of novel binding sites and inhibitors for the chikungunya virus envelope proteins. **Journal of Molecular Graphics and Modelling**, v. 44, p. 241–252, 2013.

<https://doi.org/10.1016/j.jmngm.2013.07.001>

RASHAD, A. A.; MAHALINGAM, S.; KELLER, P. A. Chikungunya virus: Emerging targets and new opportunities for medicinal chemistry. **Journal of Medicinal Chemistry**, v. 57, n. 4, p. 1147–1166, 2014. <https://doi.org/10.1021/jm400460d>

REZZA, G. et al. Infection with chikungunya virus in Italy: an outbreak in a temperate region. **Lancet**, v. 370, n. 9602, p. 1840–1846, 2007. [https://doi.org/10.1016/0035-9203\(55\)90080-8](https://doi.org/10.1016/0035-9203(55)90080-8)

ROBINSON, M. C. An epidemic of virus disease in Southern Province, Tanganyika Territory, in 1952-53. I. Clinical features. **Transactions of the Royal Society of Tropical Medicine and Hygiene**, v. 49, n. 1, p. 28–32, jan. 1955.

RODRÍGUEZ-MORALES, A. J. et al. Prevalence of Post-Chikungunya Infection Chronic Inflammatory Arthritis: A Systematic Review and Meta-Analysis. **Arthritis Care and Research**, 2016. <https://doi.org/10.1002/acr.22900>

ROUGERON, V. et al. Chikungunya, a paradigm of neglected tropical disease that emerged to be a new health global risk. **Journal of Clinical Virology**, v. 64, p. 144–152, mar. 2015. <https://doi.org/10.1016/j.jcv.2014.08.032>

RUSSO, R. R. et al. Expression, purification and virucidal activity of two recombinant isoforms of phospholipase A2 from *Crotalus durissus terrificus* venom. **Archives of Virology**, v. 164, n. 4, p. 1159–1171, 26 abr. 2019. <https://doi.org/10.1007/s00705-019-04172-6>

SAVIĆ, A. et al. Antitumor activity of organoruthenium complexes with chelate aromatic ligands, derived from 1,10-phenantroline: Synthesis and biological activity. **Journal of Inorganic Biochemistry**, v. 202, n. September 2019, p. 110869, 2020. <https://doi.org/10.1016/j.jinorgbio.2019.110869>

SCHUFFENECKER, I. et al. Genome Microevolution of Chikungunya Viruses Causing the Indian Ocean Outbreak. **PLoS Medicine**, v. 3, n. 7, p. 1058–1070, 2006.

SCHUHMACHER, A.; REICHLING, J.; SCHNITZLER, P. Virucidal effect of peppermint oil on the enveloped viruses herpes simplex virus type 1 and type 2 in vitro. **Phytomedicine**, v. 10, n. 6–7, p. 504–510, jan. 2003. <https://doi.org/10.1078/094471103322331467>

SCHWARTZ, O.; ALBERT, M. L. Biology and pathogenesis of chikungunya virus. **Nature Reviews Microbiology**, v. 8, n. 7, p. 491–500, 2010. <https://doi.org/10.1038/nrmicro2368>

SHARIFI-RAD, J. et al. Susceptibility of herpes simplex virus type 1 to monoterpenes thymol, carvacrol, p-cymene and essential oils of *Sinapis arvensis* L., *Lallemantia royleana* Benth. and *Pulicaria vulgaris* Gaertn. **Cellular and molecular biology (Noisy-le-Grand,**

France), v. 63, n. 8, p. 42–47, 30 ago. 2017. <https://doi.org/10.14715/cmb/2017.63.8.10>

SILVA, N. M. DA et al. Vigilância de chikungunya no Brasil: desafios no contexto da Saúde Pública. **Epidemiologia e serviços de saúde : revista do Sistema Unico de Saude do Brasil**, v. 27, n. 3, p. e2017127, 2018. <https://doi.org/10.5123/S1679-49742018000300003>

SILVA, L. A. et al. A Single-Amino-Acid Polymorphism in Chikungunya Virus E2 Glycoprotein Influences Glycosaminoglycan Utilization. **Journal of Virology**, v. 88, n. 5, p. 2385–2397, 2014. <https://doi.org/10.1128/JVI.03116-13>

SIMON, F. et al. Chikungunya virus infection. **Current Infectious Disease Reports**, v. 13, n. 3, p. 218–228, 2011. <https://doi.org/10.1007/s11908-011-0180-1>

SOLIGNAT, M. et al. Replication cycle of chikungunya: A re-emerging arbovirus. **Virology**, v. 393, n. 2, p. 183–197, 2009. <https://doi.org/10.1016/j.virol.2009.07.024>

STEGMANN-PLANCHARD, S. et al. Chikungunya, a Risk Factor for Guillain-Barré Syndrome. **Clinical Infectious Diseases**, v. 66, p. 37–39, 9 jul. 2019. <https://doi.org/10.1093/cid/ciz625>

STRAUSS, J. H.; STRAUSS, E. G. **The alphaviruses: Gene expression, replication, and evolution** *Microbiological Reviews*, set. 1994. <https://doi.org/10.1128/MMBR.58.3.491-562.1994>

TANG, J. et al. Virucidal activity of hypericin against enveloped and non-enveloped DNA and RNA viruses. **Antiviral Research**, v. 13, n. 6, p. 313–325, jun. 1990. [https://doi.org/10.1016/0166-3542\(90\)90015-Y](https://doi.org/10.1016/0166-3542(90)90015-Y)

TEIXEIRA, R. R. et al. Natural Products as Source of Potential Dengue Antivirals. **Molecules**, v. 19, p. 8151–8176, 2014. <https://doi.org/10.3390/molecules19068151>

THIBERVILLE, S. D. et al. Chikungunya fever: Epidemiology, clinical syndrome, pathogenesis and therapy. **Antiviral Research**, v. 99, n. 3, p. 345–370, 2013. <https://doi.org/10.1016/j.antiviral.2013.06.009>

UCHIME, O.; FIELDS, W.; KIELIAN, M. The role of E3 in pH protection during alphavirus assembly and exit. **Journal of virology**, v. 87, n. 18, p. 10255–62, 2013. <https://doi.org/10.1128/JVI.01507-13>

VAJS, J. et al. The 1,3-diaryltriazenido(p-cymene)ruthenium(II) complexes with a high in vitro anticancer activity. **Journal of Inorganic Biochemistry**, v. 153, p. 42–48, 2015. <https://doi.org/10.1016/j.jinorgbio.2015.09.005>

VIEGAS, C.; DA SILVA BOLZANI, V.; BARREIRO, E. J. OS produtos naturais e a química medicinal moderna. **Química Nova**, v. 29, n. 2, p. 326–337, 2006.

<https://doi.org/10.1590/S0100-40422006000200025>

VOLK, S. M. et al. Genome-Scale Phylogenetic Analyses of Chikungunya Virus Reveal Independent Emergences of Recent Epidemics and Various Evolutionary Rates. **Journal of Virology**, v. 84, n. 13, p. 6497–6504, 2010. <https://doi.org/10.1128/JVI.01603-09>

VU, D. M.; JUNGKIND, D.; LABEAUD, A. D. Chikungunya Virus. **Clinics in Laboratory Medicine**, v. 37, n. 2, p. 371–382, 2017. <https://doi.org/10.1016/j.cll.2017.01.008>

WINTACHAI, P. et al. Identification of Prohibitin as a Chikungunya Virus Receptor Protein. **Journal of Medical Virology**, v. 84, p. 1757–1770, 2012. <https://doi.org/10.1002/jmv.23403>

YANG, S. et al. Regulatory considerations in development of vaccines to prevent disease caused by Chikungunya virus q. **Vaccine**, v. 35, n. 37, p. 4851–4858, 2017. <https://doi.org/10.1016/j.vaccine.2017.07.065>

CAPÍTULO II

Manuscript

**Ruthenium and *para*-cymene complex inhibits
Chikungunya virus *in vitro***

*Este capítulo está em formato de manuscrito com algumas alterações estruturais para melhor se adequar ao formato da dissertação. O artigo em questão será submetido à revista *Antiviral Research*.

Ruthenium and *para*-cymene complex inhibits Chikungunya virus *in vitro*

Débora Moraes de Oliveira^a, Igor de Andrade Santos^a, Daniel Oliveira Silva Martins^{a,b}, Yasmin Garcia Gonçalves^c, Léia Cardoso Sousa^d, Robinson Sabino da Silva^d, Andres Merits^e, Mark Harris^f, Gustavo Von Poelhsitz^c, Ana Carolina Gomes Jardim^{a,b}.

^aLaboratory of Virology, Institute of Biomedical Science, Federal University of Uberlândia, MG, Brazil

^bSão Paulo State University, IBILCE, São José do Rio Preto, SP, Brazil

^cInstitute of Chemistry, Federal University of Uberlândia, MG, Brazil

^dDepartment of Physiology, Institute of Biomedical Sciences, Federal University of Uberlândia, Minas Gerais, Brazil

^eInstitute of Technology, University of Tartu, Tartu, Estonia

^fSchool of Molecular and Cellular Biology, Faculty of Biological Sciences and Centre for Structural Molecular Biology, University of Leeds, Leeds, United Kingdom

Corresponding author: Professor Ana Carolina Gomes Jardim, Institute of Biomedical Science, ICBIM/UFU, Avenida Amazonas, 4C- Room 216, Umuarama, Uberlândia, Minas Gerais, Brazil, CEP: 38405-302

Tel: +55 (34) 3225-8682

E-mail: jardim@ufu.br

Abstract

Chikungunya fever is a disease caused by the Chikungunya virus (CHIKV) that is transmitted by the bite of the female of *Aedes* mosquito. The symptoms include fever, muscle aches, skin rash and severe joint pains. The disease may develop into a chronic condition and joint pain that may last for months or years. Currently, there is no effective antiviral treatment against CHIKV infection, being necessary the development of novel therapies. Treatments based on natural compounds have been widely studied, as many drugs were produced by using natural molecules and their derivatives. *Para*-cymene (pCYM) is a naturally occurring aromatic organic compound that is a common ligand for ruthenium, forming the organometallic ruthenium and pCYM complex. Organometallic complexes have shown promising as a new generation of compounds that presented relevant biological properties, however, there is a lack of knowledge concerning the anti-CHIKV activity of these complexes. In this context, the present work evaluated the effects of the ruthenium and pCYM complex ($[\text{Ru}_2\text{Cl}_4(\eta^6\text{-p-cymene})_2]$) (RcP) and its precursors on CHIKV infection *in vitro*. To this, BHK21 cells were infected with CHIKV-*nanoluciferase* (CHIKV-*nanoluc*), a viral construct with the reporter gene -*nanoluc*, at the presence or absence of the compounds for 16 hours, and cytotoxicity (MTT) and infectivity (Luciferase) rates were accessed. The results demonstrated that RcP exhibited a strong therapeutic index judged by the selective index of 43.1 (ratio of cytotoxicity to antiviral potency). Antiviral effects of RcP on different stages of the CHIKV replicative cycle were investigated and the results showed that it reduced 77% of virus entry to the host cells at non-toxic concentrations. Further assays demonstrated the virucidal activity of the compound that completely knocked down virus infectivity. Molecular docking calculations were performed in order to investigate possible interactions between pCYM and CHIKV glycoproteins and results suggested bindings between pCYM and a site located behind the fusion loop between glycoproteins E3 and E2. Additionally, infrared spectroscopy spectral analysis indicated interactions of RcP with CHIKV glycoproteins. This data suggests that RcP may act on CHIKV viral particles, disrupting virus entry to the host cells. Additional analyses are being performed to evaluate the mode of action of this complex.

Keywords: Chikungunya virus; antiviral; arene complex; ruthenium and *para*-cymene complex; organometallic complexes.

1. Introduction

The Chikungunya virus (CHIKV) belongs to the genus Alphavirus of the family *Togaviridae* (ICTV, 2019). This virus is the causative agent of Chikungunya fever being related to epidemics mainly in tropical and subtropical regions (KHAN et al., 2002; PAIXÃO et al., 2018; STEGMANN-PLANCHARD et al., 2019).

CHIKV is a positive single strand RNA virus with a genome of approximately 12 kb (SCHUFFENECKER et al., 2006). The icosahedral capsid is covered by a lipid envelope derived from the host cell plasma membrane where the viral glycoproteins E1 and E2 are inserted into (KHAN et al., 2002; SCHUFFENECKER et al., 2006; THIBERVILLE et al., 2013).

CHIKV is transmitted through the bite of the female mosquito of *Aedes* sp (VU; JUNGKIND; LABEAUD, 2017). It was first isolated during an epidemic in Tanzania in 1953 (Robinson, 1955; Wintachai et al., 2012). In 2006, CHIKV outbreaks were reported on several Indian Ocean islands and about 250 people died from the disease on the French island of *La Réunion* (SCHUFFENECKER et al., 2006). In 2013, the virus was detected in the Americas with reported cases in the Caribbean islands (KAUR; CHU, 2013). The first case in Brazil was reported in 2014 (CARVALHO; LOURENÇO-DE-OLIVEIRA; BRAGA, 2014).

Chikungunya fever presents symptoms as fever, prostration, muscle aches, lymphopenia and arthralgia, being the latest the main symptom related to this disease (CUNHA et al., 2017; PAIXÃO et al., 2018). Pain associated to arthralgia in the phalanges, wrists and ankles occurs in up to 98% of cases (THIBERVILLE et al., 2013). The infection can progress to a chronic infection in around 70 % of infected patients (DE ANDRADE et al., 2010; SIMON et al., 2011), causing muscle pain and persistent arthralgia for periods ranging from months to years (MATHEW et al., 2017).

Currently, there is no vaccine or specific therapy against CHIKV infection (DEY et al., 2019; YANG et al., 2017). The treatment of symptomatic infections is palliative, based on the use of non-salicylate analgesics and non-steroidal anti-inflammatory drugs (MATHEW et al., 2017; PARASHAR; CHERIAN, 2014). Several of the currently used drugs for different pathologies are either from natural origin synthesized based on natural scaffolds (DA SILVA-JÚNIOR et al., 2017; TEIXEIRA et al., 2014).

Para-cymene (pCYM) is a naturally occurring organic aromatic hydrocarbon from the monoterpene class that has shown to possess important biological activities as antioxidant (DE OLIVEIRA et al., 2015), anti-inflammatory (Kummer et al., 2015), antifungal (KORDALI et al., 2008) and antiviral (ASTANI; REICHLING; SCHNITZLER, 2009). Ruthenium is a metal belonging to the iron group and studies have shown that the ruthenium complexed molecules possess effective biological properties as antimicrobial (PAVAN et al., 2010) (PAVAN et al., 2010). pCYM is a common binder for ruthenium (BENNETT et al., 2007) and the antitumoral activity of this complex has also been described (CLARKE; ZHU; FRASCA, 1999; DOUGAN; SADLER, 2007; DYSON, 2007; HABTEMARIAM et al., 2006; SAVIĆ et al., 2020; VAJS et al., 2015).

Here we evaluated the activity of ruthenium and pCYM complex (RcP) and its precursors on the CHIKV replicative cycle. These data are the first description of the ruthenium and pCYM complex possessing anti-CHIKV activity.

2. Material and methods

2.1. Compounds

The ruthenium and *para*-cymene complex ($[\text{Ru}_2\text{Cl}_4(\eta^6\text{-p-cymene})_2]$) (RcP) (Figure 1A) evaluated in this work was synthesized as previously described (JENSEN; RODGER; SPICER, 1998). The precursors ruthenium trichloride ($\text{RuCl}_3 \cdot 3\text{H}_2\text{O}$) and *para*-cymene (α -phellandrene), used in the synthesis of complex were purchased by Sigma Aldrich. The complex was dissolved in dimethyl sulfoxide (DMSO) and stored at -20°C . Dilutions of the compounds in complete media were made immediately prior to the experiments. For all the assays performed, control cells were treated with media added of DMSO at the final concentration of 0.3%.

2.2. Cell culture

BHK 21 cells were maintained in Dulbecco's modified Eagle's media (DMEM; Sigma-Aldrich) supplemented with 100 U/mL of penicillin (Hyclone Laboratories, USA), 100 mg/mL of streptomycin (Hyclone Laboratories, USA), 1% of non-essential amino acids (Hyclone 28 Laboratories, USA) and 1% of fetal bovine serum (FBS, Hyclone Laboratoires, USA) in a humidified 5% CO_2 incubator at 37°C .

2.3. Virus

The CHIKV-*nanoluciferase* (CHIKV-*nanoluc*) construct (**Figure 1A**) used for the antiviral assays was designed from a CHIKV sequence based on CHIKV LR (*Lá reunion*) added of CMV promoter and *nanoluciferase* protein sequence (MATKOVIC et al., 2018; POHJALA et al., 2011). For virus production, 2.3×10^7 BHK 21 cells seeded in a T175 cm² were transfected with 1.5 µg of CHIKV-CMV-*nanoluc* plasmid, using lipofectamine 3000® and Opti-Mem media to produce CHIKV-*nanoluc* virus particles. Forty-eight hours post transfection the supernatant was collected and stored at -80°C. To determine viral titer, 5×10^5 BHK 21 cells were seeded in each of 6 wells plate 24 hours prior to the infection. Then, the cells were infected with 10-fold serially diluted of CHIKV-*nanoluc* for 1 hour at 37°C. The inoculums were removed and the cells were washed with PBS to remove the unbound virus and added of cell culture media supplemented with 1% penicillin, 1% streptomycin, 2% FBS and 1% carboxymethyl cellulose (CMC). Infected cells were incubated for 2 days in a humidified 5% CO₂ incubator at 37°C, followed by fixation with 4% formaldehyde and stained with 0.5% violet crystal. The viral foci were counted to determine CHIKV-*nanoluc* titer.

2.4. Cell viability through MTT assay

Cell viability was measured by MTT [3-(4,5-dimethylthiazol-2-yl)-2,5-diphenyl tetrazolium bromide] (Sigma-Aldrich) assay. For viability assay, 5×10^4 BHK 21 cells were cultured in 48 well plates and treated with different concentrations of each compound for 16h at 37°C with 5% of CO₂. Sixteen hours post treatment, compound-containing media was removed and MTT solution at 1 mg/mL was added to each well, incubated for 1 hour and replaced with 100 µL of DMSO (dimethyl sulfoxide) to solubilize the formazan crystals. The absorbance was measured at 560 nm on Glomax microplate reader (Promega). Cell viability was calculated according to the equation $(T/C) \times 100\%$, which T and C represented the optical density of the treated well and control groups, respectively. DMSO was used as untreated control. The cytotoxic concentration of 50% (CC50) was calculated using Prism (Graph Pad).

2.5. Antiviral assays

To access the antiviral activity of compounds, BHK 21 cells were seeded at density of 5×10^4 cells per well into 48 well plates 24 hours prior to the infection. CHIKV-*nanoluc* (MATKOVIC et al., 2018) at a multiplicity of infection (MOI) of 0.1 and compounds were simultaneously added to cells. Samples were harvested in Renilla luciferase lysis buffer (Promega) at 16 hours post-infection (h.p.i.) and virus replication levels were quantified by measuring *nanoluciferase* activity using the Renilla luciferase Assay System (Promega). The effective concentration of 50% inhibition (EC50) was calculated using Prism (Graph Pad). The values of CC50 and EC50 were used to calculate the selectivity index ($SI = CC50/EC50$). To investigate in which step of CHIKV replicative cycle the compound was active, BHK 21 cells at the density of 5×10^4 were seeded in 48 well plate 24 hours prior to infection and treatment. To evaluate if the compound possesses protective activity to the host cells, cells were treated for 1 hour with the compound before infection, extensively washed to remove compound and added CHIKV-*nanoluc*. The effect on the entry steps was analyzed by incubating virus and compound simultaneously with BHK 21 cells for 1 hour. To investigate the activity of the compound on postentry stages of viral replicative cycle, cells were infected with CHIKV for 1 hour, washed extensively with PBS (phosphate buffered saline) to remove unbound virus and added with compound containing media. To further investigate entry stage, the virucidal activity was investigated by previously incubating virus and compound for 1 hour and then adding to the cells for extra 1 hour. Then, compound was removed and as cells added of media. To evaluate the attachment step, the cells were treated with virus and compound at for 1 hour at 4°C , and then the cells were washed to the complex removal and replaced by media. For the uncoating step, cell, virus and compound were also incubated for 1 hour at 4°C followed by 30 minutes at 37°C and then washed and replaced by media. All experiments were conducted with virus at MOI of 0.1. Luminescence levels were accessed 16h.p.i. to analyze the virus replication rates.

2.6. Docking Protein Binder

The interaction of the *para*-cymene ligand with the envelope glycoprotein of the CHIKV (PDB: 3N42) was evaluated using the GOLD program, using the parameters predefined by the program except the flexibility of the ligand, which was defined as 200%. The seven glycoprotein binding sites defined by (RASHAD; KELLER, 2013) were defined for this

purpose. Each docking was performed 10 times and the best docking positions were assessed using a ranking of the ChemPLP scoring function. The post-docking images were generated in the DS Visualizer program, Dassault Systèmes BIOVIA, Discovery Studio Visualizer, version 17, San Diego: Dassault Systèmes, 2016. The interaction between the ruthenium ligand and the complex was not evaluated due to the program not having parameters for loading metals.

2.7 Infrared spectroscopy Spectral data analysis

An ATR-FTIR spectrophotometer Vertex 70 (Bruker Optics, Reinstetten, Germany) connected to a micro-attenuated total reflectance (ATR) platform was used to record sample signature at 1800 cm^{-1} to 400 cm^{-1} regions. The ATR unit is composed by a diamond disc as internal-reflection element. The sample dehydrated pellicle penetration depth ranges between 0.1 and 2 μm and depends on the wavelength, incidence angle of the beam and the refractive index of ATR-crystal material. The infrared beam is reflected at the interface toward the sample in the ATR-crystal. All samples (1 μL) were dried using airflow on ATR-crystal for 3 min before sample spectra recorded in triplicate. The air spectrum was used as a background in all ATR-FTIR analysis. Sample spectra and background was taken with 4 cm^{-1} of resolution and 32 scans were performed for sample analysis. The spectra were normalized by the vector method and adjusted to rubber band baseline correction. The original data were plotted in the Origin Pro 9.0 (OriginLab, Northampton, MA, USA) software to create the second derivative analysis. The second derivative was obtained by applying Savitzky-Golay algorithm with polynomial order 5 and 20 points of the window. The value heights indicated the intensity of functional group evaluated.

2.8. Statistical analysis

Individual experiments were performed in triplicate and all assays were performed a minimum of three times in order to confirm the reproducibility of the results. Differences between means of readings were compared using analysis of variance (one way or two-way ANOVA) or Student's t-test using Graph Pad Prism 8.0 software (Graph Pad Software). P values \leq than 0.01 was considered to be statistically significant.

3. Results

3.1. Ruthenium (Ru) and *para*-cymene (pCYM) complex (RcP) inhibits CHIKV *in vitro*

The anti-CHIKV activity of the complex RcP (**Figure 1A**) and its precursors was evaluated by using a recombinant CHIKV that expresses the *nanoluciferase* reporter (CHIKV-*nanoluc*) (**Figure 1B**). To assess the effect of compounds on cell viability and virus infection, MTT and luminescence assays were performed. For this, the cells were infected with CHIKV-*nanoluc* and treated with the compounds at 125 μ M, a concentration previously determined as non-cytotoxic for RcP (data not shown). The efficiency of viral replication and cell viability were evaluated at 16 h.p.i. (**Figure 1C**). The results showed that RcP complex significantly inhibited 91% of CHIKV infectivity and presented no toxicity to cells (**Figure 1D**). Alternatively, pCYM and Ru at the same concentration decreased cell viability or had no effective antiviral activity, respectively (**Figure 1D**). This data demonstrated that RcP exhibited the best therapeutic index (favorable ratio of cytotoxicity to antiviral potency) and was selected for extra analysis.

We therefore performed a dose response assay to determine effective concentration 50% (EC_{50}) and cytotoxicity 50% (CC_{50}) values for RcP. BHK 21 cells were infected with CHIKV-*nanoluc* and treated with RcP at concentrations ranging from 500 to 3.9 μ M and viral replication efficiency was evaluated at 16 h.p.i. In parallel cell viability was measured by MTT assay. The results showed that the RcP was able to completely knock down the virus infectivity while the minimum cell viability was 93% (**Figure 1E**). By the use of this range of concentrations, it was determined that the RcP complex has an EC_{50} of 31,99 μ M, CC_{50} of 1379 μ M and Selective Index (SI) of 43.1 (**Figure 1E**).

3.2. RcP inhibits CHIKV entry to the host cells

The antiviral activity of the RcP at different stages of CHIKV replication was analyzed. First, cells were pretreated with RcP for 1 hour at 37 °C, washed with PBS to completely remove the compound and then were infected with CHIKV-*nanoluc*. Luminescence levels were measured 16 h.p.i. (**Figure 2A**). The RcP demonstrated a modest yet significant reduction of 23 % of luminescence levels when cells were pretreated ($p < 0.01$) (**Figure 2A**).

To evaluate virus entry to the host cells, virus and RcP were simultaneously added to BHK 21 cells for 1 hour, then washed with PBS and replaced with media. Luminescence levels were

measured 16 h.p.i. (**Figure 2B**). The results showed that RcP at 125 μ M significantly reduced 77% of the virus entry to the host cells ($p < 0.01$) (**Figure 2B**).

For the post-entry steps, the cells were first infected with CHIKV-*nanoluc* for 1 hour at 37 °C, washed to remove unbound virus and then added with compound containing media. Luminescence levels were measured 16 h.p.i. (**Figure 2C**). RcP also demonstrated a modest yet significant reduction of 21% of luminescence levels when the treatment was performed after virus entry to the cells ($p < 0.01$) (**Figure 2C**). Altogether, these data suggest that the main antiviral activity of RcP is related to its ability to inhibit the entry stage of the virus lifecycle.

Based on the results obtained, we further evaluated the activity of RcP on CHIKV entry to the cells. First, supernatant containing CHIKV-*nanoluc* was incubated with RcP 125 μ M for 1 hour at 37 °C prior to the infection of cells to investigate virucidal effect. The inoculum of virus and RcP was transferred to the naïve cells and incubated for 1 hour. Cells were washed for the complete removal of the inoculum and replaced with fresh media for 16 h.p.i. (**Figure 3A**). The results showed a strong significant virucidal activity of RcP by blocking 100% of virus entry ($p < 0.01$) (**Figure 3A**).

We also analyzed RcP effect on the virus attachment. For this, virus and RcP were incubated with the cells at 4 °C for 1 hour, when virus is able to attach to cell membrane receptor, but not to entry to the host cells. Then, cells were washed with PBS and a fresh media was added. Luminescence levels were measured 16 h.p.i. (**Figure 3B**). Data obtained from this assay showed that RcP reduced 90% of virus entry to the host cells ($p < 0.01$) (**Figure 3B**).

Next, antiviral activity of RcP on virus uncoating was investigated by incubating virus and compound for 1 hour at 4 °C and then at 37 °C for 30 minutes. Therefore, the period of treatment may include virus attachment, entry and uncoating. Cells were washed with PBS and a fresh media was added. Luminescence levels were measured 16 h.p.i. (**Figure 3C**). The results demonstrated that under this protocol of treatment, the complex inhibited up to 55% of the virus entry to the host cells ($p < 0.01$) (**Figure 3C**). These data demonstrated that RcP was able to abrogate different stages of virus entry to the host cells (**Figure 3**). However, the strongest effect was observed in virucidal and attachment protocol. This might suggest that an anti-CHIKV mechanism of action for this complex might be related to a direct action on the virus chemical structure.

3.3. Possible interactions between pCYM and CHIKV E2 glycoprotein

Based on the results that showed RcP interfering on CHIKV entry to the host cells, molecular docking calculations were performed in order to investigate possible binding mode and the interactions between pCYM and CHIKV glycoproteins. Docking analysis are not feasible with metallocenes as RcP because their chemical structure presents an unforeseen conformation named “half sandwich piano stool”. Therefore, The pCYM ligand was used for *in silico* analysis, Seven possible glycoprotein complex binding sites were explored and the scores generated by the ChemPLP scoring function of the Gold program are presented in **Table 1**. The *p*-cymene showed the best result with site 4, score 39.71 (**Table 1**). The best docking scores were obtained between the site 4, located behind the fusion loop between glycoproteins E3 and E2 (**Figure 4**).

3.4. RcP causes molecular changes in CHIKV

To further investigate the interaction between RcP and CHIKV particles, infrared spectroscopy spectral analysis was performed. The vibrational analysis between virus and RcP are shown in **Table 2**. A representative infrared average spectrum of RcP, CHIKV or RcP plus CHIKV, which contains different biochemical functional groups such as lipids, proteins, glycoproteins and nucleic acid, are represented in **Figure 5**. We were particularly interested in the interaction of RcP with CHIKV. A representative infrared average spectrum of second derivative analysis from RcP, CHIKV or RcP plus CHIKV was displayed in **Figure 6A**. In the second derivative analysis, which the value heights indicated the intensity of each functional group, a reduction in intensity of Amide II [ν (N-H), ν (C-N)] at 1540 cm^{-1} with the association of RcP with CHIKV indicates interaction with proteins of CHIKV (**Figure 6B**). The binding interaction was also revealed by spectral shifting of the 1013 cm^{-1} to 1005 cm^{-1} , which indicates interaction with ν s (CO-O-C) presents in Glycoprotein derived from RcP and/or CHIKV (**Figure 6C**). The binding interaction was also revealed by increase in intensity of 724 cm^{-1} , 679 cm^{-1} , 645 cm^{-1} and 609 cm^{-1} in RcP plus CHIKV, which indicate formation of C-H rocking of CH₂ and S-O bending. The binding interaction was additionally confirmed by the decrease in intensity of 704 cm^{-1} , 652 cm^{-1} and 632 cm^{-1} in RcP plus CHIKV, which indicate reduction in the presence of OH out-of-plane bend (**Figure 6C**).

4. Discussion

Chikungunya virus (CHIKV) has obtained attention from the public health worldwide due to the recent outbreaks (GOULD et al., 2017), but also because the infection may persist for months or even years (CUNHA; TRINTA, 2017). CHIKV was first described in the 1950s (Robinson, 1955), however, there is still no specific treatment or vaccine against this virus (MATHEW et al., 2017; STEGMANN-PLANCHARD et al., 2019). Thus, the search for new molecules with anti-CHIKV activity is necessary.

In this study, the anti-CHIKV activity of the ruthenium (Ru) and *para*-cymene (pCYM) complex (RcP) was investigated. The pCYM molecule has already been described to demonstrate biological activities as antioxidant, anti-inflammatory and antifungal (DE OLIVEIRA et al., 2015; KORDALI et al., 2008; KUMMER et al., 2015). It was also demonstrated that pCYM in lower concentrations showed moderate antiviral activity against the Herpes simplex virus (HSV), partially inhibiting the viral infection in RC-37 cells (ASTANI; REICHLING; SCHNITZLER, 2009; GAROZZO et al., 2009). However, there is a lack of studies on the effects of pCYM against CHIKV.

Our results showed that Ru or pCYM treatment did not significantly reduce CHIKV infectivity in BHK21 cells. However, the complexed molecule of Ru and pCYM, the organometallic complex RcP, demonstrated to be effective against the virus, exhibiting a strong therapeutic index judged by the high selective index. The data demonstrated that RcP showed moderate yet significant inhibitory activity when the cells were pretreated, exerting a protective effect to the host cells. Similar data was observed when the cells were treated after viral infection. Alternatively, RcP significantly reduced virus entry to the host cells at non-toxic concentrations. As the complex demonstrated to interfere on virus entry, we reevaluated the early stages of CHIKV infection. RcP demonstrated a moderate activity on the virus uncoating and strong action on inhibiting virus attachment or as a virucide. A recent study demonstrated that pCYM presented virucidal activity against HSV. The results showed that when p-cymene and HSV were incubated together, virus entry was reduced by 80% (SHARIFI-RAD et al., 2017).

The strong virucidal effect observed for RcP might suggest that an anti-CHIKV mechanism of action for this complex might be related to a direct action on the viral particle envelope (RUSSO et al., 2019; SCHUHMACHER; REICHLING; SCHNITZLER, 2003; TANG et al., 1990), which could also be responsible for the effect observed on virus attachment (CARRAVILLA et al., 2017; KONG et al., 2019). Possible interactions between

Chikungunya envelope proteins and RcP could be a reasonable explanation for the observed virucidal effect. Based on this data, molecular docking calculations were performed in order to investigate possible binding mode and the interactions between pCYM and CHIKV glycoproteins. Our results suggested that pCYM may bind to a site located behind the fusion loop between glycoproteins E3 and E2. Glycoprotein E2 is responsible for binding the virus to cell receptors (FONGSARAN et al., 2014; MOLLER-TANK et al., 2013b; SILVA et al., 2014). When small molecules attach to that site, the movement of the glycoprotein domains can be frozen and then prevent the virus from entering the cell (RASHAD; KELLER, 2013). We suggest that pCYM may be binding to such a site and preventing the virus from binding to the cell. Similarly, we can suggest that, through molecular interactions observed by the FTIR methodology, the RcP compound alters CHIKV glycoprotein and lipid sites, reaffirming that there is an interaction between the viral envelope and the complex.

In summary, we showed that ruthenium and para-cymene complex is able to strongly inhibit CHIKV infectivity, acting mainly on the entry of virus to the host cells. This is the first description of the antiviral activity of an organometallic complex against CHIKV. This data may be useful for the development of future antivirals against CHIKV that will provide a relevant advance to the public health to treat Chikungunya fever.

Acknowledgment and funding

This research was funded by the Royal Society – Newton Advanced Fellowship (grant reference NA 150195), CNPQ (National Counsel of Technological and Scientific Development – grant 445021/2014-4), FAPEMIG (Minas Gerais Research Foundation-APQ-00587-14, SICONV 793988/2013 and APQ-03385-18) and CAPES (Coordination for the Improvement of Higher Education Personnel – Code 001). ACGJ also thanks the CNPq for the productivity fellowship (311219/2019-5).

5. References

ABDELNABI, R.; NEYTS, J.; DELANG, L. Towards antivirals against chikungunya virus. **Antiviral Research**, v. 121, n. June, p. 59–68, 2015.

ASTANI, A.; REICHLING, J.; SCHNITZLER, P. Comparative study on the antiviral activity

of selected monoterpenes derived from essential oils. **Phytotherapy Research**, v. 23, n. 9, p. n/a-n/a, 2009.

BENNETT, M. A. et al. 16. (η^6 -Hexamethylbenzene)Ruthenium Complexes. In: [s.l: s.n.]. p. 74–78.

BRASIL, M. DA S. **Chikungunya: causas, sintomas, tratamento e prevenção**. Disponível em: <<http://saude.gov.br/saude-de-a-z/chikungunya>>. Acesso em: 30 jan. 2020.

BURT, F. J. et al. Chikungunya virus: an update on the biology and pathogenesis of this emerging pathogen. **The Lancet Infectious Diseases**, v. 17, n. 4, p. e107–e117, 2017.

CARRAVILLA, P. et al. Effects of HIV-1 gp41-Derived Virucidal Peptides on Virus-like Lipid Membranes. **Biophysical Journal**, v. 113, n. 6, p. 1301–1310, 2017.

CARVALHO, R. G.; LOURENÇO-DE-OLIVEIRA, R.; BRAGA, I. A. Updating the geographical distribution and frequency of *Aedes albopictus* in Brazil with remarks regarding its range in the Americas. **Memórias do Instituto Oswaldo Cruz**, v. 109, n. 6, p. 787–796, 2014.

CASTRO, A. P. C. R. DE; LIMA, R. A.; NASCIMENTO, J. DOS S. Chikungunya: vision of the pain clinician. **Revista Dor**, v. 17, n. 4, p. 299–302, 2016.

CENTERS FOR DISEASE CONTROL AND PREVENTION (CDC). Countries and territories where chikungunya cases have been reported. **Cdc**, p. 1, 2018.

CLARKE, M. J.; ZHU, F.; FRASCA, D. R. Non-platinum chemotherapeutic metallopharmaceuticals. **Chemical Reviews**, v. 99, n. 9, p. 2511–2533, 1999.

CUNHA, R. V. DA; TRINTA, K. S. Chikungunya virus: clinical aspects and treatment - A Review. **Memórias do Instituto Oswaldo Cruz**, v. 112, n. 8, p. 523–531, 2017.

CUNHA, M. S. et al. Autochthonous Transmission of East/Central/South African Genotype Chikungunya Virus, Brazil. **Emerging Infectious Diseases**, v. 23, n. 10, p. 2015–2017, 2017.

DA SILVA-JÚNIOR, E. F. et al. The medicinal chemistry of Chikungunya virus. **Bioorganic & Medicinal Chemistry**, v. 25, n. 16, p. 4219–4244, 2017.

DE ANDRADE, D. C. et al. Chronic pain associated with the Chikungunya Fever: long lasting burden of an acute illness. **BMC Infectious Diseases**, v. 10, n. 1, p. 31, 2010.

DE OLIVEIRA, T. M. et al. Evaluation of p-cymene, a natural antioxidant. **Pharmaceutical Biology**, v. 53, n. 3, p. 423–428, 2015.

DEY, D. et al. The effect of amantadine on an ion channel protein from Chikungunya virus. **PLOS Neglected Tropical Diseases**, v. 13, n. 7, p. e0007548, 2019.

DO SOCORRO SOUZA, T. et al. Travelers as sentinels for chikungunya fever, Brazil. **Emerging Infectious Diseases**, v. 18, n. 3, p. 529–530, 2012.

DOUGAN, S. J.; SADLER, P. J. The design of organometallic ruthenium arene anticancer agents. **Chimia**, v. 61, n. 11, p. 704–715, 2007.

DYSON, P. J. Systematic design of a targeted organometallic antitumour drug in pre-clinical development. **Chimia**, v. 61, n. 11, p. 698–703, 2007.

EPIDEMIOLOGICO, B. et al. N^o 59 | Dez. v. 49, 2018.

EPIDEMIOLOGICO, B. **Sumário Coordenação-Geral de Vigilância das Arboviroses (CGARB/DEIDT/SVS)***. [s.l: s.n.].

FAVRE, H. A.; POWELL, W. H. **Nomenclature of Organic Chemistry**. [s.l.] Royal Society of Chemistry, 2013.

FONGSARAN, C. et al. Involvement of ATP synthase β subunit in chikungunya virus entry into insect cells. **Archives of Virology**, v. 159, n. 12, p. 3353–3364, 2014.

GAROZZO, A. et al. In vitro antiviral activity of Melaleuca alternifolia essential oil. **Letters in Applied Microbiology**, v. 49, n. 6, p. 806–808, dez. 2009.

GOULD, E. et al. Emerging arboviruses: Why today? **One Health**, v. 4, n. April, p. 1–13, 2017.

GRANDADAM, M. et al. Chikungunya virus, Southeastern France. **Emerging Infectious Diseases**, v. 17, n. 5, p. 910–913, 2011.

HABTEMARIAM, A. et al. Structure-activity relationships for cytotoxic ruthenium(II) arene

complexes containing N,N-, N,O-, and O,O-chelating ligands. **Journal of Medicinal Chemistry**, v. 49, n. 23, p. 6858–6868, 2006.

HER, Z. et al. Active Infection of Human Blood Monocytes by Chikungunya Virus Triggers an Innate Immune Response. **The Journal of Immunology**, v. 184, n. 10, p. 5903–5913, 15 maio 2010.

HOARAU, J.-J. et al. Persistent Chronic Inflammation and Infection by Chikungunya Arthritogenic Alphavirus in Spite of a Robust Host Immune Response. **The Journal of Immunology**, v. 184, n. 10, p. 5914–5927, 15 maio 2010.

JENSEN, S. B.; RODGER, S. J.; SPICER, M. D. **Facile preparation of η^6 -p-cymene ruthenium diphosphine complexes. Crystal structure of $[(\eta^6\text{-p-cymene})\text{Ru}(\text{dppf})\text{Cl}]\text{PF}_6$** **Journal of Organometallic Chemistry**, 1998.

KAUR, P.; CHU, J. J. H. Chikungunya virus: An update on antiviral development and challenges. **Drug Discovery Today**, v. 18, n. 19–20, p. 969–983, 2013.

KHAN, A. H. et al. Complete nucleotide sequence of chikungunya virus and evidence for an internal polyadenylation site. **The Journal of general virology**, v. 83, n. Pt 12, p. 3075–84, dez. 2002.

KONG, B. et al. Virucidal nano-perforator of viral membrane trapping viral RNAs in the endosome. **Nature Communications**, v. 10, n. 1, p. 1–10, 2019.

KORDALI, S. et al. Antifungal, phytotoxic and insecticidal properties of essential oil isolated from Turkish *Origanum acutidens* and its three components, carvacrol, thymol and p-cymene. **Bioresource Technology**, v. 99, n. 18, p. 8788–8795, 2008.

KRAEMER, M. U. G. et al. The global distribution of the arbovirus vectors *Aedes aegypti* and *Ae. Albopictus*. **eLife**, v. 4, n. JUNE2015, p. 1–18, 2015a.

KRAEMER, M. U. G. et al. The global distribution of the arbovirus vectors *Aedes aegypti* and *Ae. albopictus*. **eLife**, v. 4, n. JUNE2015, jun. 2015b.

KUMMER, R. et al. Effect of p-cymene on chemotaxis, phagocytosis and leukocyte behaviors. **International Journal of Applied Research in Natural Products**, v. 8, n. 2, p.

20–27, 2015.

LUM, F. M.; NG, L. F. P. Cellular and molecular mechanisms of chikungunya pathogenesis. **Antiviral Research**, v. 120, p. 165–174, 2015.

MATHEW, A. J. et al. Chikungunya Infection : a Global Public Health Menace. p. 1–9, 2017.

MATKOVIC, R. et al. The Host DHX9 DExH-Box Helicase Is Recruited to Chikungunya Virus Replication Complexes for Optimal Genomic RNA Translation. **Journal of Virology**, v. 93, n. 4, p. 1–17, 2018.

MOLLER-TANK, S. et al. Role of the Phosphatidylserine Receptor TIM-1 in Enveloped-Virus Entry. **Journal of Virology**, v. 87, n. 15, p. 8327–8341, 2013a.

MOLLER-TANK, S. et al. Role of the Phosphatidylserine Receptor TIM-1 in Enveloped-Virus Entry. v. 87, n. 15, p. 8327–8341, 2013b.

PAIXÃO, E. S. et al. Chikungunya chronic disease: A systematic review and meta-analysis. **Transactions of the Royal Society of Tropical Medicine and Hygiene**, v. 112, n. 7, p. 301–316, 2018.

PARASHAR, D.; CHERIAN, S. Antiviral perspectives for chikungunya virus. **BioMed Research International**, v. 2014, 2014.

PAVAN, F. R. et al. Ruthenium (II) phosphine/picolinate complexes as antimycobacterial agents. **European Journal of Medicinal Chemistry**, v. 45, n. 2, p. 598–601, 2010.

POHJALA, L. et al. Inhibitors of alphavirus entry and replication identified with a stable Chikungunya replicon cell line and virus-based assays. **PLoS ONE**, v. 6, n. 12, 2011.

RASHAD, A. A.; KELLER, P. A. Structure based design towards the identification of novel binding sites and inhibitors for the chikungunya virus envelope proteins. **Journal of Molecular Graphics and Modelling**, v. 44, p. 241–252, 2013.

RASHAD, A. A.; MAHALINGAM, S.; KELLER, P. A. Chikungunya virus: Emerging targets and new opportunities for medicinal chemistry. **Journal of Medicinal Chemistry**, v. 57, n. 4, p. 1147–1166, 2014.

REZZA, G. et al. Infection with chikungunya virus in Italy: an outbreak in a temperate region. **Lancet**, v. 370, n. 9602, p. 1840–1846, 2007.

ROBINSON, M. C. An epidemic of virus disease in Southern Province, Tanganyika Territory, in 1952-53. I. Clinical features. **Transactions of the Royal Society of Tropical Medicine and Hygiene**, v. 49, n. 1, p. 28–32, jan. 1955.

RODRÍGUEZ-MORALES, A. J. et al. Prevalence of Post-Chikungunya Infection Chronic Inflammatory Arthritis: A Systematic Review and Meta-Analysis. **Arthritis Care and Research**, 2016.

ROUGERON, V. et al. Chikungunya, a paradigm of neglected tropical disease that emerged to be a new health global risk. **Journal of Clinical Virology**, v. 64, p. 144–152, mar. 2015.

RUSSO, R. R. et al. Expression, purification and virucidal activity of two recombinant isoforms of phospholipase A2 from *Crotalus durissus terrificus* venom. **Archives of Virology**, v. 164, n. 4, p. 1159–1171, 26 abr. 2019.

SAVIĆ, A. et al. Antitumor activity of organoruthenium complexes with chelate aromatic ligands, derived from 1,10-phenantroline: Synthesis and biological activity. **Journal of Inorganic Biochemistry**, v. 202, n. September 2019, p. 110869, 2020.

SCHUFFENECKER, I. et al. Genome Microevolution of Chikungunya Viruses Causing the Indian Ocean Outbreak. **PLoS Medicine**, v. 3, n. 7, p. 1058–1070, 2006.

SCHUHMACHER, A.; REICHLING, J.; SCHNITZLER, P. Virucidal effect of peppermint oil on the enveloped viruses herpes simplex virus type 1 and type 2 in vitro. **Phytomedicine**, v. 10, n. 6–7, p. 504–510, jan. 2003.

SCHWARTZ, O.; ALBERT, M. L. Biology and pathogenesis of chikungunya virus. **Nature Reviews Microbiology**, v. 8, n. 7, p. 491–500, 2010.

SHARIFI-RAD, J. et al. Susceptibility of herpes simplex virus type 1 to monoterpenes thymol, carvacrol, p-cymene and essential oils of *Sinapis arvensis* L., *Lallemantia royleana* Benth. and *Pulicaria vulgaris* Gaertn. **Cellular and molecular biology (Noisy-le-Grand, France)**, v. 63, n. 8, p. 42–47, 30 ago. 2017.

SILVA, N. M. DA et al. Vigilância de chikungunya no Brasil: desafios no contexto da Saúde Pública. **Epidemiologia e serviços de saúde : revista do Sistema Unico de Saude do Brasil**, v. 27, n. 3, p. e2017127, 2018.

SILVA, L. A. et al. A Single-Amino-Acid Polymorphism in Chikungunya Virus E2 Glycoprotein Influences Glycosaminoglycan Utilization. **Journal of Virology**, v. 88, n. 5, p. 2385–2397, 2014.

SIMON, F. et al. Chikungunya virus infection. **Current Infectious Disease Reports**, v. 13, n. 3, p. 218–228, 2011.

SOLIGNAT, M. et al. Replication cycle of chikungunya: A re-emerging arbovirus. **Virology**, v. 393, n. 2, p. 183–197, 2009.

STEGMANN-PLANCHARD, S. et al. Chikungunya, a Risk Factor for Guillain-Barré Syndrome. **Clinical Infectious Diseases**, v. 66, p. 37–39, 9 jul. 2019.

STRAUSS, J. H.; STRAUSS, E. G. **The alphaviruses: Gene expression, replication, and evolution** *Microbiological Reviews*, set. 1994.

TANG, J. et al. Virucidal activity of hypericin against enveloped and non-enveloped DNA and RNA viruses. **Antiviral Research**, v. 13, n. 6, p. 313–325, jun. 1990.

TEIXEIRA, R. R. et al. Natural Products as Source of Potential Dengue Antivirals. **Molecules**, v. 19, p. 8151–8176, 2014.

THIBERVILLE, S. D. et al. Chikungunya fever: Epidemiology, clinical syndrome, pathogenesis and therapy. **Antiviral Research**, v. 99, n. 3, p. 345–370, 2013.

UCHIME, O.; FIELDS, W.; KIELIAN, M. The role of E3 in pH protection during alphavirus assembly and exit. **Journal of virology**, v. 87, n. 18, p. 10255–62, 2013.

VAJS, J. et al. The 1,3-diaryltriazenido(p-cymene)ruthenium(II) complexes with a high in vitro anticancer activity. **Journal of Inorganic Biochemistry**, v. 153, p. 42–48, 2015.

VIEGAS, C.; DA SILVA BOLZANI, V.; BARREIRO, E. J. OS produtos naturais e a química medicinal moderna. **Quimica Nova**, v. 29, n. 2, p. 326–337, 2006.

VOLK, S. M. et al. Genome-Scale Phylogenetic Analyses of Chikungunya Virus Reveal Independent Emergences of Recent Epidemics and Various Evolutionary Rates. **Journal of Virology**, v. 84, n. 13, p. 6497–6504, 2010.

VU, D. M.; JUNGKIND, D.; LABEAUD, A. D. Chikungunya Virus. **Clinics in Laboratory Medicine**, v. 37, n. 2, p. 371–382, 2017.

WINTACHAI, P. et al. Identification of Prohibitin as a Chikungunya Virus Receptor Protein. **Journal of Medical Virology**, v. 84, p. 1757–1770, 2012.

YANG, S. et al. Regulatory considerations in development of vaccines to prevent disease caused by Chikungunya virus q. **Vaccine**, v. 35, n. 37, p. 4851–4858, 2017.

Tables

Table 1. Maximum score resulting from the dosage for each evaluated site.

	Binder color	ChemPLP	Coordinates (x, y, z)	Volume (Å ³)	Localization
Site 1	Yellow	32.53	-15.687, 2.019, -19.939	651.375	Between E1 domain II and E2 domain
Site 2	Green	38.98	-33.937, -18.731, -31.939	357.375	Between E1 domain II and E2 beta-sheet
Site 3	Blue	37.10	-33.437, -6.731, -33.189	156.125	Adjacent to site 2
Site 4	Purple	39.71	-42.937, -28.731, -22.939	183.875	Behind the fusion loop, between E3 B domains, E2 domain B, and E2 domain A
Site 5	Brown	18.38	-44.437, -14.731, -23.439	124	Between the E2 and E3 beta sheet
Site 6	-	*	-16.187, -18.231, -36.439	20.5	Inside the E3 cavity
Site 7	Black	4.56	-59.187, -15.731, -26.189	22.5	Replacing the furin loop

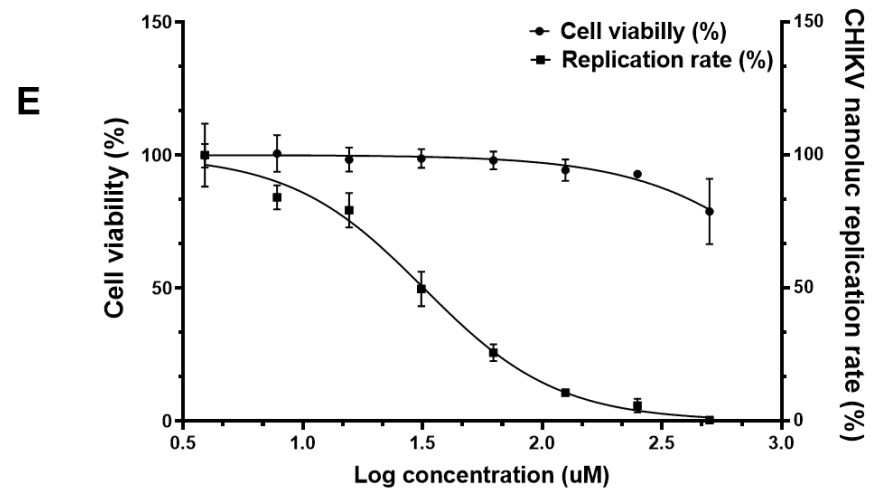
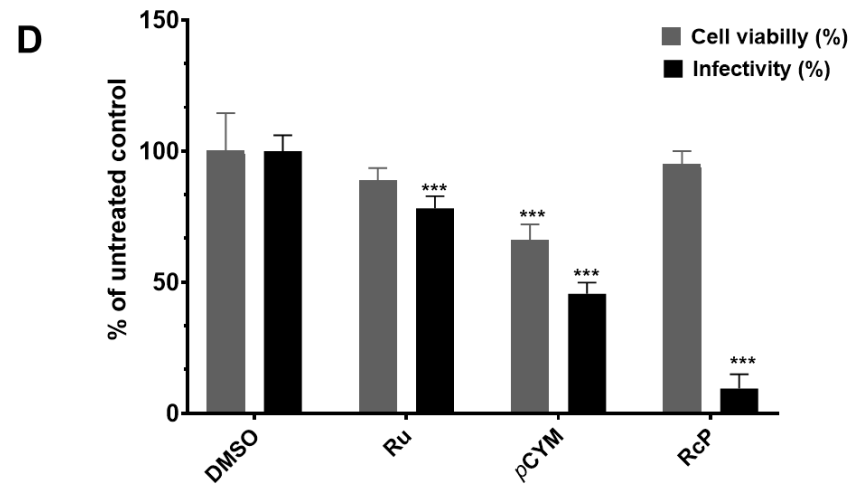
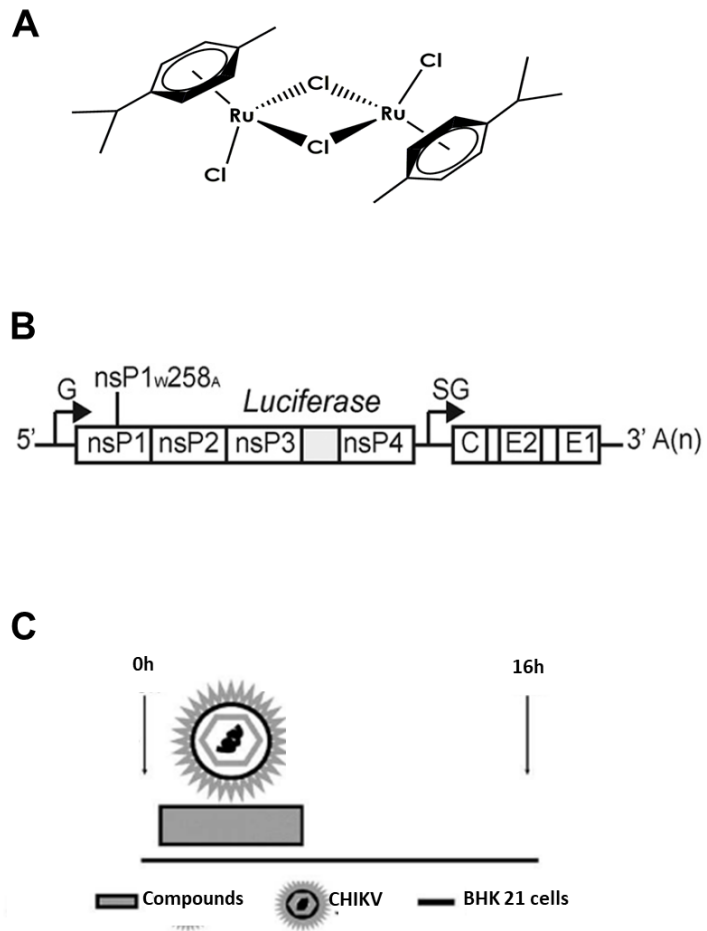
* No docking results

FONT: Adapted (RASHAD E KELLER, 2013)

Table 2. Vibrational modes present in each vibrational mode and identification of the respective functional group in the sample.

Vibrational mode (cm ⁻¹)	Proposed vibrational mode	Molecular source
1540	Amide II [ν (N-H), ν (C-N)]	Protein
1013	vs (CO-O-C)	Glycoprotein/ Carbohydrates
1005	vs (CO-O-C)	Glycoprotein/ Carbohydrates
724	C-H rocking of CH ₂	Fatty acids, proteins Inespecific
704	Unsaignment band	Sulphates components
679	S-O bending	Protein and lipids
652	OH out-of-plane bend	Inespecific
645	Unsaignment band	Protein, Lipids
632	OH out-of-plane bend	Sulphates components
609	S-O bending	

Assignments of main wavenumbers of sample ATR-FTIR spectra. Abbreviations: ν = stretching vibrations, δ = bending vibrations, s = symmetric vibrations and as = asymmetric vibrations.



Figures and legends

Figure 1. CHIKV activity of ruthenium(Ru) and paracycymene(pCYM) complex (RcP). (A) RcP chemical structure (B) Schematic representation of CHIKV-*nanoluc* construction. (C) Schematic representation of infectivity assays. (D) BHK 21 cells were infected with CHIKV-*nanoluc* at MOI 0.1 and treated with compounds at 125 μ M for 16h. Infectivity and cell viability assays were performed. (E) Cells were treated with concentrations of RcP ranging from 500 to 3.9 μ M and the effective concentration of 50% (EC₅₀) and cytotoxic concentration of 50% (CC₅₀) of RcP were determined. CHIKV replication was measured by luciferase assay (indicated by \square) and cellular viability measured using an MTT assay (indicated by \bullet). Mean values of three independent experiments each measured in quadruple including the standard deviation are shown.

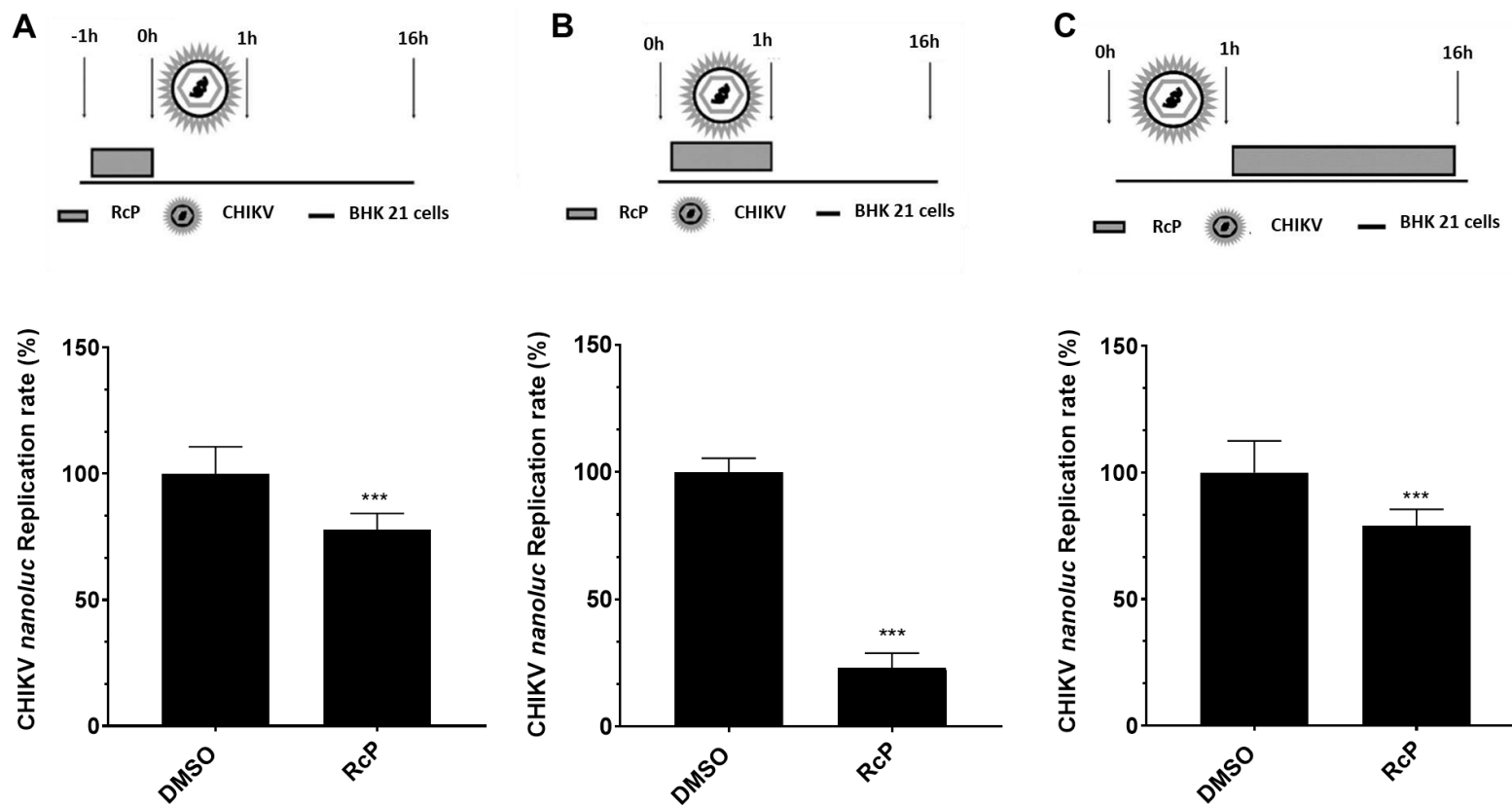


Figure 2. Antiviral effects of RcP at different stages of CHIKV replicative cycle. (A) BHK 21 cells were treated with RcP at 125 μ M for 1h. Then, cells were extensively washed and infected with CHIKV-*nanoluc* at a MOI 0.1 for 1h, compound containing media was removed and replaced by fresh media. (B) BHK 21 cells were infected with CHIKV-*nanoluc* (MOI 0.1) and simultaneously treated with RcP at 125 μ M for 1 h. Cells were washed and replaced with fresh media. (C) The cells were first infected with CHIKV-*nanoluc* (MOI 0.1) for 1h, washed to remove unbound virus and added of compound containing media. For all assays, CHIKV replication was measured by *nanoluc* activity at 16 h.p.i. Mean values of a minimum of three independent experiments each measured in triplicate. $P < 0.01$ was considered significant.

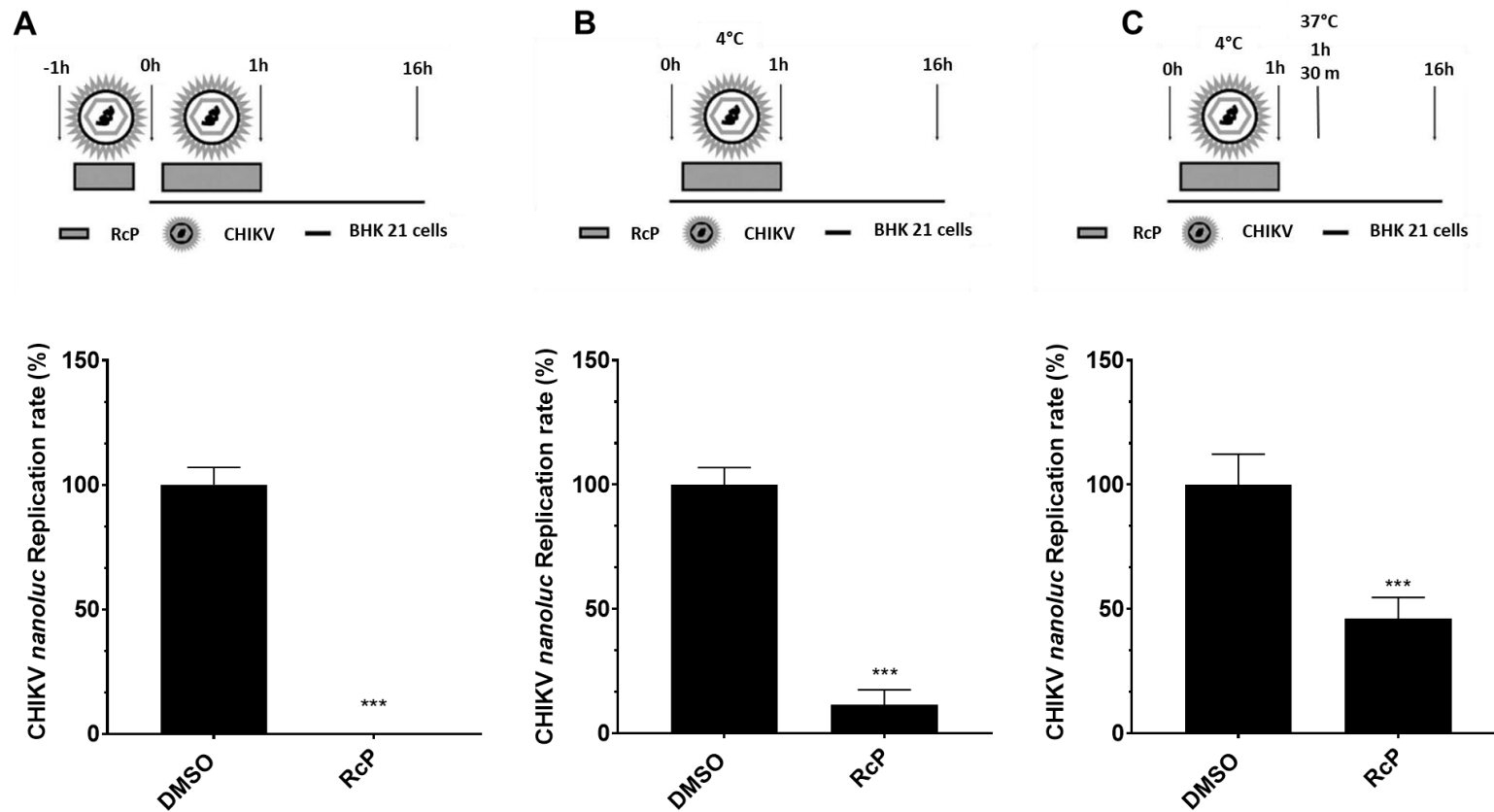


Figure 3. RcP activity on CHIKV entry to the host cells. (A) CHIKV-*nanoluc* and compound were incubated for 1 h and then for one additional hour in the cells. Then, the compound was removed and the cells added of media. (B) BHK 21 cells were infected with virus and simultaneously treated for 1 h at 4°C. The cells were washed to remove virus and compound and replaced with fresh media. (C) BHK 21 cells were infected with virus and simultaneously treated for 1 h at 4°C. Then, cells were incubated for a further 30 min with compound and virus at 37°C, were then washed to remove virus and compound and replaced with media. For all assays, CHIKV replication was measured by *nanoluc* activity at 16h.p.i.. Mean values of a minimum of three independent experiments each measured in triplicate P<0.01 was considered significant.

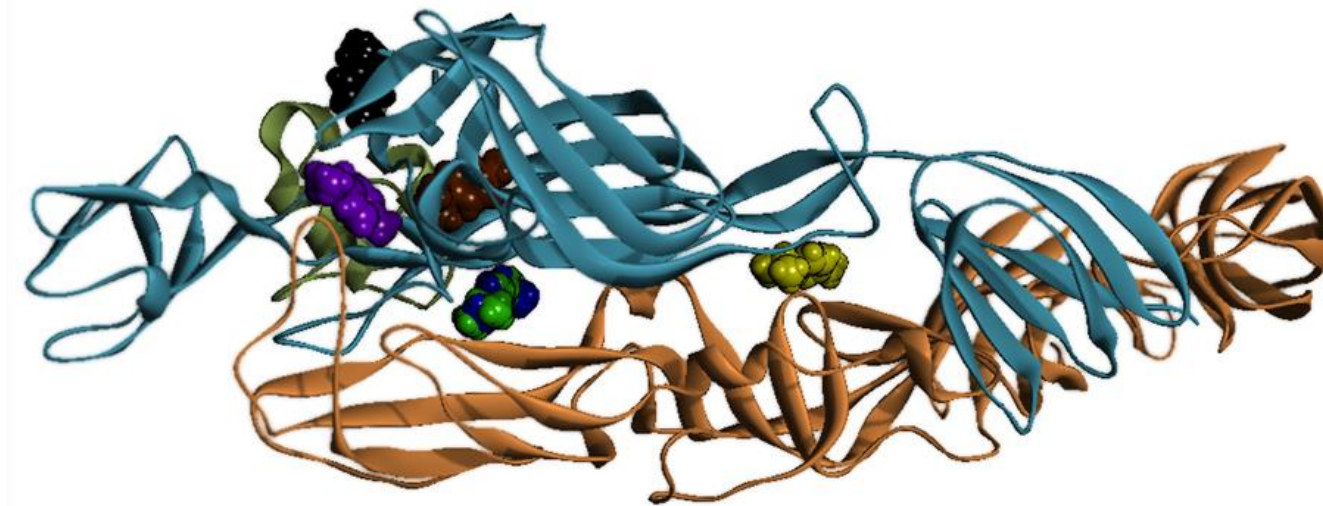


Figure 4. The CHIKV envelope glycoproteins E1 (Brown), E2 (Blue) and E3 (green), complexed with para-cymene, sites 1 (yellow), 2 (green), 3 (blue), 4 (purple), 5 (brown) and 7 (black).

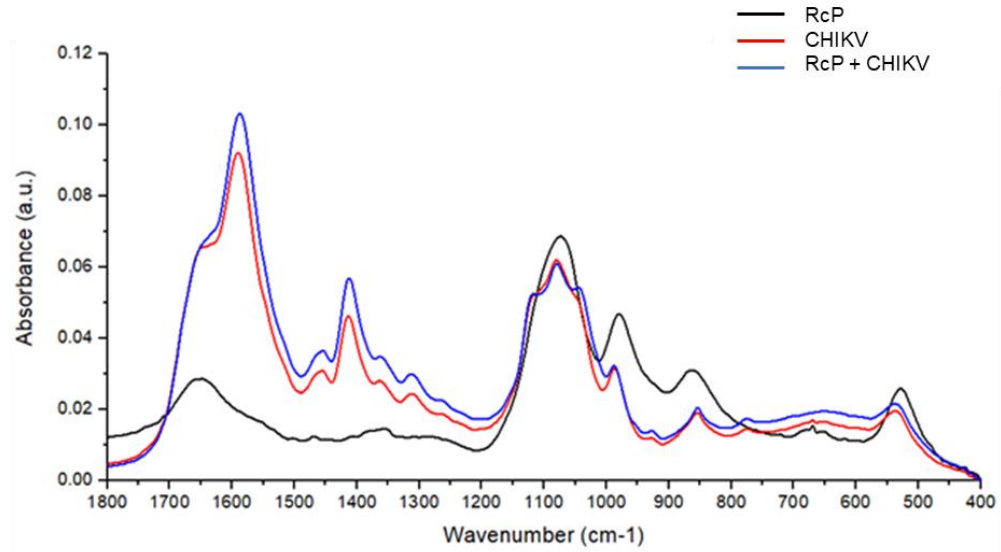


Figure 5. Representative infrared average spectrum of RcP, CHIKV and RcP plus CHIKV, which contains different biochemical functional groups such as lipids, proteins, glycoproteins and nucleic acid.

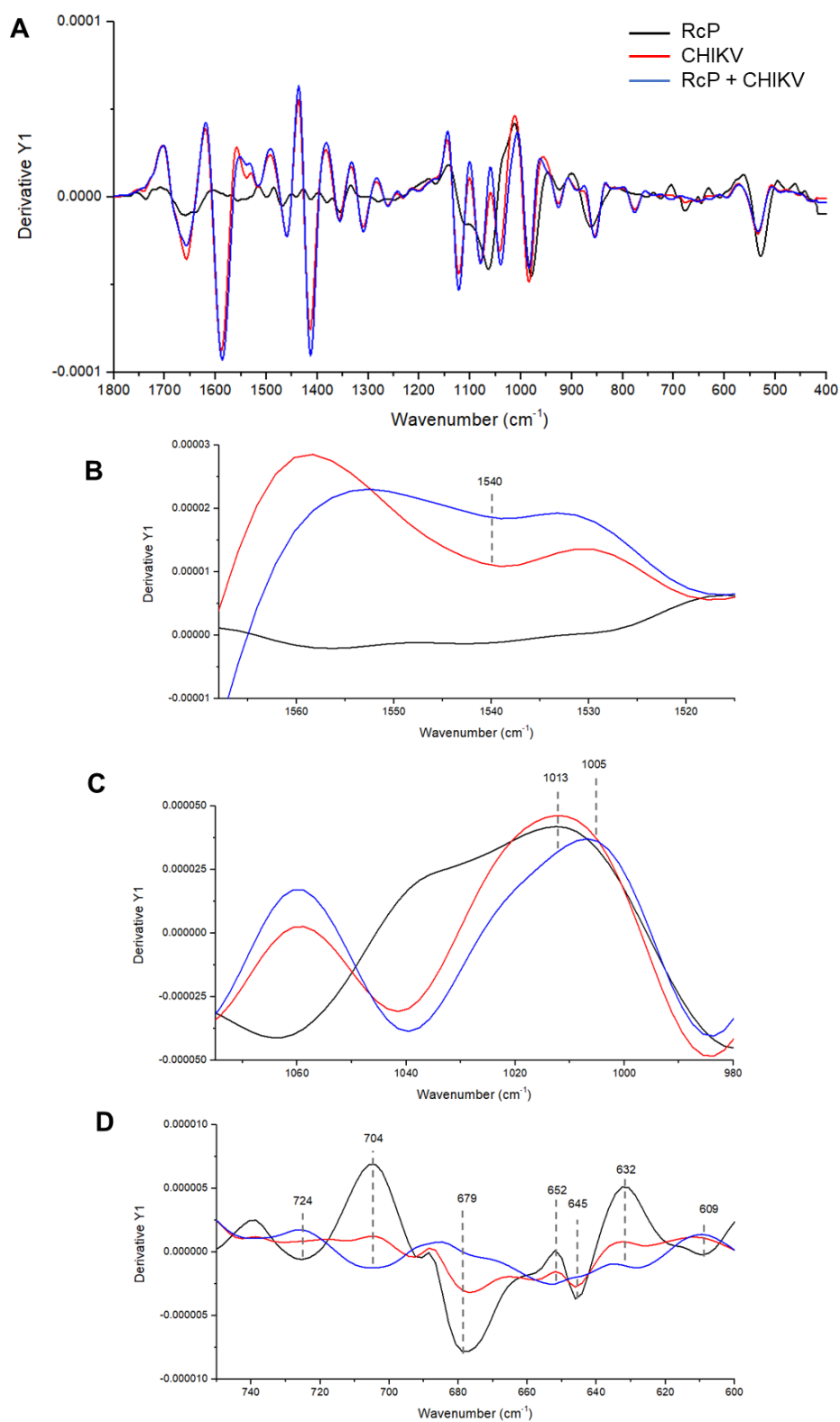


Figure 6. (A) Representative infrared average spectrum of second derivative analysis from RcP, CHIKV and RcP plus CHIKV. (B, C, D) Second derivative analysis, which the value heights indicate the intensity of each functional group.

CAPÍTULO III

Considerações finais

Considerações Finais

Os resultados deste estudo demonstram que o composto avaliado neste trabalho pode servir de base para novos estudos em busca de novos antivirais. Mais estudos são necessários para avaliar mecanismos de ação antiviral desse complexo, além dos testes *in vivo* e o estudo das vias de entrega desse composto.

Este trabalho fornecerá informação potencial para o desenvolvimento de novas terapias antivirais.

Material Suplementar

Artigos publicados ou aceitos para publicação



viruses

an Open Access Journal by MDPI



CERTIFICATE OF ACCEPTANCE



Certificate of acceptance for the manuscript (viruses-656877) titled:
Antivirals against Chikungunya virus: is the solution in nature

Authored by:

Daniel Oliveira Silva Martins; Igor de Andrade Santos; Débora Moraes de Oliveira; Victória Riquena Grosche; Ana Carolina Gomes Jardim

has been accepted in *Viruses* (ISSN 1999-4915) on 07 February 2020



Academic Open Access Publishing
since 1996

Basel, February 2020

Review

Antivirals against Chikungunya Virus: Is the Solution in Nature?

Daniel Oliveira Silva Martins ^{1,2,†}, Igor de Andrade Santos ^{1,†}, Débora Moraes de Oliveira ¹,
Victória RiquenaGrosche¹and Ana Carolina Gomes Jardim.^{1,2,*}

¹Laboratory of Virology, Institute of Biomedical Science, ICBIM, Federal University of Uberlândia, Uberlândia, MG 38408-100, Brazil; danielosmartins@gmail.com(D.O.S.M.); igoras244@gmail.com (I.A.S.); deboramoraes@hotmail.com (D.M.d.O.); victoriagrosche@live.com (V.R.G.)

²São Paulo State University, Institute of Biosciences, Letters and Exact Sciences (IBILCE), State University of São Paulo, São José do Rio Preto, SP 15054-000, Brazil

*Correspondence: jardim@ufu.br; Tel.: +55-(34)-3225-8679

[†]These authors contributed equally to this work.

Received: 15 November 2019; Accepted: 7 February 2020; Published: date

Abstract: The worldwide outbreaks of the chikungunya virus (CHIKV) in the last years demonstrated the need for studies to screen antivirals against CHIKV. The virus was first isolated in Tanzania in 1952 and was responsible for outbreaks in Africa and Southwest Asia in subsequent years. Between 2007 and 2014, some cases were documented in Europe and America. The infection is associated with low rates of death; however, it can progress to a chronic disease characterized by severe arthralgias in infected patients. This infection is also associated with Guillain–Barré syndrome. There is no specific antiviral against CHIKV. Treatment of infected patients is palliative and based on analgesics and non-steroidal anti-inflammatory drugs to reduce arthralgias. Several natural molecules have been described as antiviruses against viruses such as dengue, yellow fever, hepatitis C, and influenza. This review aims to summarize the natural compounds that have demonstrated antiviral activity against chikungunya virus in vitro.

Keywords:chikungunya virus; antiviral; natural compounds

1. Introduction

Chikungunya fever is a tropical disease caused by the chikungunya virus (CHIKV) which is transmitted to humans by the bite of an infected mosquito of *Aedes* sp. The first case of chikungunya fever was reported in 1952 in Tanzania [1]. In February 2005, a major outbreak of chikungunya occurred on the islands of the Indian Ocean [2]. A large number of cases occurred in Europe and India in 2006 and 2007, respectively [2]. Several other countries in Southeast Asia were also affected [3]. In December 2013, autochthonous cases were confirmed in the French part of the Caribbean island of St Maarten [4]. Since then, local transmission has been confirmed in over 60 countries in Asia, Africa, Europe, and the Americas. In 2014, more than 1 million suspected cases were reported in the Americas, with 1,379,788 suspected cases and 191 deaths in the Caribbean islands, Latin American countries, and the United States of America (USA) [5]. Canada, Mexico,

and USA have also recorded imported cases. The countries reporting the most cases were Brazil (265,000 suspected cases), and Bolivia and Colombia (19,000 suspected cases each) [6]. The first autochthonous transmission of chikungunya reported in Argentina occurred in 2016 following an outbreak of more than 1000 suspected cases [7]. In the African region, Kenya reported an outbreak of chikungunya resulting in more than 1700 suspected cases. In 2017, Pakistan continues to respond to an outbreak which started in 2016 [8]. These virus outbreaks have raised concerns on studies of CHIKV epidemiology and antiviral research [9].

CHIKV belongs to the Alphavirus genus and the *Togaviridae* family. It is a positive-sense, single-stranded RNA (12 kb in length) virus, with an enveloped icosahedral capsid [10]. The virus lifecycle starts via the attachment of the viral glycoproteins to the cell membrane receptors, mainly to MXRA8 [11,12] but also to prohibitin (PHB) [13], phosphatidylserine (PtdSer) [14], and glycosaminoglycans (GAGs) [15] receptors in mammalian and to ATP synthase β in mosquito cells [16], forming a pore. Then, a virus capsid is released into the cytoplasm, where the replication process takes place. Viral genome is uncoated and directly translated into nonstructural (NS) proteins nP1–4. The NS proteins form the viral replicase complex that catalyzes the synthesis of a negative strand, a template to synthesize the full-length positive sense genome, and the subgenomic mRNA. The subgenomic mRNA is translated in a polyprotein, which is cleaved to produce the structural proteins C, E3, E2, 6k, and E1, followed by the assembly of the viral components and virus release (Figure 1) [17,18].

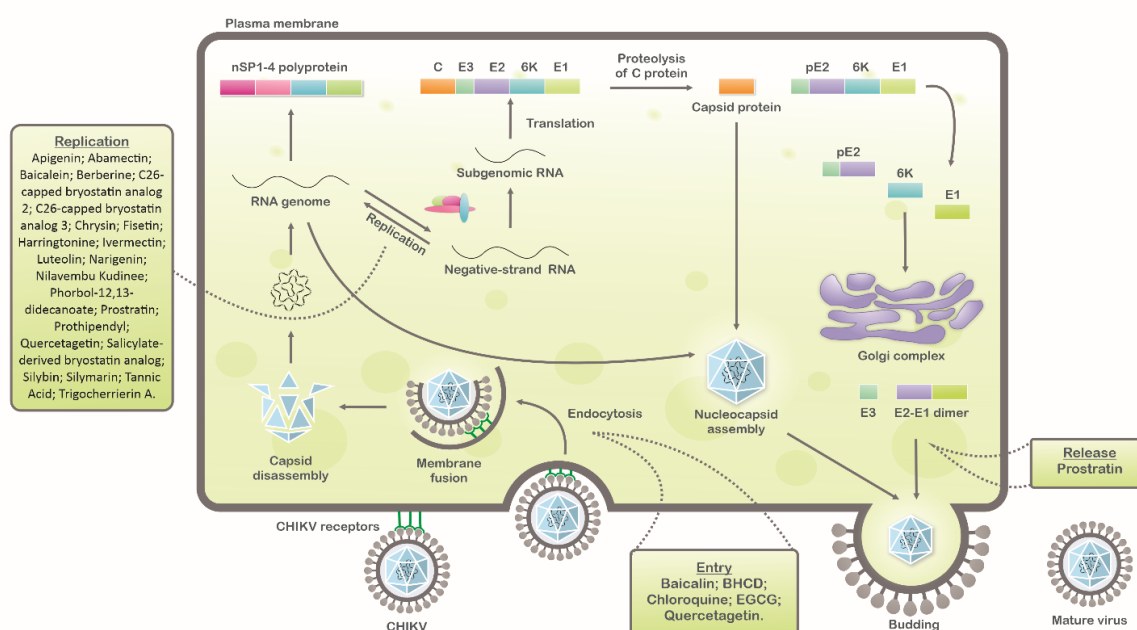


Figure 1. Schematic representation of chikungunya virus (CHIKV) replication cycle: Natural compounds with antiviral activity against CHIKV are indicated in each step of virus replication cycle (entry, replication, and release).

Chikungunya fever is characterized by strong fever, arthralgia, backache, headache, and fatigue. In some cases, cutaneous manifestation and neurological complications can occur [19,20]. There is no Food and Drug Administration (FDA) approved specific antiviral or vaccine against CHIKV. Therefore, the treatment of infected patients is based on palliative care, using analgesics for pain and non-steroidal anti-inflammatory drugs to reduce arthralgia in chronic infections [10].

Due to the lack of efficient anti-CHIKV therapy, researches have been developed to identify new drug candidates for the future treatment of chikungunya fever [21]. Among them, antiviral research based on natural molecules is a potential approach. Many natural compounds showed antiviral activity against a variety of human viruses such as dengue (DENV) [22–25], yellow fever

(YFV) [25–27], hepatitis C (HCV) [28–32], influenza [33,34], and zika (ZIKV) [33,35,36]. Here, we aim to summarize the natural compounds previously described to possess anti-CHIKV activity.

2. Inhibitors of CHIKV Replicative Cycle

2.1. Epigallocatechin Gallate (Green Tea)

Epigallocatechin gallate (EGCG) is the major catechin constituent in green tea that has shown antiviral activity against CHIKV in vitro [37]. HEK 293T cells (human kidney cells) were infected with the pseudo particles CHIKV-mCherry-490 with a multiplicity of infection of 1 (MOI = 1) in the presence or absence of EGCG at 10 µg/mL, which blocked up to 60% of CHIKV entry. Through lentiviral expression of CHIKV glycoprotein, the authors evaluated the antiviral activity of EGCG on entry steps and suggested that EGCG interferes with CHIKV entry due to their effect on CHIKV envelope protein [37].

2.2. Chloroquine

According to the studies of Khan and coworkers, a synthetic compound derived from the natural Chloroquine used to treat malaria infection has shown antiviral activity against CHIKV [38]. To do this, Vero cells were infected with the African East-Central-South (ECSA) CHIKV genotype, DRE-06 strain, and incubated with the compound at 5, 10, or 20 µM to evaluate its antiviral activity. Three treatment strategies were used for the plaque assay: 1) pretreatment of the cells 24 h before infection; 2) concurrent treatment by simultaneously adding virus and chloroquine; and 3) treatment of cells up to 6 h post-CHIKV infection of Vero cells. Chloroquine at 20 µM was nontoxic to the cells and inhibited CHIKV entry by approximately 94% when cells were pretreated, 70% in the concurrent treatment, and 65% in the post-infection treatment. The results suggested that this compound presents strong antiviral activity, mainly when administered 24 h prior to infection [38].

2.3. Apigenin, Chrysin, Luteonin, Narigenin, Silybin, and Prothipendyl

Pohjala and colleagues demonstrated the anti-CHIKV activity of five natural compounds by using either a replicon cell line expressing the nonstructural proteins of CHIKV and the *eGFP* and Renilla luciferase (*Rluc*) markers or the full-length virus genetically modified with the reporter *Rluc*. Firstly, BHK21 (baby hamster kidney) cells were infected with the full length CHIKV-*Rluc* (MOI = 0.001) and simultaneously treated with different concentrations of each compound ranging from 0.01 to 100 µM for 16 h. The compounds apigenin (inhibitory concentration (IC₅₀) = 70.8 µM), chrysin (IC₅₀ = 126.6 µM), narigenin (IC₅₀ = 118.4 µM), silybin (IC₅₀ = 92.3 µM), and prothipendyl (IC₅₀ = 97.3 µM) significantly inhibited CHIKV-*Rluc* replication [39].

In addition, Muralli and coworkers also tested the antiviral activity of apigenin and luteonin ethanolic fraction from *Cynodondactylon* in Vero cells and found that the fractions inhibited 98% of CHIKV activity at concentration of 50 µg/mL through the cytopathic effect [40]. Using a reverse transcriptase polymerase chain-reaction (RT-PCR) the authors also demonstrated that virus RNA levels decreased under treatment. In another study, apigenin and luteonin were isolated from a fraction of the *Cynodondactylon* plant, obtained from the National Institute of Virology of India, and were used to assess the cytotoxicity and antiviral activity in Vero cells. Results showed that concentrations ranging from 5 to 200 µg/mL were nontoxic as determined by 3-(4,5-dimethylthiazol-2-yl)-2,5-diphenyltetrazolium bromide cell proliferation assay (MTT assay). In addition, treatment of cells at 10, 25, and 50 µg/mL showed a reduction of viral activity by decreasing 68%, 88%, and 98% of the cytopathic effect of the virus, respectively [39,40].

2.4. Flavaglines

As CHIKV uses prohibitin as a receptor to entry into mammalian cells [13], Wintachai and colleagues investigated the anti-CHIKV activity of the plant-derived compounds sulfonyl amidines

1M and the flavaglines FL3 and FL23 [41], previously reported to interact with this receptor. These compounds demonstrated antiviral activity against the CHIKV strain E1:226V East-Central-South-Africa (ECSA) genotype of a Thai isolate. The cell line HEK-293T/17 was added to each compound at specific concentrations (1, 5, 10, and 20 nM) for one hour and then infected with 10 pfu/cell of CHIKV. After 20 h, cell pellets were submitted to flow cytometry and the supernatant to a plaque assay to measure CHIKV titers. All three compounds significantly reduced the percentage of viral production in the infected cells at 10 and 20 nM concentrations. Sulfonyl amidine 1M and FL23 at 20 nM reduced viral cytopathic effect by approximately 40%, and FL3 at 20 nM reduced viral yield by 50% [41].

2.5. Compounds from *Tectona grandis*

The antiviral activity of three isolated and characterized compounds from *Tectonagrandis* had its antiviral activity tested against the CHIKV strains ECSA KC 969208 and Asian KC969207 in Vero cells [42]. The authors determined IC₅₀ of the compounds 2-(butoxycarbonyl) benzoic acid (BCB), 3,7,11,15-tetramethyl-1-hexadecanol (THD), and benzene-1-carboxylic acid-2-hexadecanoate (BHCD). They demonstrated that the most potent anti-CHIKV activity was observed for BHCD with selectivity index (SI) of 116 for the Asian strain and 4.66 for ECSA. In silico analyses were performed and showed that the compound possessed strong interactions with CHIKV envelope protein 1 (E1) and poor interactions with nonstructural proteins (nSP) that may suggest that this compound could act on CHIKV entry [42].

2.6. *Trigocherrierin A*

The work of Bourjot and colleagues showed that compounds isolated from the *Trigonostemoncherrieri* presented inhibitory activity against CHIKV replication [43]. Vero cells were used in cell proliferation assay (MTS) to evaluate the anti-CHIKV activity of compounds by decreasing the cell death induced by the virus infection [43]. Among the isolated compounds, trigocherrierin A inhibited death of cells caused by the virus with a concentration that induced half of the maximum effect (EC₅₀) of 0.6 ± 0.1 μM, CC₅₀ of 43 ± 16 μM, and the SI of 71.7. Thus, trigocherrierin A has been shown to be the most potent tested compound against CHIKV replication in this study [43].

2.7. *Harringtonine*

Harringtonine, a natural compound derived from the Japanese plant *Cephalotaxusharringtonia*, demonstrated antiviral activity against CHIKV replication [44]. The authors investigated the anti-CHIKV activity of this compound by using the cell lines BHK-21, C6/36 (embryonic tissue cells of the *Aedes albopictus* mosquito), and HSMM (human skeletal muscle myoblasts) and the virus strains CHIKV-0708 (Singapore 07/2008, lacking the A226V mutation in E1 protein) and CHIKV-122508 (SGEHICHD 122508, having the A226V mutation in the E1 protein) [44]. In BHK-21 cells, harringtonine at 1 and 10 μM showed potent anti-CHIKV action, inhibiting up to 90% of viral replication with cell viability higher than 80%. Aiming to investigate the harringtonine mechanism of action, the authors performed a time addition assay. Compounds were added at different concentrations, prior to infection (-2 h) and at 0, 2, 6, 12, and 16 hours post infection (h.p.i.). Treatments showed inhibition of CHIKV replication at 2 h.p.i, indicating that harringtonine inhibits the early steps of the CHIKV replicative cycle. Additionally, cells were infected and treated for 6 h, and western blot and qRT-PCR assays were performed. The results showed that harringtonine reduced negative- and positive-sense RNAs of CHIKV and the production of nSP3 and E2 proteins [44].

2.8. *Diterpene Ester (phorbol-12,13-didecanoate)*

Twenty-nine diterpenoids isolated from *Euphorbiaceae* species had their antiviral activity tested against CHIKV (Indian Ocean strain 899) in vitro through MTS assay [45,46]. First, media with serial dilutions of each compound was added to empty 96-well microplate, and then, each well was added of media containing Vero cells (2.5×10^3 cells per well) and CHIKV for 6–7 days. Among the tested compounds, phorbol-12,13-didecanoate was shown to be the strongest candidate as an antiviral against CHIKV replication, with an EC_{50} 6.0 ± 0.9 nM [45,46].

2.9. Daphnanane Diterpenoid Ortho Esters

A panel of diterpenoids or thioesters isolated from *Trigonostemon cherrieri* was used to evaluate the antiviral activity against CHIKV [47]. Vero cells were used to determine the cytotoxicity of compounds, and antiviral properties were accessed by plaque assay. Among the tested compounds, Trigoocherrins A, B, and F were shown to be potent inhibitors of CHIKV replication with SIs of 23, 36, and 8, respectively [45].

2.10. Aplysiatoxin-Related Compounds

Five bioactive compounds from the cyanobacteria *Trichodesmium erythraeum* had their antiviral activity evaluated [47]. Cell viability was measured and a dose-dependent anti-CHIKV assay was performed to access the antiviral activity of the compounds under pre- or post-treatment conditions. The Debromo analogues 2 and 5 showed significant antiviral activity in post-treatment of infected BHK 21 cells with EC_{50} of 1.3 and 2.7 μ M and SI of 10.9 and 9.2, respectively. The authors suggested that the antiviral activity of these compounds blocks the replication step of the CHIKV replicative cycle [47].

2.11. Tannic Acid

Tannic acid (TA) is a compound found in different species of plants, but its structure varies according to their sources. It previously demonstrated antiviral activity against viruses as Herpes (HSV) and HCV [48,49]. The anti-CHIKV activity of TA was investigated by KONISHI and HOTTA by performing plaque reduction assay using BHK-21 cells [50]. TA reduced 50% of the virus infectivity in lower concentrations and demonstrated inhibition of virus post-entry steps in BHK-21 cells. To investigate which chemical group of TA is associated with its antiviral activity, the authors tested TA analogues on their virus-inhibiting capacities. The results demonstrated that phenolic hydroxyl groups may be related to the antiviral activity, since the displacement of these groups make the molecule ineffective [50].

2.12. Silymarin

Silymarin is a polyphenolic compound from flavonoids family, is extracted from *Silybum marianum*, and is described to possess antiviral activity against HCV [51]. A study tested the activity of silymarin on CHIKV genotype ECSA with A226V mutation in E1 protein from a clinical strain isolated in an outbreak in 2008. BHK-21 and Vero cells were used to evaluate different steps of the viral replicative cycle, and silymarin showed inhibition of post-entry stages of CHIKV with an EC_{50} of 16.9 μ g/mL and SI of 25.1. By using a stable cell line expressing CHIKV replicon and *EGFP* and *Rluc* markers [39], it was demonstrated that silymarin suppressed 93.4% of CHIKV replication. Western blot assay was performed, showing that silymarin treatment decreased the amounts of nSP1, nSP3, and E2 proteins [52].

2.13. Baicalein, Fisetin, and Quercetin

Baicalein, fisetin, and quercetin are compounds from the flavonoids family that exhibited antiviral activity against DENV [22] and enterovirus A71 [53]. Lani and colleagues infected Vero cells with the CHIKV genotype ECSA strain from the outbreak of 2008 and evaluated their effects in reducing the cytopathic effect resulting from viral infection [54]. All three compounds were found

to inhibit CHIKV replication in a dose-dependent manner and reduced E2, nSP1, and nSP3 protein synthesis, as showed by Western blot analysis. Baicalein and quercetagenin showed anti-CHIKV activity by inactivating the virus, preventing the attachment of the virus to the host cells and blocking post-entry stages, with EC₅₀ of 1.891 µg/mL and 13.85 µg/mL, respectively. Fisetin only inhibited post-entry steps with EC₅₀ of 8.44 µg/mL [54].

2.14. Bryostatin

Bryostatin is a macrolide lactone derived from a marine animal named *Bugula neritina* [55]. It was described by the antineoplastic activity [56], affects Alzheimer's disease [57], and has been related to the eradication of human immunodeficiency virus reservoirs [58]. The anti-CHIKV activities of the Bryostatin analogs salicylate-derived analog 1, C26-capped analog 2, and C26-capped analog 3 were assessed by evaluating the cytopathic effect (CPE) caused by CHIKV Indian Ocean lineage strain 899 replication under treatment with these three compounds [59]. All of the Bryostatin analogs inhibited the CHIKV replicative cycle, decreasing infectious progeny and viral RNA copies, confirmed by supernatant titration and RT-PCR. A time-addition assay showed that these compounds inhibited late stages of CHIKV replication, with EC₅₀ rates of 4 µM, 8 µM, and 7.5 µM, respectively. Additionally, salicylate-derived analog 1 but not the other compounds blocked entry of CHIKV pseudoparticles into Buffalo green monkey kidney cells (BGM) [59].

2.15. Prostratin

Bourjot and coworkers described the effect of prostratin, a compound derived from *Trigonostemonhowii*, on CHIKV infection in Vero cells by a CPE assay (EC₅₀ = 2.6 µM) [60]. Another work used CHIKV lineage Indian Ocean 899 to infected Vero, BGM, or Human embryonic lung fibroblasts (HEL) cells at MOI of 0.001 under the treatment with prostratin and obtained EC₅₀ of 8 µM, 7.6 µM, and 7.1 µM, respectively. Using a delay treatment associated with a RT-PCR or CHIKV pseudoparticle techniques, it was demonstrated that prostratin decreased both the number of CHIKV genome copies and the production of infectious progeny virus particles. A western blot assay was used to detect CHIKV proteins and showed that prostratin also reduced the accumulation of nSP1 and capsid proteins [60].

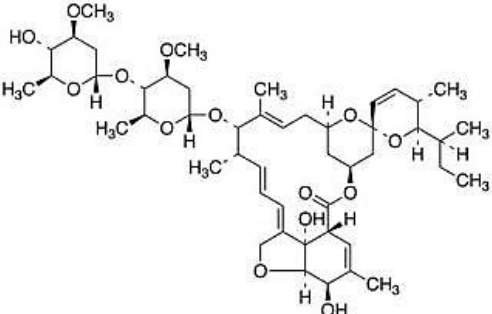
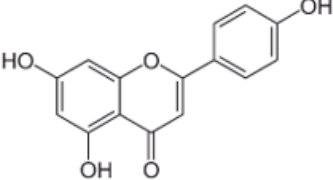
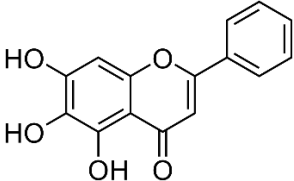
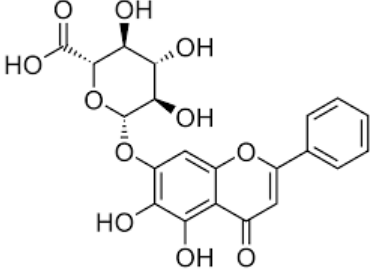
2.16. Berberine

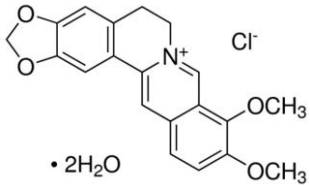
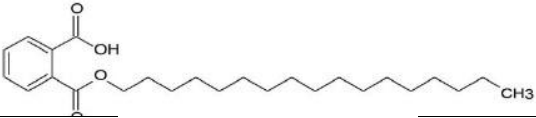
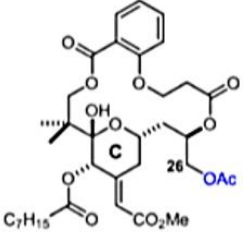
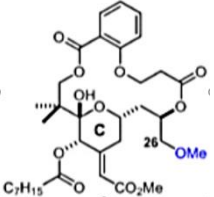
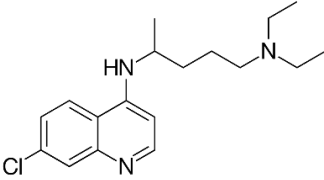
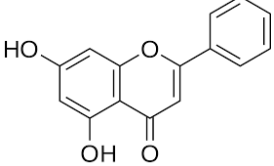
Berberine is a compound found in plants from the *Berberis* genus, family *Berberidaceae*, that previously demonstrated antiviral activity against other viruses [61]. Varghese and colleagues analyzed the antiviral effect of berberine on the CHIKV replication cycle using the CHIKV lineage LR2006 OPY1 with the *Rluc* marker to infect HEK-293T, HOS (human bone osteosarcoma), and CRL-2522 cells. The berberine EC₅₀ for each cell line were 4.5, 12.2, and 35.3 µM, respectively. This compound was also active against the different CHIKV strains LR2006 OPY1, SGP11, and CNR20235, showing EC₅₀ of 37.6, 44.2, and 50.9 µM, respectively. Berberine showed no inhibition on CHIKV entry or replication but decreased viral RNA and viral protein synthesis, suggesting that berberine is indirectly perturbing CHIKV replication by affecting host components [61].

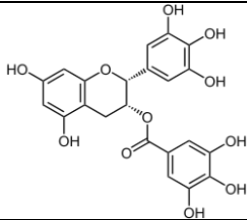
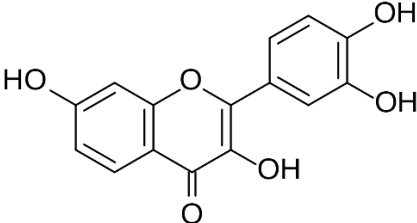
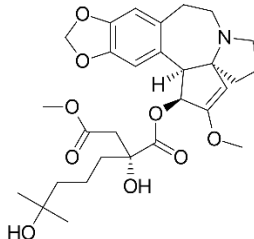
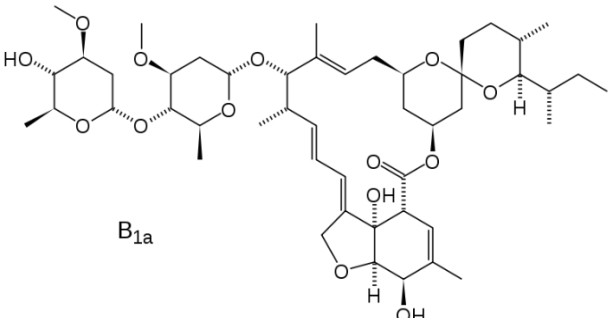
2.17. Avermectin derivatives

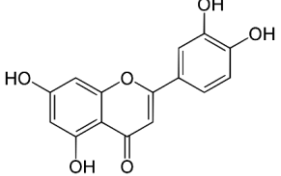
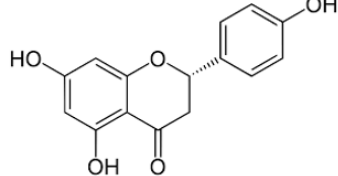
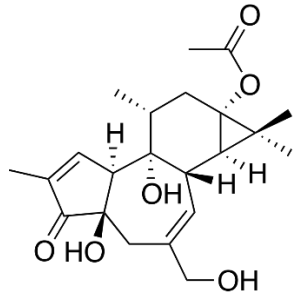
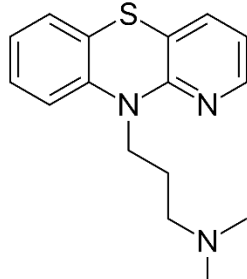
Avermectin is naturally produced in *Streptomyces avermitilis* bacteria and showed different biological properties including antiparasitic [62], antiviral [63], and antibacterial [64,65] activities. Ivermectin (IVN) and abamectin (ABN) are chemically modified derivatives of avermectin. The activity of these derivatives on the CHIKV replication cycle was described in a study that used BHK-21 with CHIKV containing the *Rluc* gene [66]. IVN and ABN demonstrated EC₅₀ of 0.6 µM and 1.5 µM, respectively, and strongly reduced nSP1 and nSP3 even in high MOIs. A time-of-addition assay demonstrated that IVN and ABN interfered in earlier stages of CHIKV cycle but not when

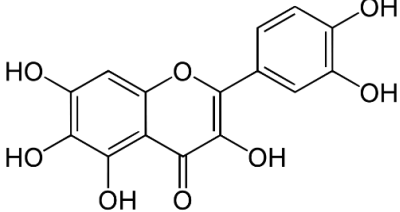
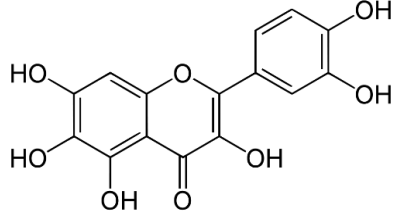
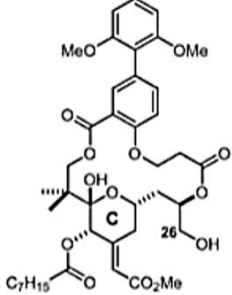
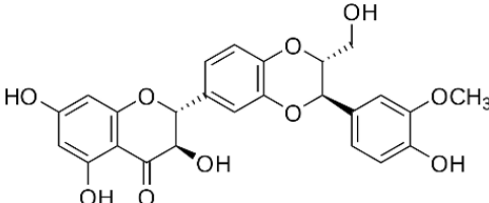
cells were pretreated. Alternatively, the activity of these compounds was decreased in the later stages of the CHIKV replicative cycle [66].

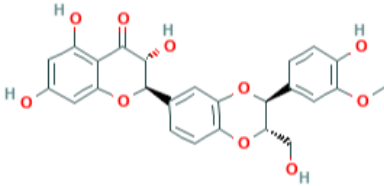
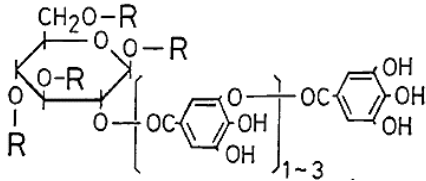
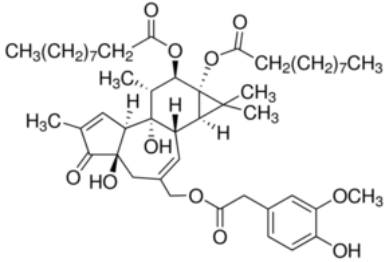
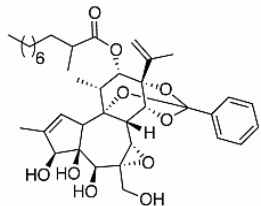
Compound	Structure	Inhibition	SI or EC ₅₀	Cell Line
Abamectin [66]		Replication	1.5 μM	BHK-21
Apigenin [40,39]		Infection/Replication	70.8 μM	BHK 21
Baicalein [54]		Infection and replication	1.891 μg/mL	BHK-21
Baicalein [54]		Entry, binding	6.997 μM	Vero

Berberine [61]		Replication (interfering in host components)	≤35.3 μM	CRL-2522, HEK-293T, and HOS
BHCD [42]		Entry	116 (Asian strain) and 4.66 (ECSA)	Vero and in silico
C26-capped bryostatin analog 2 [59]		Replication	8 μM	Vero
C26-capped bryostatin analog 3 [59]		Replication	7.5 μM	Vero
Chloroquine [38]		Entry	37.14	Vero
Chrysin [39]		Infection	126.6 μM	BHK 21

EGCG [37]		Entry steps; cell attachment	6.54 $\mu\text{g/mL}$	HEK 293T
Fisetin [54]		Replication	8.44 $\mu\text{g/mL}$	BHK-21
Harringtonine [44]		Early stages of replication	0.24 μM	BHK 21
Ivermectin [66]		Replication	0.6 μM	BHK-21

Luteolin [40]		Replication	NS	Vero
Narigenin [39]		Infection	118.4 μ M	BHK 21
Prostratin [60]		Replication and release	2,6 μ M and \pm 8 μ M	Vero, BGM, and HEL
Prothipendyl [39]		Replication	97.3 μ M	BHK 21

Quercetagetin [54]		Entry and binding	43.52 μ M	Vero
Quercetagetin [54]		Entry and replication	13.85 μ g/mL	BHK-21
Salicylate-derived bryostatin analog [59]		Entry and replication	4 μ M	Vero
Silybin [39]		Infection	92.3 μ M	BHK 21

Silymarin [52]		Replication	16.9 µg/mL	BHK-21 and Vero
Tannic Acid [50]		Replication	NS	BHK-21
Phorbol-12,13-didecanoate [46]		Replication	6 ± 0.9 nM	Vero
Trigocherrierin [43]		Replication	0.6 ± 0.1 µM	Vero

NS = Not shown, data not shown.

3. Prospects

The aim of this review was to summarize data from literature concerning the natural compounds described to possess anti-CHIKV activity. Altogether, data is heterogeneous since authors developed a variety of assays using different cell lines and CHIKV strains or replicons. Some studies did not elucidate the mechanism of action (MOA) of the compound, retaining their information as EC₅₀, CC₅₀, and/or SI. For most of the compounds presented in this review, it would be desirable to demonstrate the MOA in order to elucidate the biochemical and molecular basis of the compound–virus or compound–cell interactions and to be able to predict and promote strategies for pharmacological outcomes in further studies [67]. Also, the investigation of the effects of each compound in different cell lines would provide important information concerning the effects of these compounds on the host cells [68,69]. Besides that, all data summarized here represent a relevant source of knowledge concerning the antiviral potential of molecules isolated from nature.

From the natural compounds cited in this review, chloroquine was the only compound tested *in vivo*, in non-human primates, and in human clinical trials. Chloroquine is already used for the treatment of malaria [70]. However, despite the *in vitro* results, chloroquine demonstrated no relevant results *in vivo* in decreasing viremia or in reducing clinical manifestations during acute stage of CHIKV infection [71]. Therefore, the results demonstrated by *in vitro* analysis were not correlated with the *in vivo* analysis that showed that chloroquine was not suitable for patients with CHIKV. Additionally, the remaining compounds described here have not been tested *in vivo* yet, representing a delay in anti-CHIKV drug development.

Apart from the chloroquine case, all compounds that demonstrated antiviral activity have the potential to be further investigated by their therapeutically properties against chikungunya fever. Furthermore, natural compounds may present as a source of molecules with potent biological activities that could be used as templates to the development of novel antivirals.

4. Conclusion

The spread of CHIKV in the last years demonstrated the need to develop effective antiviruses to treat chikungunya fever and to prevent future outbreaks. In this context, natural compounds have shown potent antiviral activity against a range of viruses. This review summarized the natural compounds described to possess anti-CHIKV activity by blocking early and/or late stages of virus replication *in vitro*. Apart from the great antiviral activity of the described compounds, further research is needed for the development of future treatments.

Funding: We would like to thank the Royal Society – Newton Advanced Fellowship (grant reference NA 150195), CNPQ (National Counsel of Technological and Scientific Development – grant 445021/2014-4), FAPEMIG (Minas Gerais Research Foundation - APQ-00587-14, SICONV 793988/2013 and APQ-03385-18) and CAPES (Coordination for the Improvement of Higher Education Personnel – Code 001), for financial support. ACGJ also thanks the CNPq for the productivity fellowship (311219/2019-5).

Conflicts of Interest: The authors declare no conflict of interest.

References

1. Ross, R.W. The virus: Isolation, Pathogenic properties and relationship to the epidemic. *Newala Epidemic* **1956**, 177–191.
2. Panning, M.; Grywna, K.; van Esbroeck, M.; Emmerich, P.; Drosten, C. Chikungunya Fever in Travelers Returning to Europe from the Indian Ocean Region, 2006. *Emerg. Infect. Dis.* **2008**, *14*, 416–422.

3. Schuffenecker, I.; Frangeul, L.; Vaney, M.; Iteman, I.; Michault, A.; Lavenir, R.; Pardigon, N.; Reynes, J.; Biscornet, L.; Diancourt, L. Genome Microevolution of Chikungunya Viruses Causing the Indian Ocean Outbreak. *PLoS Med.* **2006**, *3*, 1058–1070.
4. Henry, M.; Francis, L.; Asin, V.; Polson-Edwards, K.; Olowokure, B. Chikungunya virus outbreak in Sint Maarten, 2013-2014. *Rev. Panam. Salud Publica Pan Am. J. Public Health* **2017**, *41*, e61.
5. Morens, D.M.; Fauci, A.S. Chikungunya at the Door — Déjà Vu All Over Again? *N. Engl. J. Med.* **2014**, *371*, 885–887.
6. PAHO PAHO WHO. Chikungunya. Data, Maps and statistics. Available online: https://www.paho.org/hq/index.php?option=com_topics&view=Drdmore&cid=5927&itemid=40931&lang=En (accessed on 28 Dec, 2019).
7. Carbajo, A.E.; Vezzani, D. Waiting for chikungunya fever in Argentina: Spatio-temporal risk maps. *Mem. Inst. Oswaldo Cruz* **2015**, *110*, 259–262.
8. Badar, N.; Salman, M.; Ansari, J.; Ikram, A.; Qazi, J.; Alam, M.M. Epidemiological trend of chikungunya outbreak in Pakistan: 2016-2018. *PLoS Negl. Trop. Dis.* **2019**, *13*, 2018–2019.
9. Renault, P.; Solet, J.; Sissoko, D.; Balleydier, E.; Larrieu, S.; Filleul, L.; Lassalle, C.; Thiria, J.; Rachou, E.; Valk, H. De; et al. A Major Epidemic of Chikungunya Virus Infection on Réunion Island. *Am. Soc. Trop. Med. Hyg.* **2007**, *77*, 727–731.
10. Thiberville, S.D.; Moyen, N.; Dupuis-Maguiraga, L.; Nougairede, A.; Gould, E. a.; Roques, P.; de Lamballerie, X. Chikungunya fever: Epidemiology, clinical syndrome, pathogenesis and therapy. *Antiviral Res.* **2013**, *99*, 345–370.
11. Song, H.; Zhao, Z.; Chai, Y.; Jin, X.; Li, C.; Yuan, F.; Liu, S.; Gao, Z.; Wang, H.; Song, J.; et al. Molecular Basis of Arthritogenic Alphavirus Receptor MXRA8 Binding to Chikungunya Virus Envelope Protein. *Cell* **2019**, *177*, 1714–1724.e12.
12. Zhang, R.; Earnest, J.T.; Kim, A.S.; Winkler, E.S.; Desai, P.; Adams, L.J.; Hu, G.; Bullock, C.; Gold, B.; Cherry, S.; et al. Expression of the Mxra8 Receptor Promotes Alphavirus Infection and Pathogenesis in Mice and Drosophila. *Cell Rep.* **2019**, *28*, 2647–2658.e5.
13. Wintachai, P.; Wikan, N.; Kuadkitkan, A.; Jaimipuk, T.; Ubol, S.; Pulmanasakakil, R.; Auewarakul, P.; Kasinrerak, W.; Weng, W.-Y.; Panyasrivanit, M.; et al. Identification of Prohibitin as a Chikungunya Virus Receptor Protein. *J. Med. Virol.* **2012**, *84*, 1757–1770.
14. Moller-Tank, S.; Kondratowicz, A.S.; Davey, R.A.; Rennert, P.D.; Maury, W. Role of the Phosphatidylserine Receptor TIM-1 in Enveloped-Virus Entry. *J. Virol.* **2013**, *87*, 8327–8341.
15. Silva, L.A.; Khomandiak, S.; Ashbrook, A.W.; Weller, R.; Heise, M.T.; Morrison, T.E.; Dermody, T.S.; Lyles, D.S. A Single-Amino-Acid Polymorphism in Chikungunya Virus E2 Glycoprotein Influences Glycosaminoglycan Utilization. *J. Virol.* **2014**, *88*, 2385–2397.
16. Fongsaran, C.; Jirakanwisal, K.; Kuadkitkan, A.; Wikan, N.; Wintachai, P.; Thepparit, C.; Ubol, S.; Phaonakrop, N.; Roytrakul, S.; Smith, D.R. Involvement of ATP synthase β subunit in chikungunya virus entry into insect cells. *Arch. Virol.* **2014**, *159*, 3353–3364.
17. Abdelnabi, R.; Neyts, J.; Delang, L. Towards antivirals against chikungunya virus. *Antiviral Res.* **2015**, *121*, 59–68.
18. Gould, E.A.; Coutard, B.; Malet, H.; Morin, B.; Jamal, S.; Weaver, S.; Gorbalenya, A.; Moureau, G.; Baronti, C.; Delogu, I.; et al. Understanding the alphaviruses: Recent research on important emerging pathogens and progress towards their control. *Antiviral Res.* **2010**, *87*, 111–124.
19. Lima, M.E. de S.; Bachur, T.P.R.; Aragão, G.F. Guillain-Barre syndrome and its correlation with dengue, Zika and chikungunya viruses infection based on a literature review of reported cases in Brazil. *Acta Trop.* **2019**, *197*, 105064.
20. W.H.O. Chikungunya. Available online: <https://www.who.int/news-room/fact-sheets/detail/chikungunya> (accessed on 28 Dec, 2019).
21. Yactayo, S.; Staples, J.E.; Millot, V.; Cibrelus, L.; Ramon-Pardo, P. Epidemiology of Chikungunya in the Americas. *J. Infect. Dis.* **2016**, *214*, S441–S445.
22. Zandi, K.; Teoh, B.-T.; Sam, S.-S.; Wong, P.-F.; Mustafa, M.R.; AbuBakar, S. Novel antiviral activity of baicalein against dengue virus. *BMC Complement. Altern. Med.* **2012**, *12*, 1185.

23. Jain, J.; Kumar, A.; Narayanan, V.; Ramaswamy, R.S.; Sathiyarajeswaran, P.; Shree Devi, M.S.; Kannan, M.; Sunil, S. Antiviral activity of ethanolic extract of NilavembuKudineer against dengue and chikungunya virus through in vitro evaluation. *J. Ayurveda Integr. Med.***2019**.
24. Gómez-Calderón, C.; Mesa-Castro, C.; Robledo, S.; Gómez, S.; Bolivar-Avila, S.; Diaz-Castillo, F.; Martínez-Gutierrez, M. Antiviral effect of compounds derived from the seeds of *Mammea americana* and *Tabernaemontana cymosa* on Dengue and Chikungunya virus infections. *BMC Complement. Altern. Med.***2017**, *17*, 57.
25. Mastrangelo, E.; Pezzullo, M.; De burghgraeve, T.; Kaptein, S.; Pastorino, B.; Dallmeier, K.; De lamballerie, X.; Neyts, J.; Hanson, A.M.; Frick, D.N.; et al. Ivermectin is a potent inhibitor of flavivirus replication specifically targeting NS3 helicase activity: New prospects for an old drug. *J. Antimicrob. Chemother.***2012**, *67*, 1884–1894.
26. Julander, J.G. Experimental therapies for yellow fever. *Antiviral Res.***2013**, *97*, 169–179.
27. Danielle, V.; Muller, M.; Rinaldi, R.; Cristina, A.; Cintra, O.; Aurélio, M.; Alves-paiva, R.D.M.; Tadeu, L.; Figueiredo, M.; Vilela, S.; et al. Toxicon Crotoxin and phospholipases A 2 from *Crotalus durissus terri* fi cus showed antiviral activity against dengue and yellow fever viruses. *Toxicon***2012**, *59*, 507–515.
28. Calland, N.; Dubuisson, J.; Rouillé, Y.; Séron, K. Hepatitis C virus and natural compounds: A new antiviral approach? *Viruses***2012**, *4*, 2197–2217.
29. Campos, G.R.F.; Bittar, C.; Jardim, A.C.G.; Shimizu, J.F.; Batista, M.N.; Paganini, E.R.; Assis, L.R. de; Bartlett, C.; Harris, M.; Bolzani, V. da S.; et al. Hepatitis C virus in vitro replication is efficiently inhibited by acridone Fac4. *J. Gen. Virol.***2017**, *98*, 1693–1701.
30. Stankiewicz-drogon, A.; Palchykovska, L.G.; Kostina, V.G.; Alexeeva, I. V.; Shved, A.D.; Boguszewska-chachulska, A.M. New acridone-4-carboxylic acid derivatives as potential inhibitors of Hepatitis C virus infection. *Bioorg. Med. Chem.***2008**, *16*, 8846–8852.
31. Jardim, A.C.G.; Igloi, Z.; Shimizu, J.F.; Santos, V.A.F.F.M.; Felipe, L.G.; Mazzeu, B.F.; Amako, Y.; Furlan, M.; Harris, M.; Rahal, P. Natural compounds isolated from Brazilian plants are potent inhibitors of hepatitis C virus replication in vitro. *Antiviral Res.***2015**, *115*, 39–47.
32. Shimizu, J.F.; Lima, C.S.; Pereira, C.M.; Bittar, C.; Batista, M.N.; Nazaré, A.C.; Polaquini, C.R.; Zothner, C.; Harris, M.; Rahal, P.; et al. Flavonoids from *Pterogynenitens* Inhibit Hepatitis C Virus Entry. *Sci. Rep.***2017**, *7*, 16127.
33. Varghese, F.S.; Rausalu, K.; Hakanen, M.; Saul, S.; Kümmerer, B.M.; Susi, P.; Merits, A.; Ahola, T. Obatoclox Inhibits Alphavirus Membrane Fusion by Neutralizing the Acidic Environment of Endocytic Compartments. *Antimicrob. Agents Chemother.***2017**, *61*, 1–17.
34. Song, J.M.; Lee, K.H.; Seong, B.L. Antiviral effect of catechins in green tea on influenza virus. *Antiviral Res.***2005**, *68*, 66–74.
35. Li, C.; Deng, Y.; Wang, S.; Ma, F.; Aliyari, R.; Huang, X.-Y.; Zhang, N.-N.; Watanabe, M.; Dong, H.-L.; Liu, P.; et al. 25-Hydroxycholesterol Protects Host against Zika Virus Infection and Its Associated Microcephaly in a Mouse Model. *Immunity***2017**, *46*, 446–456.
36. Carneiro, B.M.; Batista, M.N.; Braga, A.C.S.; Nogueira, M.L.; Rahal, P. The green tea molecule EGCG inhibits Zika virus entry. *Virology***2016**, *496*, 215–218.
37. Weber, C.; Sliva, K.; Von Rhein, C.; Kümmerer, B.M.; Schnierle, B.S. The green tea catechin, epigallocatechin gallate inhibits chikungunya virus infection. *Antiviral Res.***2015**, *113*, 1–3.
38. Khan, M.; Santhosh, S.R.; Tiwari, M.; Rao, P.V.L.; Parida, M. Assessment of In Vitro Prophylactic and Therapeutic Efficacy of Chloroquine Against Chikungunya Virus in Vero Cells. **2010**, *824*, 817–824.
39. Pohjala, L.; Utt, A.; Varjak, M.; Lulla, A.; Merits, A.; Ahola, T.; Tammela, P. Inhibitors of Alphavirus Entry and Replication Identified with a Stable Chikungunya Replicon Cell Line and Virus-Based Assays. *PLoS ONE***2011**, *6*, e28923.
40. Murali, K.S.; Sivasubramanian, S.; Vincent, S.; Murugan, S.B.; Giridaran, B.; Dinesh, S.; Gunasekaran, P.; Krishnasamy, K.; Sathishkumar, R. Anti-chikungunya activity of luteolin and apigenin rich fraction from *Cynodondactylon*. *Asian Pac. J. Trop. Med.***2015**, *8*, 352–358.
41. Wintachai, P.; Thuaud, F.; Basmadjian, C.; Roytrakul, S.; Ubol, S.; Désaubry, L.; Smith, D.R. Assessment of flavaglines as potential chikungunya virus entry inhibitors. *Microbiol. Immunol.***2015**, *59*, 129–141.

42. Sangeetha, K.; Purushothaman, I.; Rajarajan, S. Spectral characterisation, antiviral activities, in silico ADMET and molecular docking of the compounds isolated from *Tectonagrandis* to chikungunya virus. *Biomed. Pharmacother.* **2017**, *87*, 302–310.
43. Bourjot, M.; Leyssen, P.; Neyts, J.; Dumontet, V.; Litaudon, M. Trigocherrierin A, a potent inhibitor of chikungunya virus replication. *Molecules* **2014**, *19*, 3617–3627.
44. Kaur, P.; Thiruchelvan, M.; Lee, R.C.H.; Chen, H.; Chen, K.C.; Ng, M.L.; Chu, J.J.H. Inhibition of Chikungunya virus replication by harringtonine, a novel antiviral that suppresses viral protein expression. *Antimicrob. Agents Chemother.* **2013**, *57*, 155–167.
45. Allard, P.M.; Leyssen, P.; Martin, M.T.; Bourjot, M.; Dumontet, V.; Eydoux, C.; Guillemot, J.C.; Canard, B.; Poullain, C.; Guéritte, F.; et al. Antiviral chlorinated daphnane diterpenoid orthoesters from the bark and wood of *Trigonostemoncherrieri*. *Phytochemistry* **2012**, *84*, 160–168.
46. Nothias-Scaglia, L.-F.; Pannecouque, C.; Renucci, F.; Delang, L.; Neyts, J.; Roussi, F.; Costa, J.; Leyssen, P.; Litaudon, M.; Paolini, J. Antiviral Activity of Diterpene Esters on Chikungunya Virus and HIV Replication. *J. Nat. Prod.* **2015**, *78*, 1277–1283.
47. Gupta, D.K.; Kaur, P.; Leong, S.T.; Tan, L.T.; Prinsep, M.R.; Chu, J.J.H. Anti-Chikungunya viral activities of aplysiatoxin-related compounds from the marine cyanobacterium *Trichodesmiumerythraeum*. *Mar. Drugs* **2014**, *12*, 115–127.
48. Liu, S.; Chen, R.; Hagedorn, C.H. Tannic Acid Inhibits Hepatitis C Virus Entry into Huh7.5 Cells. *PLoS ONE* **2015**, *10*, e0131358.
49. Orłowski, P.; Kowalczyk, A.; Tomaszewska, E.; Ransozek-Soliwoda, K.; Węgrzyn, A.; Grzesiak, J.; Celichowski, G.; Grobelny, J.; Eriksson, K.; Krzyzowska, M. Antiviral Activity of Tannic Acid Modified Silver Nanoparticles: Potential to Activate Immune Response in Herpes Genitalis. *Viruses* **2018**, *10*, 524.
50. Konishi, E.; Hotta, S. Effects of Tannic Acid and Its Related Compounds upon Chikungunya Virus. *Microbiol. Immunol.* **1979**, *23*, 659–667.
51. Wagoner, J.; Negash, A.; Kane, O.J.; Martinez, L.E.; Nahmias, Y.; Bourne, N.; Owen, D.M.; Grove, J.; Brimacombe, C.; McKeating, J.A.; et al. Multiple effects of silymarin on the hepatitis C virus lifecycle. *Hepatol. Baltim. Md* **2010**, *51*, 1912–1921.
52. Lani, R.; Hassandarvish, P.; Chiam, C.W.; Moghaddam, E.; Chu, J.J.H.; Rausalu, K.; Merits, A.; Higgs, S.; Vanlandingham, D.; Abu Bakar, S.; et al. Antiviral activity of silymarin against chikungunya virus. *Sci. Rep.* **2015**, *5*, 11421.
53. Li, X.; Liu, Y.; Wu, T.; Jin, Y.; Cheng, J.; Wan, C.; Qian, W.; Xing, F.; Shi, W. The Antiviral Effect of Baicalin on Enterovirus 71 In Vitro. *Viruses* **2015**, *7*, 4756–4771.
54. Lani, R.; Hassandarvish, P.; Shu, M.-H.; Phoon, W.H.; Chu, J.J.H.; Higgs, S.; Vanlandingham, D.; Abu Bakar, S.; Zandi, K. Antiviral activity of selected flavonoids against Chikungunya virus. *Antiviral Res.* **2016**, *133*, 50–61.
55. HALFORD, B. THE BRYOSTATINS' TALE. *Chem. Eng. News Arch.* **2011**, *89*, 10–17.
56. Plimack, E.R.; Tan, T.; Wong, Y.-N.; von Mehren, M.M.; Malizzia, L.; Roethke, S.K.; Litwin, S.; Li, T.; Hudes, G.R.; Haas, N.B. A Phase I Study of Temsirolimus and Bryostatatin-1 in Patients With Metastatic Renal Cell Carcinoma and Soft Tissue Sarcoma. *The Oncologist* **2014**, *19*, 354–355.
57. Schrott, L.M.; Jackson, K.; Yi, P.; Dietz, F.; Johnson, G.S.; Basting, T.F.; Purdum, G.; Tyler, T.; Rios, J.D.; Castor, T.P.; et al. Acute oral Bryostatatin-1 administration improves learning deficits in the APP/PS1 transgenic mouse model of Alzheimer's disease. *Curr. Alzheimer Res.* **2015**, *12*, 22–31.
58. Mehla, R.; Bivalkar-Mehla, S.; Zhang, R.; Handy, I.; Albrecht, H.; Giri, S.; Nagarkatti, P.; Nagarkatti, M.; Chauhan, A. Bryostatatin Modulates Latent HIV-1 Infection via PKC and AMPK Signaling but Inhibits Acute Infection in a Receptor Independent Manner. *PLoS ONE* **2010**, *5*, e11160.
59. Abdelnabi, R.; Staveness, D.; Near, K.E.; Wender, P.A.; Delang, L.; Neyts, J.; Leyssen, P. Comparative analysis of the anti-chikungunya virus activity of novel bryostatatin analogs confirms the existence of a PKC-independent mechanism. *Biochem. Pharmacol.* **2016**, *120*, 15–21.
60. Bourjot, M.; Delang, L.; Nguyen, V.H.; Neyts, J.; Guéritte, F.; Leyssen, P.; Litaudon, M. Prostratin and 12- O - Tetradecanoylphorbol 13-Acetate Are Potent and Selective Inhibitors of Chikungunya Virus Replication. *J. Nat. Prod.* **2012**, *75*, 2183–2187.

61. Varghese, F.S.; Thaa, B.; Amrun, S.N.; Simarmata, D.; Rausalu, K.; Nyman, T.A.; Merits, A.; McInerney, G.M.; Ng, L.F.P.; Ahola, T. The Antiviral Alkaloid Berberine Reduces Chikungunya Virus-Induced Mitogen-Activated Protein Kinase Signaling. *J. Virol.***2016**, *90*, 9743–9757.
62. Campbell, W.C.; Fisher, M.H.; Stapley, E.O.; Albers-Schönberg, G.; Jacob, T.A. Ivermectin: A potent new antiparasitic agent. *Science***1983**, *221*, 823–828.
63. Wagstaff, K.M.; Sivakumaran, H.; Heaton, S.M.; Harrich, D.; Jans, D.A. Ivermectin is a specific inhibitor of importin α/β -mediated nuclear import able to inhibit replication of HIV-1 and dengue virus. *Biochem. J.***2012**, *443*, 851–856.
64. Muhammed Ameen, S.; Drancourt, M. Ivermectin lacks antituberculous activity. *J. Antimicrob. Chemother.***2013**, *68*, 1936–1937.
65. Laing, R.; Gillan, V.; Devaney, E. Ivermectin – Old Drug, New Tricks? *Trends Parasitol.***2017**, *33*, 463–472.
66. Varghese, F.S.; Kaukinen, P.; Gläsker, S.; Bespalov, M.; Hanski, L.; Wennerberg, K.; Kümmerer, B.M.; Ahola, T. Discovery of berberine, abamectin and ivermectin as antivirals against chikungunya and other alphaviruses. *Antiviral Res.***2016**, 117–124.
67. Toxicology, N.R.C. (US) C. on A. of T.T. to P. *Application to the Study of Mechanisms of Action*; National Academies Press: Washington, DC, USA, 2007.
68. Kaur, G.; Dufour, J.M. Cell lines. *Spermatogenesis***2012**, *2*, 1–5.
69. Ulrich, A.B.; Pour, P.M. Cell Lines. In *Encyclopedia of Genetics*; Brenner, S., Miller, J.H., Eds.; Academic Press: New York, NY, USA, 2001; pp. 310–311.
70. Slater, A.F. Chloroquine: Mechanism of drug action and resistance in *Plasmodium falciparum*. *Pharmacol. Ther.***1993**, *57*, 203–235.
71. Roques, P.; Thiberville, S.-D.; Dupuis-Maguiraga, L.; Lum, F.-M.; Labadie, K.; Martinon, F.; Gras, G.; Lebon, P.; Ng, L.F.P.; de Lamballerie, X.; et al. Paradoxical Effect of Chloroquine Treatment in Enhancing Chikungunya Virus Infection. *Viruses***2018**, *10*, 268.



© 2019 by the authors. Submitted for possible open access publication under the terms and conditions of the Creative Commons Attribution (CC BY) license (<http://creativecommons.org/licenses/by/4.0/>).

OPEN **A diarylamine derived from anthranilic acid inhibits ZIKV replication**

Suely Silva^{1,2}, Jacqueline Farinha Shimizu^{1,2}, Débora Moraes de Oliveira¹, Leticia Ribeiro de Assis³, Cintia Bittar³, Melina Mottin⁴, Bruna Katiele de Paula Sousa⁴, Nathalya Cristina de Moraes Roso Mesquita⁵, Luis Octávio Regasini³, Paula Rahal², Glaucius Oliva⁵, Alexander Luke Perryman^{6,7}, Sean Ekins⁸, Carolina Horta Andrade⁴, Luiz Ricardo Goulart⁹, Robinson Sabino-Silva¹⁰, Andres Merits¹¹, Mark Harris¹² & Ana Carolina Gomes Jardim^{1,2*}

Zika virus (ZIKV) is a mosquito-transmitted Flavivirus, originally identified in Uganda in 1947 and recently associated with a large outbreak in South America. Despite extensive efforts there are currently no approved antiviral compounds for treatment of ZIKV infection. Here we describe the antiviral activity of diarylamines derived from anthranilic acid (FAMs) against ZIKV. A synthetic FAM (E3) demonstrated anti-ZIKV potential by reducing viral replication up to 86%. We analyzed the possible mechanisms of action of FAM E3 by evaluating the intercalation of this compound into the viral dsRNA and its interaction with the RNA polymerase of bacteriophage SP6. However, FAM E3 did not act by these mechanisms. *In silico* results predicted that FAM E3 might bind to the ZIKV NS3 helicase suggesting that this protein could be one possible target of this compound. To test this, the thermal stability and the ATPase activity of the ZIKV NS3 helicase domain (NS3^{Hel}) were investigated *in vitro* and we demonstrated that FAM E3 could indeed bind to and stabilize NS3^{Hel}.

Zika virus (ZIKV) is a mosquito-transmitted virus first isolated in 1947 from a *Rhesus* monkey in the Zika forest, Uganda¹. ZIKV remained endemic to the African and Asian regions until 2007, since then the virus has spread to other continents²⁻⁶. Notably, in 2015, the ZIKV outbreak had a worldwide impact and was considered a serious public health problem due to the large number of people infected and the development of neurological disorders in neonates (microcephaly) and adults (Guillain Barre syndrome)⁷.

Similar to other arboviruses such as Dengue virus (DENV), Yellow Fever virus (YFV) and Chikungunya virus (CHIKV), ZIKV is mainly transmitted by *Aedes spp.* of mosquitoes⁸⁻¹⁰. Nevertheless, other sources of infection acquisition have been reported, including blood transfusion⁹, sexual^{11,12}, perinatal and transplacental transmissions^{5,13}. Recently, it has been suggested that ZIKV may also have a sylvatic transmission cycle which could increase the frequency of human reinfection¹⁴.

ZIKV belongs to the *Flaviviridae* family and genus *Flavivirus*¹⁵. As other members of the genus, the viral genome is a positive single-stranded RNA with one open reading frame (ORF), translated in a polyprotein that is

¹Laboratory of Virology, Institute of Biomedical Science, ICBIM, Federal University of Uberlândia, Uberlândia, MG, Brazil. ²São Paulo State University, IBILCE, S. José do Rio Preto, SP, Brazil. ³Laboratory of Antibiotics and Chemotherapeutics, São Paulo State University, IBILCE, S. José do Rio Preto, SP, Brazil. ⁴LabMol - Laboratory of Molecular Modeling and Drug Design, Faculdade de Farmácia, Universidade Federal de Goiás, Goiânia, GO, 74605-170, Brazil. ⁵Institute of Physics of São Carlos, University of São Paulo, São Carlos, Brazil. ⁶Department of Pharmacology, Physiology and Neuroscience, Rutgers University–New Jersey Medical School, Newark, NJ 07103, United States. ⁷Present address: Repare Therapeutics, 7210 Rue Frederick-Banting, Suite 100, Montreal, QC, H4S 2A1, Canada. ⁸Collaborations Pharmaceuticals, Inc., 840 Main Campus Drive, Lab 3510, Raleigh, NC, 27606, United States. ⁹Laboratory of Nanobiotechnology, Federal University of Uberlândia, Uberlândia, MG, Brasil. ¹⁰Integrative Physiology and Salivary Nanobiotechnology Group, Federal University of Uberlândia, Uberlândia, MG, Brasil. ¹¹Institute of Technology, University of Tartu, Nooruse 1, 50411, Tartu, Estonia. ¹²School of Molecular and Cellular Biology, Faculty of Biological Sciences and Astbury Centre for Structural Molecular Biology, University of Leeds, Leeds, LS2 9JT, United Kingdom. *email: jardim@ufu.br

cleaved by host and viral proteases into 10 proteins. The polyprotein yields seven nonstructural proteins involved in the viral replication process (NS1, NS2A, NS2B, NS3, NS4A, NS4B and NS5), and three structural proteins (capsid (C), pre-membrane (prM) and the envelope (E) proteins), which comprise the viral particles^{16–18}.

There are currently no approved antiviral compounds targeting ZIKV infection. The treatment of infected individuals is palliative and consists of fluid intake and rest. Therefore, there is an urgent need for research to develop effective antivirals. In this context, the therapeutic properties of natural compounds have been historically described for the treatment of several viral diseases, such as hepatitis C virus (HCV)^{19,20}, human immunodeficiency virus (HIV-1)²¹, CHIKV²², DENV and West Nile virus (WNV)²³. Natural products present advantages such as high chemical diversity, low cost of production and efficient metabolism^{24,25}. However, compounds isolated from natural sources are not patentable and the isolation process is time consuming^{24,26}. An attractive alternative is to use the structure of the natural products as scaffolds for the synthesis of new molecules that can enhance the bioactivity and are more amenable to large scale manufacture^{26–28}.

Natural and synthetic acids have attracted attention due to their potent antiviral properties. This is exemplified by glycyrrhizic acid which prevents the release of HCV infectious particles²⁹ and inhibits hepatitis A virus (HAV) penetration into the host cell³⁰, and 3,5-dicaffeoylquinic acid, 1-methoxyoxalyl-3,5-dicaffeoylquinic acid, and L-choric acid that were described to prevent HIV-1 viral replication³¹. Similarly, nordihydroguaiaretic acid (NDGA) and its derivative tetra-*o*-methyl nordihydroguaiaretic acid were demonstrated to block DENV, HCV³², WNV and ZIKV³³ replication.

Here we evaluated the antiviral activity of synthetic diarylamines derived from anthranilic acid (FAMs) on ZIKV infection *in vitro* and *in silico*. Our data showed that FAM E3 significantly inhibited the ZIKV genome replication.

Results

ZIKV infection can be inhibited by synthetic FAMs. A panel of FAMs synthesized based on natural scaffolds was screened using a recombinant ZIKV that expresses the Nanoluciferase reporter (ZIKV-Nanoluc) (Fig. 1A). This recombinant virus was shown previously to exhibit a similar replication rate to wild type virus³⁴. To assess cytotoxicity, Vero cells were treated with differing concentrations of each FAM (0.4, 2, 10 and 50 μ M) and cell viability was measured 72 h post-treatment. Then, Vero cells were infected with ZIKV-Nanoluc at a MOI of 0.1 in the presence or absence of each compound at specific concentrations and Nanoluciferase activity levels, proportional to viral replication, were assessed 72 h post infection (h.p.i).

From all compounds evaluated, FAM E3 (Fig. 1B) showed the highest inhibition rate (Table S1). We therefore performed a dose response assay to determine effective concentration 50% (EC₅₀) and cytotoxicity 50% (CC₅₀) values for FAM E3. ZIKV-Nanoluc infected Vero cells were therefore treated with FAM E3 at concentrations ranging from 1 to 10 μ M and virus replication efficiency was evaluated 72 h.p.i. In parallel cell viability was measured by MTT assay. Our data showed that FAM E3 was able to inhibit >99% of virus replication, while the minimum cell viability remained above 60% (Fig. 1C). Using a wider range of FAM E3 concentrations, it was determined that the compound has an EC₅₀ of 2.59 μ M, CC₅₀ of 8.0 μ M and SI of ~3 (Fig. 1D). For further analysis, cells were treated with FAM E3 at 3 μ M, which inhibited approximately 96% of ZIKV infectivity with cell viability >88% (Fig. 1C). To confirm that the activity of FAM E3 against ZIKV was not specific to the laboratory isolate, it was also tested against a primary clinical isolate of ZIKV (provided by the Evandro Chagas Institute in Belém, Pará³⁵) (ZIKV^{BR}). For this, Vero cells were infected with ZIKV^{BR} at MOI = 0.1 and treated with FAM E3 3 μ M or controls for 72 h. Then, intracellular virus was titrated by analysing focus-forming units per milliliters (Ffu/mL). The results corroborated to the data from ZIKV-Nanoluc (Fig. 1E).

The antiviral effect of FAM E3 was also investigated in the ZIKV human permissive cell lines Huh-7 and 293 T. Infected cells were treated with 3 μ M of FAM E3 and both cell viability and ZIKV infectivity were evaluated. The results showed that FAM E3 was able to significantly decrease ZIKV replication levels in both cell types (Fig. 1F). However, 293 T cells appeared to be acutely sensitive to the cytotoxic effect of FAM E3.

FAM E3 inhibits the post-entry stage of ZIKV replication. To analyze the effects of FAM E3 on different stages of the ZIKV replicative cycle, time of addition experiments were performed. To evaluate the activity of compound on virus entry, FAM E3 and ZIKV-Nanoluc were simultaneously added to the cells for 2 h at 37 °C. Then, the inoculum was removed, cells were extensively washed with PBS, fresh media was added, and the cells were incubated for 72 h (Fig. 2A). In contrast to the control obatoxacin (OLX) that is known to inhibit the entry of ZIKV³⁶, the results showed that FAM E3 had no effect on ZIKV entry into the host cell (Fig. 2A).

We further investigated whether FAM E3 could elicit a protective effect. For this, cells were pretreated by incubation in medium containing FAM E3 for 2 h. prior to infection with ZIKV-Nanoluc for 72 h as shown in Fig. 2B. FAM E3 had no significant effect on ZIKV infection, suggesting that this compound is not acting by rendering the cells refractory to infection with ZIKV (Fig. 2B).

Finally, we analyzed the effect of FAM E3 on post-entry steps of ZIKV infection. For this, Vero cells were incubated with ZIKV-Nanoluc for 2 h, and then the inoculum was replaced by medium containing FAM E3. The data showed that FAM E3 decreased viral replication up to 86% whilst retaining cell viability above 90% (Fig. 2C). These data suggest that the antiviral activity of FAM E3 is related to its ability to inhibit a post-entry stage of the virus lifecycle, most likely viral RNA replication.

Potential mechanisms of action of FAM E3. To investigate possible mechanisms of action of FAM E3, we analyzed the ability of FAM E3 to intercalate into dsRNA, the replication intermediate of all positive-strand RNA viruses. Fifteen nanomoles of an *in vitro* synthesized dsRNA was incubated with FAM E3 or controls (DMSO or the well characterized intercalating agent doxorubicin (DOX)) and the obtained RNA/compound complexes were analyzed in 1% agarose gel. Densitometry analysis showed that FAM E3 did not intercalate with dsRNA (Fig. 3A).

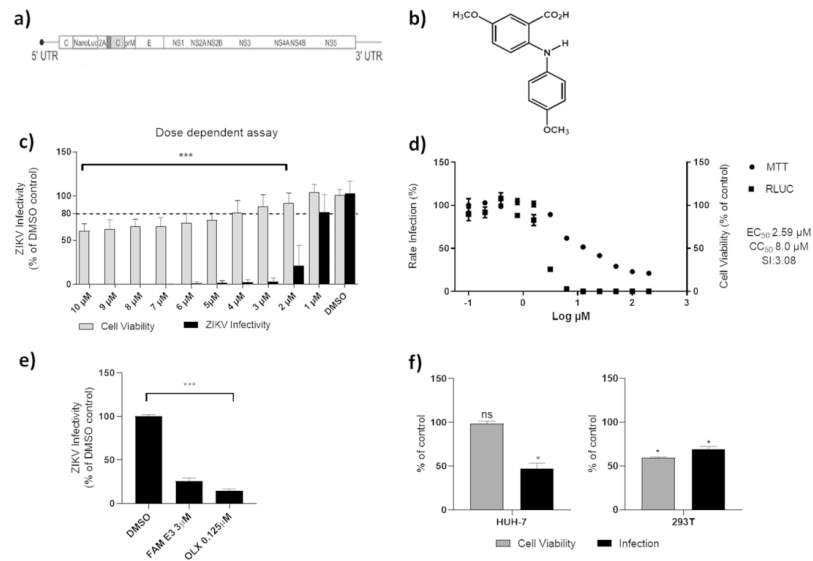


Figure 1. Inhibitory activity of FAM E3 on ZIKV replication. Schematic representation of ZIKV-Nanoluc that continuously expresses the Nanoluciferase reporter (a). Chemical structure of FAM E3 (b). Dose response assay: ZIKV-Nanoluc infected cells (MOI 0.1) were treated with FAM E3 at concentrations ranging from 1 to 10 μM and virus replication efficiency was evaluated 72 h.p.i. Simultaneously, Vero cells were equally treated with FAM E3 and cells viability was measured 72 h later (c). Effective and cytotoxic concentration of 50%: Vero cells were treated with increasing concentrations of FAM E3 ranging from 0.10 to 200 μM . ZIKV replication was measured by luciferase assay (indicated by ■) and cellular viability measured using an MTT assay (indicated by ●) (d). Vero cells were infected with ZIKV^{BR} and treated with FAM E3 at 3 μM and virus replication was accessed 72 h.p.i. The intracellular virus was titrated by analysing focus-forming units per milliliters (Ffu/mL), DMSO and OLX were used as negative and positive controls, respectively (e). Huh-7 or 293 T cell lines were infected with ZIKV-Nanoluc and treated with FAM E3 (3 μM) or DMSO (0.1%) for 72 h (f). Mean values of three independent experiments each measured in quadruplicate including the standard deviation are shown. $P < 0.05$ was considered significant compared to DMSO control.

As an assay for the RNA-dependent RNA polymerase activity of ZIKV NS5 was not available, we attempted to elucidate whether FAM E3 interacts with RNA synthesis carried out by the unrelated bacteriophage SP6 DNA-dependent RNA polymerase. For this, an *in vitro* transcription assay using SP6 RNA polymerase was performed in the presence or absence of FAM E3. Reaction products were analyzed using agarose gel electrophoresis and densitometry. As shown in Fig. 3B FAM E3 was unable to inhibit synthesis of ZIKV RNAs by SP6 RNA polymerase.

To test whether FAM E3 interfered with the cell lipid metabolism of the host cells. Vero cells infected with ZIKV-Nanoluc and treated with FAM E3, DMSO or OLX were fixed and stained with DAPI (to detect nuclear DNA), Bodipy to detect lipid droplets and an anti-NS3 antibody. As expected ZIKV infection increased lipid droplet accumulation and this was reduced by FAM E3 treatment. However, FAM E3 did not significantly reduce lipid droplet accumulation in non-infected Vero cells. Based on this result, the decrease in lipid droplets in infected Vero cells treated with FAM E3 is likely a consequence of the inhibition of virus replication, suggesting other mechanism of action for FAM E3 (Fig. 4).

FAM E3 is able to bind to and stabilize the ZIKV NS3^{Hdel} protein. Molecular docking calculations were performed in order to investigate the possible binding mode and the interactions between FAM E3 and ZIKV proteins. The proteins NS2B-NS3 protease, NS3 helicase, NS5 methyltransferase and NS5 polymerase, capsid and envelope were selected due to the availability of their experimentally obtained 3D structures in the protein data bank (PDB). The two best docking scores were obtained for NS3 helicase (NS3^{Hdel}) (-8.7 and -7.8 Kcal $\cdot\text{mol}^{-1}$, for RNA and ATP binding sites, respectively) (Figs. 5 and 6). As shown in Fig. 5, FAM E3 is predicted to bind into the NS3^{Hdel} RNA binding pocket: the carboxylic acid moiety of FAM E3 participating in hydrogen bonding interactions with the amino acid residues Arg598, His486 and adenine (A1) (Fig. 5A,B). Moreover, the aromatic rings and hydrophobic groups of FAM E3 were predicted to make hydrophobic packing interactions with residues Ala264, Ser268, Met536, Leu541, Pro542, Val543, Val599 and Ala605 (Fig. 5A,B).

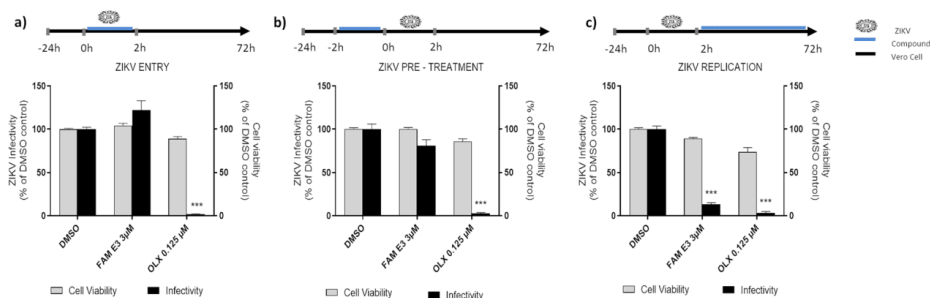


Figure 2. Effects of FAM E3 on the different stages of the ZIKV replicative cycle. Vero cells were infected with ZIKV-Nanoluc at a MOI = 0.5 and simultaneously treated with FAM E3 for 2 h; cells were washed to remove the virus and replaced with fresh media. ZIKV replication was measured by Nanoluc activity at 72 h.p.i (a). Vero cells were treated with FAM E3 for 2 h. Then, cells were extensively washed and infected with ZIKV-Nanoluc at a MOI = 0.5 for 2 h. The inoculum was removed and the cells were washed and replaced with fresh media. ZIKV replication was measured by Nanoluc activity at 72 h.p.i (b). Vero cells were infected with ZIKV-Nanoluc at a MOI = 0.5 for 2 h. The virus was removed, cells were washed and added of fresh media containing FAM E3. ZIKV replication was measured by Nanoluc activity at 72 h.p.i (c). For all assays, non-infected Vero cells were equally treated with FAM E3 and cell viability was measured 72 h later using MTT assay. DMSO was used as negative control and OLV as positive control for infectivity inhibition. Mean values of three independent experiments each measured in quadruplicate including the standard deviation are shown. $P < 0.05$ was considered significant.

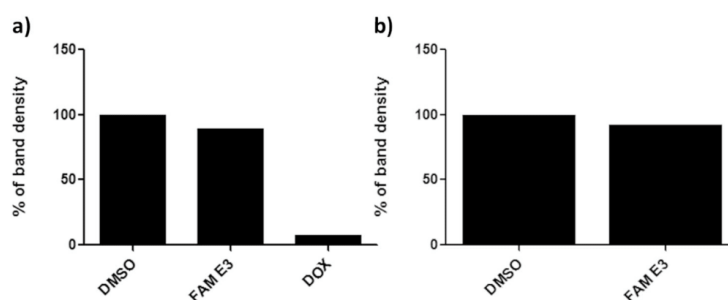


Figure 3. Analysis of FAM E3 intercalation into the viral dsRNA and its interaction with the activity of phage SP6 RNA polymerase. Fifteen nanomoles of dsRNA were incubated with the FAM E3 or intercalating controls (DMSO) or (DOX) for 45 minutes at room temperature. The reaction products were subjected to 1% agarose electrophoresis gel containing Ethidium Bromide followed by densitometry analysis (a). FAM E3 and 5 µg of purified pCCL-SP6-ZIKV amplicon was used for *in vitro* transcription using SP6 RNA polymerase at the presence or absence of FAM E3. Reaction products were analysed by agarose gel electrophoresis followed by densitometry analysis (b). Results of a representative of three independent reproducible experiments are shown.

FAM E3 was also predicted to bind into the NS3^{Hdel} ATP binding pocket (Fig. 6), in this case the carboxylic acid moiety of FAM E3 is predicted to form hydrogen bonding interactions with the amino acid residues Gln197, Gly199, Lys200 and Thr201. The ether group of FAM E3 can make a hydrogen bond with Gln455 (Fig. 6A,B). It is noteworthy that a similar interaction is observed in the crystal structure of NS3^{Hdel}, between the Gln455 residue and ATP³⁷. Moreover, FAM E3 made hydrophobic interactions with the residues Pro196, Ala235, Ala317 and Met414 (Fig. 6A,B).

In order to experimentally validate the results obtained by docking calculations, a thermal stability assay of the ZIKV NS3^{Hdel} domain was performed by Differential Scanning Fluorimetry (DSF). The thermal denaturation curves of NS3^{Hdel} in the presence of FAM E3 or non-treated control showed that FAM E3 was able to increase the NS3^{Hdel} melting temperature (T_m). This data suggests that FAM E3 could bind to and stabilize the NS3^{Hdel} protein (Fig. 7A). Additionally, a Micro-Scale Thermophoresis assay was carried out to evaluate the affinity of FAM E3 by NS3^{Hdel}. As observed in Fig. 7B, a sigmoidal slope was obtained, showing that FAM E3 could bind to NS3^{Hdel}. A fitting with the Hill function, a K_d of (0.42 ± 0.03) mM was obtained into the *in vitro* assay, showing a low affinity of

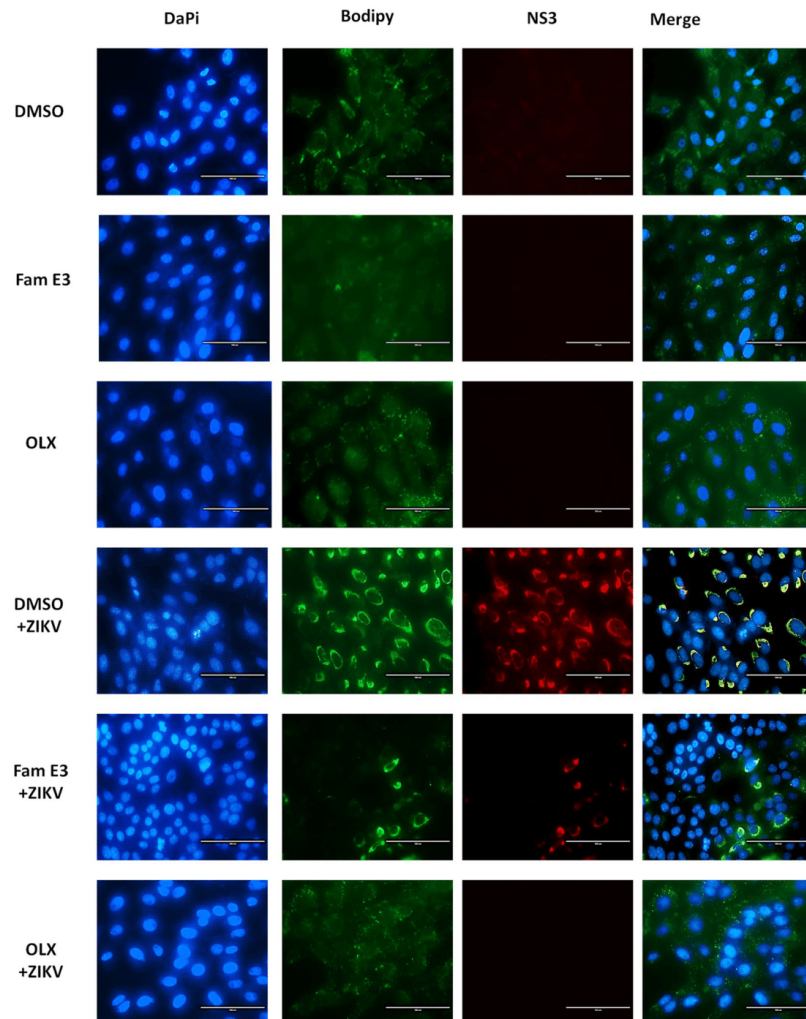


Figure 4. FAM E3 interference with the cell lipid metabolism of the host cells. Vero cells were infected with ZIKV at MOI = 0.1 and treated with FAM E3 3 μ M or DMSO 0.1% or OLX controls for 72 h. Naïve Vero cells were treated with DMSO were used as non-infected cells control. After treatment, cells were fixed and nuclei, lipid droplets (LDs) and ZIKV NS3 were labeled using DAPI (blue), BODIPY 493/503 (green) and ZIKV anti-NS3 antibody (red), respectively. Scale bar 100 nm.

the compound to the protein, in absence of ATP on NTP binding site. Finally, the effect of FAM E3 on the NTPase activity of NS3^{His} was also investigated by performing an NTPase activity assay using ATP as substrate and analyzing the amount of phosphate released by the protein in the reaction. FAM E3 did not significantly decrease the amount of phosphate released, compared to the non-treated control (Fig. 7C).

Discussion

In this study we evaluated the ability of synthetic diarylamines derived from anthranilic acid (FAMs), designed based on their natural scaffolds, to inhibit ZIKV infection. From this screen we selected FAM E3 for further analysis as it demonstrated the highest level of inhibition against ZIKV. FAM E3 is an intermediary molecule obtained during the production of synthetic acridones. The chemical structure of the FAMs is based on two aromatic rings

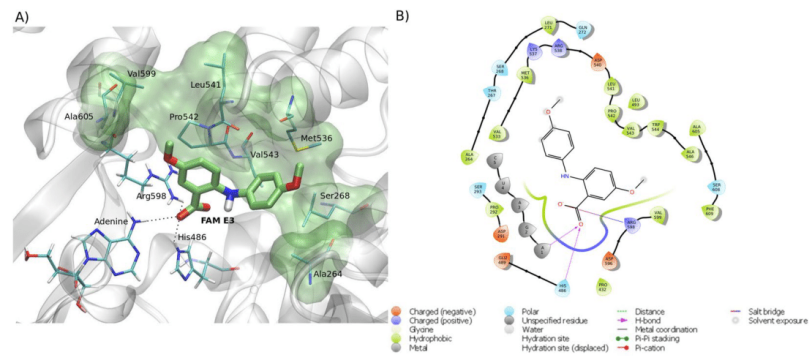


Figure 5. Predicted intermolecular interactions between FAM E3 and the RNA binding site of ZIKV NS3^{H^{el}}. 3D structure of the RNA binding site of ZIKV NS3^{H^{el}} docked with FAM E3, highlighting the main interactions between FAM E3 and amino acid residues, through hydrogen bonds (dotted black lines) and hydrophobic interactions (transparent green surface) (a). 2D representation of the protein-ligand interactions (b).

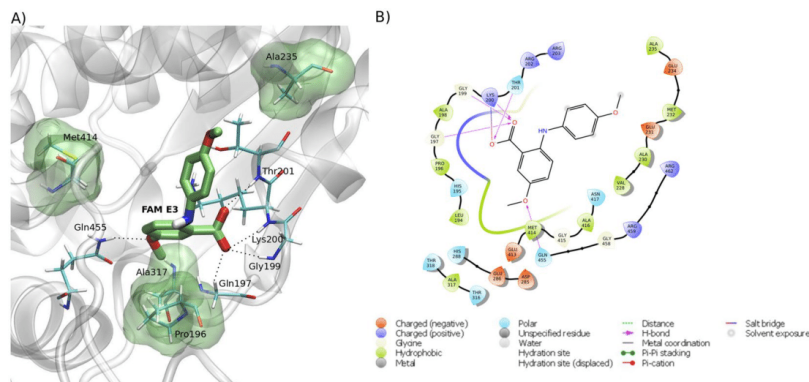


Figure 6. Predicted intermolecular interactions between FAM E3 and the ATP binding site of ZIKV NS3^{H^{el}}. 3D structure of the ATP binding site of ZIKV NS3^{H^{el}} docked with FAM E3, highlighting the main interactions between FAM E3 and amino acid residues, through hydrogen bonds (dotted black lines) and hydrophobic interactions (transparent green surface) (a). 2D representation of the protein-ligand interactions (b).

and one hydrogen atom linked to an amine group³⁸. Our results demonstrated that FAM E3 was able to inhibit ZIKV by blocking viral RNA replication, but it had no effect on ZIKV cell entry.

The observed inhibition of ZIKV RNA replication may result from different biological effects of FAM E3, including effects on viral RNA polymerase activity, interference with replicase complex formation, and suppression of interaction of viral polymerase proteins with host components. Previous studies have shown that acid derivative-containing compounds have interfered in the replicative cycle of different virus families. Zanella and coworkers showed that N-sulfonyl anthranilic acid derivatives inhibited the replication of DENV by inactivating the RNA-dependent RNA polymerase, quinic acid derivatives inhibited the replication of DENV-3 assayed using a sub-genomic replicon in RepDV3-Huh 7.5 cells³⁹. Additionally, anthranilic acid derivatives were reported to act as allosteric inhibitors by binding to HCV NS5B polymerase and inhibiting viral genome replication^{40,41}.

Antiviral mechanisms of action already described for some compounds are associated with the ability to interact with viral proteins^{42–44}. In the absence of functional ZIKV NS5 RNA polymerase and informed by the observation that viral RNA polymerases present structural and functional similarities⁴⁵, we tested whether FAM E3 could inhibit the synthesis of ZIKV genomic RNA *in vitro* by purified bacteriophage SP6 RNA polymerase. However, no significant inhibition of viral RNA transcription was observed. This indirect data, together with molecular docking results, suggests that the observed replication inhibition was unlikely to be due to the direct inhibition of RNA polymerase activity. Similarly, our results demonstrated that FAM E3 did not intercalate with dsRNA, a

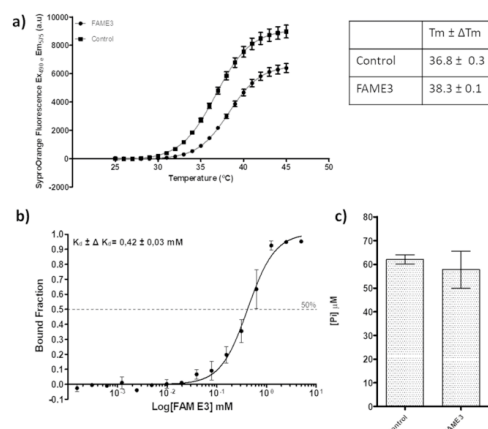


Figure 7. FAM E3 activity on NS3^{Hdel}. Thermal denaturation curves of NS3^{Hdel} and Boltzmann fitting in the presence of DMSO (Control) or FAM E3. T_m of NS3^{Hdel} obtained after Boltzmann fitting is represented on the table (a). MicroScale Thermophoretic analysis of the interaction between FAM E3 and NS3^{Hdel}. Data from four experiments were normalized to the fraction of bound ligand and averaged. K_d constant was obtained after a sigmoidal shape fitting with the Hill function (black continuous line) (b). NTPase activity of ZIKV NS3^{Hdel} in the presence or absence of FAM E3 and using ATP as substrate (c).

mechanism of action described for compounds which inhibit HCV replication, another member of *Flaviviridae* family^{45,46}.

Knowing that host cell lipids provide a replication platform for viruses, including members of genus *Flavivirus*, several studies have shown that the antiviral potential of some compounds is related to their interference to the cellular lipid metabolism, and as a consequence prevent viral morphogenesis. We investigated whether FAM E3 interferes with host cell lipid metabolism which could contribute to inhibition of viral replication. However, the results showed that FAM E3 did not interfere in the morphogenesis of lipid droplets (LDs) in non-infected Vero cells. In contrast, treatment of ZIKV infected Vero cells with FAM E3 resulted in a reduction in the numbers of LDs, although this is likely to be a consequence of its anti-ZIKV activity, decreasing replication levels. Heaton *et al.* showed that the NS3 protein of DENV is responsible for recruitment of fatty acid synthase (FASN) to virus replication sites⁴⁷. Since our results suggested that FAM E3 binds to and stabilizes ZIKV NS3^{Hdel}, we speculate that this interaction may result in a reduction of lipid recruitment to the virus replicase complex, which interferes in viral replication. NS3^{Hdel} is a promising target for antiviral drug discovery due to its essential role in the replication of the viral genome⁴⁸. Some examples of helicase inhibitors include ivermectin^{49,50}, suramin⁵¹ and benzoxazole⁵², which presented activity against both YFV⁴⁹ and DENV helicases^{51–53}. The *Flavivirus* helicases possess two enzymatic activities: adenosine triphosphatase (ATPase) which provides the chemical energy, and RNA triphosphatase (RTPase) that unwinds viral RNA during the replication process³⁷.

In summary, we have shown that the synthetic compound FAM E3 can inhibit ZIKV infection by blocking the genome replication stage. Through molecular docking it was possible to predict a possible interaction between FAM E3 and the ZIKV NS3 helicase, an essential protein for ZIKV replication. Based on this, the thermal stability and the ATPase activity of the helicase domain of ZIKV (NS3^{Hdel}) were investigated *in vitro* and demonstrated that FAM E3 could bind to and stabilize NS3^{Hdel}. The results may be useful for further development of antiviral against ZIKV infection, as well as for a better understanding of how exactly this synthetic compound inhibits viral replication.

Material and Methods

Synthesis, purification and structural elucidation of FAM E3. To a mixture of 2-bromo-5-methoxybenzoic acid (20.0 mmol) and 4-methoxyaniline (20.0 mmol) in *n*-pentanol (50 mL) were added 50 mg of copper and 3.0 g of K₂CO₃. The mixture was stirred under reflux for 24 hours and monitored by TLC. After cooling, solvent was evaporated under reduced pressure. The powder was solubilized in ethyl acetate (250 mL) followed by liquid-liquid extraction with HCl solution 1.0 mol/L (200 mL × 2). Organic phase was washed with deionized water (200 mL), dried with Na₂SO₄ and evaporated under reduced pressure. The crude product was purified by column chromatography over silica gel, using a mixture of ethyl acetate and hexane as mobile phase^{45,54}. Structure of FAME3 was confirmed by ¹H and ¹³C NMR data analyses. NMR spectra were recorded on Varian INOVA-500[®] (11.7 T) spectrometers, operating at 500 MHz for ¹H NMR and 126 MHz for ¹³C NMR. Chemical shifts (δ) were referenced to non-deuterated solvent signals. Signal multiplicities were reported as singlet (s), broad singlet (brs), doublet (d) and double doublet (dd). Amorphous yellow solid; yield 45%; ¹H NMR (500 MHz; DMSO-*d*₆): δ_H = 3.70 (s, 5-OCH₃), 3.74 (s, 4'-OCH₃), 6.92 (d, J = 2.0 and 9.0, H-3' and H-5'), 6.97 (d, J = 9.5, H-3), 7.02 (dd,

$J = 3.0$ and 9.5 Hz, H-4), 7.12 (d, $J = 9.0$ Hz, H-2' and H-6'), 7.37 (d, $J = 3.0$ Hz, H-6), 9.10 (brs, NH). ^{13}C NMR (126 MHz; DMSO- d_6): $\delta_c = 55.2$ (4'-OCH $_3$), 55.4 (5-OCH $_3$), 112.1 (C-3), 114.3 (C-1), 114.7 (C-3' and C-5'), 115.2 (C-6), 122.1 (C-4), 123.7 (C-2' and C-6'), 134.1 (C-1'), 142.8 (C-2), 150.2 (C-5), 155.4 (C-4'), 169.5 (COOH)^{45,54}.

The compounds were dissolved in dimethyl sulfoxide (DMSO) and stored at -20°C . Dilutions of the compounds in complete medium were made immediately prior to the experiments to reach a maximum final concentration of 0.1% DMSO. For all the assays performed, control cells were treated with medium added of DMSO at the final concentration of 0.1%. Obatoclax (OLX) at $0.125\ \mu\text{M}$ (AdooQ Bioscience) was used as a positive control for inhibition of ZIKV infectivity⁵⁵.

ZIKV construction. The ZIKV-Nanoluciferase (Nanoluc) construct (Fig. 1A) used in these assays was described previously⁵⁴. For maintenance and propagation of the plasmid containing the pCCI-SP6-ZIKV-Nanoluc, the *E. coli* Turbo strain (New England Biolabs) was used.

Complete amplification of the viral genome was performed using a PCR reaction with Phusion High Fidelity (Thermo Fisher) enzyme and the designed primers ZIKV-Forward (5' CG ATT AAG TTG GGT AAC GCC AGG GT 3') and ZIKV-Reverse (5' T AGA CCC ATG GAT TTC CCC ACA CC 3'). The PCR product containing SP6 promoter followed by complete viral cDNA was purified with the DNA clean and concentration kit (Zymo Research). *In vitro* transcription was performed using the RiboMAX™ Large-scale RNA Production Systems kit (Promega), as instructed by the manufacturers.

Cell culture

Vero cells were cultured in Dulbecco's modified Eagle's medium (DMEM; Sigma–Aldrich) supplemented with 100 U/mL penicillin (Gibco Life Technologies), 100 mg/mL streptomycin (Gibco Life Technologies), 1% (v/v) non-essential amino acids (Gibco Life Technologies) and 10% (v/v) fetal bovine serum (FBS; Hyclone) at 37°C in a humidified 5% CO $_2$ incubator.

Cell viability assay. Cell viability was measured by MTT [3-(4, 5-dimethylthiazol-2-yl)-2, 5-diphenyl tetrazolium bromide] (Sigma–Aldrich) method. Vero cells were seeded in a 96-well plate at a density of 1×10^4 cells per well and incubated overnight at 37°C in a humidified 5% CO $_2$ incubator. Drug-containing medium at different concentrations was added to the cell culture. After 72 h of incubation at 37°C , the media was removed and a solution containing MTT at the final concentration of 1 mg/mL was added to each well, incubated for 30 min at 37°C in a humidified 5% CO $_2$ incubator after which media was replaced with 100 μL of DMSO to solubilize the formazan crystals. Absorbance was measured by optical density (OD) of each well at 562 nm, using a spectrophotometer. Cell viability was calculated according to the equation $(T/C) \times 100\%$, where T and C represent the mean optical density of the treated group and vehicle control group, respectively. The cytotoxic concentration of 50% (CC $_{50}$) was calculated using Prism (Graph Pad).

Virus assays. For virus rescue, 8×10^6 Vero cells were electroporated with 10 μg of RNA viral transcript using 4 mm cuvettes (450 V, 600 μF , two pulses with an interval of 8 seconds). After electroporation, cells were suspended in culture media supplemented with 2% FBS and placed into 25 cm 2 cell culture flask and monitored for signs of infection during 5 days. At the end of this time, the viral supernatant was collected and stored at -80°C . To determine the viral titer, Vero cells at a density of 3×10^5 per well were seeded in a 6 well plate for 24 h prior to infection. Cells were infected with ZIKV-Nanoluc at 10-fold serially dilutions for 2 h at 37°C . The inoculum was removed and the cells were washed with PBS to completely remove the unbound virus followed by addition of cell culture media supplemented with 2% FBS and 2% carboxymethyl cellulose (CMC). Infected cells were incubated for 5 days at a CO $_2$ incubator at 37°C . The media was removed and cells were fixed with 4% formaldehyde, stained with 0.5% violet crystal and the plaques were counted.

Antiviral assays. For the initial screening of compounds, Vero cells were seeded at density of 1×10^4 cells per well into 96-well plates 24 h prior to the infection. ZIKV-Nanoluc at a multiplicity of infection (MOI) of 0.1 and compounds were simultaneously added to cells. Samples were harvested in *Renilla* luciferase lysis buffer (Promega) at 72 h post-infection (h.p.i.) and virus replication was quantified by measuring Nanoluciferase activity using the *Renilla* luciferase Assay System (Promega) (Fig. 1B). The effective concentration of 50% inhibition (EC $_{50}$) was calculated using Prism (Graph Pad). The values of CC $_{50}$ and EC $_{50}$ were used to calculate the selectivity index ($SI = CC_{50}/EC_{50}$). 0.1% DMSO and $0.125\ \mu\text{M}$ OLX were used as vehicle and positive controls, respectively.

To evaluate the dose-dependence of the antiviral effect, FAM E3 at concentrations ranging from $1\ \mu\text{M}$ to $10\ \mu\text{M}$, and ZIKV-Nanoluc (MOI = 0.1) were added to the cells simultaneously for 72 h. The cells were washed with PBS and harvested in *Renilla* luciferase lysis buffer prior to measurement of luminescence. Cell viability was analyzed concomitantly.

The effect of FAM E3 against a wild type ZIKV strain was tested by using the primary clinical isolate of ZIKV (provided by the Evandro Chagas Institute in Belém, Pará³⁵) (ZIKV^{BR}). Vero cells were infected with ZIKV^{BR} at MOI = 0.1 and treated with FAM E3 $3\ \mu\text{M}$ or controls for 72 h. Then, intracellular virus was titrated by analysing focus-forming units per milliliters (Ffu/mL).

Time-of-addition assay. To assess the effect of FAM E3 on ZIKV entry to the host cells, inoculum containing ZIKV-Nanoluc (MOI = 0.5) and compounds were simultaneously added to cells (1×10^4) and incubated for 2 h at 37°C . Cells were extensively washed with PBS to completely remove virus and compounds and were replaced with fresh media. Samples were harvested in *Renilla* luciferase lysis buffer (Promega) at 72 h.p.i. and virus infectivity was quantified by measuring luciferase activity using the *Renilla* luciferase Assay System (Promega).

Alternatively, cells were infected with ZIKV-Nanoluc (MOI = 0.5) for 2 h, the viral inoculum was completely removed by extensive washing with PBS, and compounds were added. The inhibition of ZIKV replication was measured by quantifying Renilla luciferase activity 72 h.p.i, as previously described.

Finally, Vero cells at a density of 1×10^4 cell per well were incubated with the compound for 2 h at 37 °C in a humidified 5% prior to infection. After incubation, cells were washed extensively and infected with ZIKV-Nanoluc (MOI = 0.5) for 2 h. Then, the inoculum was removed, cells were washed to completely remove non-endocytosed virus and fresh media was added. At 72 h.p.i cells were analyzed as described above. In all Time-of-Addition experiments DMSO and OLX were used as controls as described above.

DsRNA intercalation assay. To investigate whether the compound interacts with the dsRNA, an experiment using the previously described protocol was performed⁵⁶. Briefly, fifteen nanograms of the dsRNA were incubated with 3 μ M of FAM E3 at room temperature for 45 min and electrophoresed on a 1% agarose gel prior to analysis by densitometry. DMSO and Doxorubicin (DOX) at 100 μ M were used as negative and positive control, respectively.

SP6 RNA polymerase transcription assay. Assuming that viral RNA polymerases have similar topology and functions^{45,57}, we used SP6 RiboMAX™ Large-scale RNA Production Systems kit (Promega) to evaluate the effect of the compound at *in vitro* RNA transcription. The pCCI-SP6-ZIKV-Nanoluc was used as target with the addition of 3 μ M FAM E3. Complete amplification and purification of transcripts corresponding to the viral genome was performed as per manufacturers instructions. The RNA was quantified, samples were resolved in a 1% agarose gel, and results were analyzed by densitometry. DMSO was used as control.

NS3^{Hdel} cloning, overexpression and purification. The coding region of NS3^{Hdel} from the MR766 strain was cloned into the expression vector pETTrx-1a/LIC by Celco Biotec, generating the NS3^{Hdel}_pETTrx-1a/LIC expression vector. Rosetta (DE3) *E. coli* (Novagen) cells were transformed with NS3^{Hdel}_pETTrx-1a/LIC and grown in ZYM 5052 autoinduction medium, supplemented with 50 μ g.ml⁻¹ kanamycin and 34 μ g.ml⁻¹ chloramphenicol at 37 °C, until the OD₆₀₀ reached 0.6. Protein was expressed at 18 °C for 24 h. Cells were harvested by centrifugation and cell pellets was resuspended in 20 mM Tris pH 7.0, 500 mM NaCl, 20 mM Imidazole, 10% glycerol. Cells were lysed by sonication and cell debris was separated by centrifugation. NS3^{Hdel} was purified using five steps: a HisTrap HP 5.0 mL with a Ni Sepharose resin (GE Healthcare), a buffer exchanged with HisTrap Desalting 5 ml (GE Healthcare), a TEV protease cleavage from 6His-TRX-tag, another HisTrap HP 5.0 ml with a Ni Sepharose resin (GE Healthcare) and size-exclusion chromatography on a XK 26/1000 Superdex 200 column (GE Healthcare) pre-equilibrated in buffer 20 mM Bis-Tris pH 7.0, 500 mM NaCl, 10% glycerol. The final protein sample was analyzed in SDS-PAGE 10% to confirm its purity. Concentration was determined spectrophotometrically in a Nanodrop 1000 spectrophotometer (Thermo Scientific).

Thermal stability assay by differential scanning fluorimetry (DSF). To investigate the thermal stability of helicase domain of ZIKV (NS3^{Hdel}), FAM E3 was diluted to 1.25 mM in 100% DMSO (Synth) and Helicase in 20 mM Bis-Tris (Sigma), pH7, 500 mM NaCl (Sigma), 10% glycerol. A solution consisting 20 μ M Helicase, 5x Sypro® Orange (Sigma Aldrich) was prepared and transferred into each well of the 96-well assay plate (Axygen). 200 μ M of FAM E3 was added and an optical adhesive (Hampton) was used to seal the plate. The thermal stability measurements were performed by monitoring the fluorescence of Sypro® Orange ($\lambda_{excitation} = 490$ nm and $\lambda_{emission} = 575$ nm) while the samples were heated from 25 to 74 °C at a rate of 1 °C/min in a conventional quantitative PCR instrument Mx3005P. Thermal denaturation curves were obtained using GraphPad Prism 5.0 and an approximation through the Boltzmann equation as described by Huynh and Partch⁵⁸. DMSO was used as reference. The experiments were performed in duplicate.

NS3^{Hdel} NTPase activity assay by malachite green assay. Assays to evaluate the ATPase activity of the NS3^{Hdel} were performed using the commercial QuantiChrom™ ATPase/GTPase Assay Kit (BioAssay Systems) as described by Cao *et al.*⁵⁹. The assay was standardized for NS3^{Hdel} as described in the kit manual. Protein was incubated in 20 mM Bis-Tris buffer, pH7, 500 mM NaCl, 10% glycerol previously supplemented with 8.0 mM MgCl₂ (Sigma) in a 96-well plate (Greiner Crystal Clear). FAM E3 at 320 μ M in 20 mM Bis-Tris buffer, pH7, 500 mM NaCl, 10% glycerol was added into each well to a final concentration of 40 μ M in the reaction. The reaction was started with ATP (Sigma) at 2.0 mM and incubated for 30 min at 25 °C. Reactions were terminated with the addition of reagent buffer supplied by the manufacturer and incubated again for 45 min at room temperature before absorbance measurement at $\lambda = 620$ nm, which is associated with amount of phosphate released due to ATP hydrolysis. The tests were performed in duplicates. DMSO (1% vol/vol) was used as reference. The results were analyzed and plotted using the GraphPad Prism 5.0 program.

Microscale thermophoresis. Experiments were performed on a Monolith® NT.115 (Nanotemper technologies). NS3^{Hdel} was labelled on cysteine residues with NT-647-Maleimide dye (Nanotemper Technologies) using the Monolith NTTM Protein Labeling Kit RED-MALEIMIDE as per manufacturer's instructions. The concentration of protein indicated for MicroScale Thermophoresis experiments was 40 nM and a serial dilution of FAM E3 from 5 mM to 150 nM⁶⁰. The dissociation constant K_d was obtained by fitting the binding curve with the Hill function.

Immunofluorescence assay. For immunofluorescence assay, 2×10^5 Vero cells were grown in 6-well plates 24 h prior infection. ZIKV-Nanoluc (MOI = 0.1) and compounds were simultaneously added to cells. Naïve Vero

cells treated with DMSO were used as non-infected control. Cells were fixed at 72 h.p.i with 4% paraformaldehyde and washed with PBS and blocking buffer (BB) containing: 0.1% Triton X-100 (Vetec Labs, BR), 0.2% bovine albumin (BSA) and PBS for 30 min. Then, cells were incubated with primary rabbit polyclonal anti-NS3 antibody diluted in BB for 1 h. Alexa Fluor 594 conjugated anti-rabbit IgG was used as secondary antibody. Cells were washed and labelled for nuclei and lipid droplets (LDs) with DAPI and BODYPI 493/503, respectively. Images were analyzed at EVOs cell imaging systems fluorescence microscopy (Thermo Fisher Scientific).

Molecular docking. FAM E3 was docked into six available crystallographic ZIKV protein structures using the Autodock Vina 1.1.2 software⁶¹. The crystallographic structures of NS2B-NS3 protease (PDB ID: 5H4I)⁶²; NS3 helicase (PDB ID: 5GJB³⁷, helicase with RNA strand); NS5 methyltransferase (PDB ID: 5KQR)⁶³; NS5 polymerase (PDB ID: 5TFR)⁶⁴, capsid protein (PDB ID: 5YGH)⁶⁵ and envelope protein (PDB ID: 5LBV)⁶⁶ were obtained from the Protein Data Bank (<https://www.rcsb.org>). The target proteins were prepared as part of the OpenZika project⁶⁷ by using the MolProbity^{68,69} server to add the hydrogen atoms; the open source version of PyMOL⁷⁰ was then used to align all target models onto a single coordinate reference frame (using the align by alpha carbons command line); followed by using AutoDockTools 1.5.6⁷¹, to format the atom types, calculate Gasteiger-Marsili charges, and merge the non-polar hydrogens onto their respective heavy atoms, using the default AutoDockTools preparation protocol for proteins, described elsewhere⁷¹.

The SMILES structure of FAM E3 was obtained from the PubChem database (<https://pubchem.ncbi.nlm.nih.gov/>). Then, the ligand was prepared in the Avogadro software 1.2.0⁷², by adding hydrogen atoms at pH 7.4 and minimizing the geometry using the MMFF94 force field. The minimized structure was then prepared in AutoDockTools 1.5.6⁷¹, following the standard preparation protocol for ligands (allowing full ligand flexibility)⁷¹.

The protein grid coordinates were built based on ZIKV protein binding pockets described in the literature: NS2B-NS3 protease (pocket of co-crystallized inhibitor boronate⁷³ and ((1H-benzo[d]imidazole-1-yl) methanol))⁶², NS3 helicase (RNA and ATP binding sites), NS5 methyltransferase (Guanosine-5'-triphosphate (GTP), S-Adenosyl methionine (SAM) and active), NS5 polymerase (RNA, nucleoside triphosphate (NTP) and active site) and E protein (predicted pocket)⁷⁴. The capsid pockets were predicted using the PockDrug server⁷⁵: pocket 1 (between N-terminal - α 1 helix of the monomers) and pocket 2 (between α 4 helices of the monomers)¹⁸. The analysis of docking results was based on docking scores, 2D protein-ligand interaction map and visual inspection of the docked 3D binding modes. Visual Molecular Dynamics program (VMD)⁷⁶ was used to render the 3D molecular image.

Statistical analysis. Individual experiments were performed in triplicate and all assays were performed a minimum of three times in order to confirm the reproducibility of the results. Differences between means of readings were compared using analysis of variance (one-way or two-way ANOVA) or Student's *t*-test using Graph Pad Prism 5.0 software (Graph Pad Software). *P* values of less than 0.05 (***) were considered to be statistically significant.

Received: 25 January 2019; Accepted: 29 October 2019;

Published online: 27 November 2019

References

- Dick, G. W., Kitchen, S. & Haddock, A. Zika Virus (I). Isolations and serological specificity. *Trans. R. Soc. Trop. Med. Hyg.* **46**, 509–520 (1952).
- Song, B.-H., Yun, S.-I., Woolley, M. & Lee, Y.-M. Zika virus: History, epidemiology, transmission, and clinical presentation. *J. Neuroimmunol.* **308**, 50–64 (2017).
- Duffy, M. R. *et al.* Zika Virus Outbreak on Yap Island, Federated States of Micronesia. *N. Engl. J. Med.* **360**, 2536–2543 (2009).
- Lanciotti, R. S. *et al.* Genetic and serologic properties of Zika virus associated with an epidemic, Yap State, Micronesia, 2007. *Emerg. Infect. Dis.* **14**, 1232–1239 (2008).
- Chan, J. F. W., Choi, G. K. Y., Yip, C. C. Y., Cheng, V. C. C. & Yuen, K.-Y. Zika fever and congenital Zika syndrome: An unexpected emerging arboviral disease. *J. Infect.* **72**, 507–524 (2016).
- Cao-Lormeau, V.-M. Zika Virus, French Polynesia, South Pacific, 2013. *Emerg. Infect. Dis.* **20**, 1960–1960 (2014).
- WHO. The History of Zika Virus. *WHO World Health Organization* doi:entity/emergencies/zika-virus/history/en/index.html (2016).
- Paupy, C., Delatte, H., Bagny, L., Corbel, V. & Fontenille, D. Aedes albopictus, an arbovirus vector: From the darkness to the light. *Microbes Infect.* **11**, 1177–1185 (2009).
- Musso, D. *et al.* Potential Sexual Transmission of Zika Virus. *Emerg. Infect. Dis.* **21**, 359–361 (2015).
- Wong, P. S. J., Li, Mzhil., Chong, C. S., Ng, L. C. & Tan, C. H. Aedes (Stegomyia) albopictus (Skuse): A Potential Vector of Zika Virus in Singapore. *PLoS Negl. Trop. Dis.* **7**, e2348 (2013).
- McCarthy, M. Zika virus was transmitted by sexual contact in Texas, health officials report. *BMJ* **352**, i720 (2016).
- Nicastri, E. *et al.* Persistent detection of Zika virus RNA in semen for six months after symptom onset in a traveller returning from Haiti to Italy, February 2016. *Eurosurveillance* **21** (2016).
- Ventura, C. V. *et al.* Ophthalmological findings in infants with microcephaly and presumable intra-uterine Zika virus infection. *Arq. Bras. Oftalmol.* **79**, 1–3 (2016).
- Terzian, A. C. B. *et al.* Evidence of natural Zika virus infection in neotropical non-human primates in Brazil. *Sci. Rep.* **8**, 16034 (2018).
- Kuno, G., Chang, G. J., Tsuchiya, K. R., Karabatsos, N. & Cropp, C. B. Phylogeny of the genus Flavivirus. *J. Virol.* **72**, 73–83 (1998).
- Hou, W. *et al.* Molecular cloning and characterization of the genes encoding the proteins of Zika virus. *Gene* **628**, 117–128 (2017).
- Sirohi, D. & Kuhn, R. J. Zika Virus Structure, Maturation, and Receptors. *J. Infect. Dis.* **216**, S935–S944 (2017).
- Sirohi, D. *et al.* The 3.8 Å resolution cryo-EM structure of Zika virus. *Science* (80-.). **5316**, 1–7 (2016).
- Calland, N., Dubuisson, J., Rouillé, Y. & Séron, K. Hepatitis C Virus and Natural Compounds: A New Antiviral Approach? *Viruses* **4**, 2197–2217 (2012).
- Jardim, A. C. G. *et al.* Natural compounds isolated from Brazilian plants are potent inhibitors of hepatitis C virus replication *in vitro*. *Antiviral Res.* **115**, 39–47 (2015).

21. Wan, Z. & Chen, X. Triptolide inhibits human immunodeficiency virus type 1 replication by promoting proteasomal degradation of Tat protein. *Retrovirology* **11**, 88 (2014).
22. da Silva-Júnior, E. F., Leoncini, G. O., Rodrigues, É. E. S., Aquino, T. M. & Araújo-Júnior, J. X. The medicinal chemistry of Chikungunya virus. *Bioorg. Med. Chem.* **25**, 4219–4244 (2017).
23. Vázquez-Calvo, Á., de Oya, N. J., Martín-Acebes, M. A., García-Moruno, E. & Saiz, J. C. Antiviral properties of the natural polyphenols delphinidin and epigallocatechin gallate against the flaviviruses West Nile Virus, Zika Virus, and Dengue Virus. *Front. Microbiol.* **8** (2017).
24. Kitazato, K., Wang, Y. & Kobayashi, N. Viral infectious disease and natural products with antiviral activity. *Drug Discov. Ther.* **1**, 14–22 (2007).
25. Li, J. W.-H. & Vederas, J. C. Drug Discovery and Natural Products: End of an Era or an Endless Frontier? *Science* (80-). **325**, 161–165 (2009).
26. Martínez, J. P., Sasse, F., Brönstrup, M., Diez, J. & Meyerhans, A. Antiviral drug discovery: broad-spectrum drugs from nature. *Nat. Prod. Rep.* **32**, 29–48 (2015).
27. Newman, D. J., Cragg, G. M. & Snader, K. M. The influence of natural products upon drug discovery (Antiquity to late 1999). *Nat. Prod. Rep.* **17**, 215–234 (2000).
28. Butler, M. S. Natural products to drugs: natural product-derived compounds in clinical trials. *Nat. Prod. Rep.* **25**, 475–516 (2008).
29. Matsumoto, Y. *et al.* Antiviral activity of glycyrrhizin against hepatitis C virus *in vitro*. *PLoS One* **8**, e68992 (2013).
30. Crance, J. M. *et al.* Studies on mechanism of action of glycyrrhizin against hepatitis A virus replication *in vitro*. *Antiviral Res.* **23**, 63–76 (1994).
31. Robinson, W. E., Reinecke, M. G., Abdel-Malek, S., Jia, Q. & Chow, S. a. Inhibitors of HIV-1 replication that inhibit HIV integrase. *Proc. Natl. Acad. Sci. USA* **93**, 6326–6331 (1996).
32. Soto-Acosta, R., Bautista-Carbajal, P., Syed, G. H., Siddiqui, A. & Del Angel, R. M. Nordihydroguaiaretic acid (NDGA) inhibits replication and viral morphogenesis of dengue virus. *Antiviral Res.* **109**, 132–140 (2014).
33. Merino-Ramos, T., J de Oya, N., Saiz, J.-C. & Martín-Acebes, M. A. Antiviral Activity of Nordihydroguaiaretic Acid and Its Derivative Tetra- O -Methyl Nordihydroguaiaretic Acid against West Nile Virus and Zika Virus. *Antimicrob. Agents Chemother.* **61**, e00376–17 (2017).
34. Mutso, M. *et al.* Reverse genetic system, genetically stable reporter viruses and packaged subgenomic replicon based on a Brazilian Zika virus isolate. *J. Gen. Virol.* <https://doi.org/10.1099/jgv.0.000938> (2017).
35. Cugola, F. R. *et al.* The Brazilian Zika virus strain causes birth defects in experimental models. *Nature* **534**, 267–271 (2016).
36. Kuivaneen, S. *et al.* Obatoclax, salphenylhalamide and gemcitabine inhibit Zika virus infection *in vitro* and differentially affect cellular signaling, transcription and metabolism. *Antiviral Res.* **139**, 117–128 (2017).
37. Tian, H. *et al.* Structural basis of Zika virus helicase in recognizing its substrates. *Protein Cell* **7**, 562–570 (2016).
38. Layer, Robert W. Amines, Aromatic, Diarylamines. *Encyclopedia of Chemical Technology*. 1–8 (2000).
39. Zanello, P. R. *et al.* Quinic acid derivatives inhibit dengue virus replication *in vitro*. *Virol. J.* **12**, 223 (2015).
40. Nittoli, T. *et al.* Identification of anthranilic acid derivatives as a novel class of allosteric inhibitors of hepatitis C NS5B polymerase. *J. Med. Chem.* **50**, 2108–2116 (2007).
41. Vrontaki, E., Melagraki, G., Mavromoustakos, T. & Afantitis, A. Searching for anthranilic acid-based thumb pocket 2 HCV NS5B polymerase inhibitors through a combination of molecular docking, 3D-QSAR and virtual screening. *J. Enzyme Inhib. Med. Chem.* **31**, 38–52 (2016).
42. Leung, D. *et al.* Activity of recombinant dengue 2 virus NS3 protease in the presence of a truncated NS2B co-factor, small peptide substrates, and inhibitors. *J. Biol. Chem.* **276**, 45762–71 (2001).
43. Lim, Hjung *et al.* Inhibitory effect of flavonoids against NS2B-NS3 protease of ZIKA virus and their structure activity relationship. *Biotechnol. Lett.* **39**, 415–421 (2017).
44. Macdonald, A. *et al.* The hepatitis C virus non-structural NS5A protein inhibits activating protein-1 function by perturbing Ras-ERK pathway signaling. *J. Biol. Chem.* **278**, 17775–17784 (2003).
45. Stankiewicz-Drogon, A. *et al.* New acridone-4-carboxylic acid derivatives as potential inhibitors of Hepatitis C virus infection. *Bioorg. Med. Chem.* **16**, 8846–8852 (2008).
46. Campos, G. R. F. *et al.* Hepatitis C virus *in vitro* replication is efficiently inhibited by acridone Fac4. *J. Gen. Virol.* **98**, 1693–1701 (2017).
47. Heaton, N. S. *et al.* Dengue virus nonstructural protein 3 redistributes fatty acid synthase to sites of viral replication and increases cellular fatty acid synthesis. *Proc Natl Acad Sci USA* **107**, 17345–17350 (2010).
48. Mottin, M. *et al.* The A-Z of Zika drug discovery. *Drug Discov. Today*, <https://doi.org/10.1016/j.drudis.2018.06.014> (2018).
49. Mastrangelo, E. *et al.* Ivermectin is a potent inhibitor of flavivirus replication specifically targeting NS3 helicase activity: New prospects for an old drug. *J. Antimicrob. Chemother.* **67**, 1884–1894 (2012).
50. Wagstaff, K. M., Sivakumaran, H., Heaton, S. M., Harrich, D. & Jans, D. A. Ivermectin is a Specific Inhibitor of Importin α/β -Mediated Nuclear Import able to Inhibit Replication of HIV-1 and Dengue Virus. *Biochem. J.* **443** (2012).
51. Basavannacharya, C. & Vasudevan, S. G. Suramin inhibits helicase activity of NS3 protein of dengue virus in a fluorescence-based high throughput assay format. *Biochem. Biophys. Res. Commun.* **453**, 539–544 (2014).
52. Byrd, C. M. *et al.* Novel benzoxazole inhibitor of dengue virus replication that targets the NS3 helicase. *Antimicrob. Agents Chemother.* **57**, 1902–1912 (2013).
53. Albulescu, I. C., Kovacicova, K., Tas, A., Snijder, E. J. & van Hemert, M. J. Suramin inhibits Zika virus replication by interfering with virus attachment and release of infectious particles. *Antiviral Res.* **143**, 230–236 (2017).
54. Singh, P., Kaur, J., Yadav, B. & Komath, S. S. Design, synthesis and evaluations of acridone derivatives using *Candida albicans*-Search for MDR modulators led to the identification of an anti-candidiasis agent. *Bioorganic Med. Chem.* **17**, 3973–3979 (2009).
55. Saiz, J. & Martín-Acebes, M. A. The Race To Find Antivirals for Zika Virus. *Antimicrob. Agents Chemother.* **61**, e00411–17 (2017).
56. Krawczyk, M., Wasowska-Lukawska, M., Oszczapowicz, I. & Boguszewska-Chachulska, A. M. Amidinoanthracylines – a new group of potential anti-hepatitis C virus compounds. *Biol. Chem.* **390**, 351–360 (2009).
57. Gniazdowski, M., Denny, W., Nelson, S. M. & Czyz, M. Effects of anticancer drugs on transcription factor–DNA interactions. *Expert Opin. Ther. Targets* **9**, 471–489 (2005).
58. Huynh, K. & Partch, C. L. Analysis of protein stability and ligand interactions by thermal shift assay. *Curr. Protoc. Protein Sci.* **2015**, 19.26.1–19.26.14 (2015).
59. Cao, X., Li, Y., Jin, X., Guo, F. & Jin, T. Molecular mechanism of divalent-metal-induced activation of NS3 helicase and insights into Zika virus inhibitor design. *Nucleic Acids Res* **44**, 10505–10514 (2016).
60. NanoTemper Technologies GmbH. User Manual for the Monolith NT.115. 1–10 (2007).
61. Trott, O. & Olson, A. AutoDock Vina: improving the speed and accuracy of docking with a new scoring function, efficient optimization and multithreading. *J. Comput. Chem.* **31**, 455–461 (2010).
62. Zhang, Z. *et al.* Crystal structure of unlinked NS2B-NS3 protease from Zika virus. *Science* (80-). **354**, 1597–1600 (2016).
63. Coloma, J., Jain, R., Rajashankar, K. R., Garcia-Sastre, A. & Aggarwal, A. K. Structures of NS5 Methyltransferase from Zika Virus. *Cell Rep.* **16**, 3097–3102 (2016).
64. Upadhyay, A. K. *et al.* Crystal structure of full-length Zika virus NS5 protein reveals a conformation similar to Japanese encephalitis virus NS5 research communications. *Acta Crystallogr. Sect. F* **5**, 116–122 (2017).

65. Shang, Z., Song, H., Shi, Y., Qi, J. & Gao, G. F. Crystal Structure of the Capsid Protein from Zika Virus. *J. Mol. Biol.* **430**, 948–962 (2018).
66. Barba-Spaeth, G. *et al.* Structural basis of potent Zika–dengue virus antibody cross-neutralization. *Nature* **536**, 48–53 (2016).
67. Ekins, S., Perryman, A. L. & Horta Andrade, C. OpenZika: An IBM World Community Grid Project to Accelerate Zika Virus Drug Discovery. *PLoS Negl. Trop. Dis.* **10** (2016).
68. Chen, V. B. *et al.* MolProbity: All-atom structure validation for macromolecular crystallography. *Acta Crystallogr. Sect. D Biol. Crystallogr.* **66**, 12–21 (2010).
69. Chen, V. B. *et al.* research papers MolProbity: all-atom structure validation for macromolecular crystallography research papers. October 12–21, <https://doi.org/10.1107/S0907444909042073> (2010).
70. Schrödinger. The PyMOL Molecular Graphics System. Schrödinger LLC *www.pymol.org* **Version 1**, <http://www.pymol.org> (2015).
71. GM, M. *et al.* AutoDock4 and AutoDockTools4: Automated docking with selective receptor flexibility. *J. Comput. Chem.* **30**, 2785–2791 (2009).
72. Hanwell, M. D. *et al.* Avogadro: an advanced semantic chemical editor, visualization, and analysis platform. *J. Cheminform.* **4**, 17 (2012).
73. Lei, J. *et al.* Crystal structure of Zika virus NS2B-NS3 protease in complex with a boronate inhibitor. *Science* (80-). **353**, 503–505 (2016).
74. Sharma, N., Murali, A., Singh, S. K. & Giri, R. Epigallocatechin gallate, an active green tea compound inhibits the Zika virus entry into host cells via binding the envelope protein. *Int. J. Biol. Macromol.* **104**, 1046–1054 (2017).
75. Hussein, H. A. *et al.* PockDrug-Server: a new web server for predicting pocket druggability on holo and apo proteins. *Nucleic Acids Res.* **43**, W436–W442 (2015).
76. Humphrey, W., Dalke, A. & Schulten, K. VMD: Visual molecular dynamics. *J. Mol. Graph.* **14**, 33–38 (1996).

Acknowledgements

We would like to thank the Royal Society – Newton Advanced Fellowship (Grant reference NA 150195), CNPQ (National Counsel of Technological and Scientific Development – grant 445021/2014-4), CNPq/FAPEG DCR (Grant 300508/2017-4 and 201710267000063), FAPEMIG (Minas Gerais Research Foundation - APQ-00587-14, SICONV 793988/2013) and CAPES (Coordination for the Improvement of Higher Education Personnel – Code 001), for financial support. The authors thank the Brazilian funding agencies CNPq, CAPES and FAPEMIG for providing financial support to the National Institute of Science and Technology in Theranostics and Nanobiotechnology - INCT-Teranano (CNPq-465669/2014-0; MCTIC/FNDCT-CNPq/MEC-CAPES/MS-DECIT; Preventing and Combating the Zika Virus #440610/2016-8). Research in the MH laboratory was funded by a Wellcome Trust Investigator Award (grant reference 096670). CHA also thanks the “L’Oréal-UNESCO-ABC Para Mulheres na Ciência” and “L’Oréal-UNESCO International Rising Talents Program” for the awards and fellowships received. CHA has CNPq productivity fellowship. We also thank the computational contribution of the collaborators and volunteers of the OpenZika project (<http://openzika.ufg.br>), as well as the support from IBM’s World Community Grid team.

Author contributions

Acquisition of data and results analysis: S.S., J.F.S., D.M.O., L.R.A., M.M., B.K.P.S., N.C.M.R.M., C.B. and A.C.G.J.; Drafting of the manuscript: S.S. and J.F.S.; Study design, supervision and critical revision: C.B., L.O.R., P.H., C.H.A., G.O., A.L.P., S.E., L.R.G., R.S.S., A.M., M.H. and A.C.G.J. All authors reviewed the manuscript.

Competing interests

The authors declare no competing interests.

Additional information

Supplementary information is available for this paper at <https://doi.org/10.1038/s41598-019-54169-z>.

Correspondence and requests for materials should be addressed to A.C.G.J.

Reprints and permissions information is available at www.nature.com/reprints.

Publisher’s note Springer Nature remains neutral with regard to jurisdictional claims in published maps and institutional affiliations.



Open Access This article is licensed under a Creative Commons Attribution 4.0 International License, which permits use, sharing, adaptation, distribution and reproduction in any medium or format, as long as you give appropriate credit to the original author(s) and the source, provide a link to the Creative Commons license, and indicate if changes were made. The images or other third party material in this article are included in the article’s Creative Commons license, unless indicated otherwise in a credit line to the material. If material is not included in the article’s Creative Commons license and your intended use is not permitted by statutory regulation or exceeds the permitted use, you will need to obtain permission directly from the copyright holder. To view a copy of this license, visit <http://creativecommons.org/licenses/by/4.0/>.

© The Author(s) 2019